## Chapter 4

# Density-Functional Theory

In this chapter, we provide a density-functional theory (DFT) that becomes the basis of Quantum ESPRESSO. In order to understand how the DFT code works, we explain and apply the DFT on a simple example of the ground-state calculation of a helium atom. A simple Python code is also given for the helium atom calculation. This chapter will help the readers to understand Quantum ESPRESSO's techniques in Chapter 3, such as the self-consistent field (SCF) calculation, the ground-state total energy, the pseudopotential, etc.

## 4.1 "Black box" Quantum ESPRESSO

By giving input files to Quantum ESPRESSO, we can obtain output files containing the materials' information and properties. Therefore, Quantum ESPRESSO works like a black box, as shown in Fig. 4.1 (a). The readers may run a computer program successfully without understanding the black box. However, a successful run does not mean that you have run it properly. To understand what you are running, the readers need to know what is inside the black box.

*Quantum ESPRESSO Course for Solid-State Physics*
Nguyen T. Hung, Ahmad R. T. Nugraha, and Riichiro Saito

ISBN 978-981-4968-37-9 (Hardcover), 978-1-003-29096-4 (eBook)
www.jennystanford.com

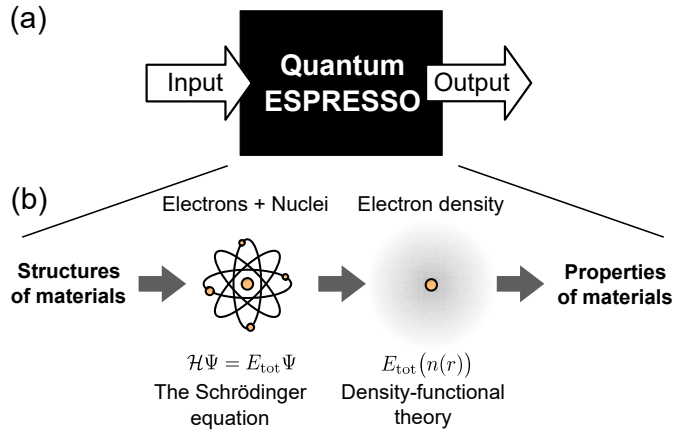


**Figure 4.1** (a) Quantum ESPRESSO as a black box. (b) Density-functional theory is used in Quantum ESPRESSO to solve the Schrödinger equation of materials.

The purpose of Quantum ESPRESSO is to calculate the properties of materials at the atomic scale. Since "*materials* = *electrons* + *nuclei*", the properties of the materials are given by the complicated interactions of the electrons and nuclei. The electrons and nuclei hold together in the materials with a detailed balance between the repulsive and attractive Coulomb interactions between them. These interactions are described by an equation in quantum mechanics, the so-called **Schrödinger equation** (Eq. (4.1)) [Schrödinger (1926)]. An analytical solution of the Schrödinger equation only exists for systems of one electron (e.g., a hydrogen atom), while most atoms, molecules, and materials consist of many electrons and nuclei. For any system of more than two electrons, the Schrödinger equation can be solved only after using some approximations due to the complexity of the Coulomb interactions. Therefore, a good approximation is necessary to solve the Schrödinger equation. In Quantum ESPRESSO, the **density-functional theory (DFT)** is used as an approximation to solve the Schrödinger equation, as shown in Fig. 4.1 (b).

## 4.2 The Schrödinger equation

A system of electrons and nuclei is described by the Schrödinger equation as

$$\mathcal{H}\Psi = E_{\text{tot}}\Psi, \tag{4.1}$$

where $\mathcal{H}$ is the Hamiltonian of the system, $E_{\text{tot}}$ is *the total energy of the electrons and nuclei*, and $\Psi(\boldsymbol{r}_1, ..., \boldsymbol{r}_{N_e}, \boldsymbol{R}_1, ..., \boldsymbol{R}_{N_n})$ is the wavefunction of many particles (electrons and nuclei). By using the atomic units listed in Table 4.1, a general Hamiltonian in Eq. (4.1) is given by kinetic energies $\mathcal{T}$ and potential energies $\mathcal{V}$ of the electrons and nuclei as

$$\begin{aligned}\mathcal{H} &= \mathcal{T}_n + \mathcal{V}_n + \mathcal{T}_e + \mathcal{V}_e + \mathcal{V}_{en} \\ &= \underbrace{-\sum_{I=1}^{N_n} \frac{\nabla_{\boldsymbol{R}_I}^2}{2M_I} + \frac{1}{2}\sum_{I\neq J}^{N_n} \frac{Z_I Z_J}{|\boldsymbol{R}_I - \boldsymbol{R}_J|}}_{\text{nuclei}} \\ &\quad \underbrace{-\sum_{i=1}^{N_e} \frac{\nabla_{\boldsymbol{r}_i}^2}{2} + \frac{1}{2}\sum_{i\neq j}^{N_e} \frac{1}{|\boldsymbol{r}_i - \boldsymbol{r}_j|}}_{\text{electrons}} + \underbrace{\sum_{i=1}^{N_e}\sum_{I=1}^{N_n} \frac{-Z_I}{|\boldsymbol{r}_i - \boldsymbol{R}_I|}}_{\text{mixed}}.\end{aligned} \tag{4.2}$$

| | | | |
|---|---|---|---|
| $\mathcal{T}_n$: | kinetic energy of nuclei | $\mathcal{T}_e$: | kinetic energy of electrons |
| $\mathcal{V}_n$: | Coulomb repulsion between a pair of nuclei | $\mathcal{V}_e$: | Coulomb repulsion between a pair of electrons |
| $\mathcal{V}_{en}$: | Coulomb attraction between electrons and nuclei | $\nabla$: | nabla operators |
| $\boldsymbol{R}$: | nuclear position | $\boldsymbol{r}$: | electronic position |
| $N_n$: | number of nuclei | $N_e$: | number of electrons |
| $I, J$: | label for a nucleus | $i, j$: | label for an electron |
| $M$: | nuclear mass | $Z$: | nuclear charge (atomic number) |

Notice that a factor of 1/2 appears in the sums of $\mathcal{V}_n$ and $\mathcal{V}_e$ to take into account the double counting on the summation $i$ and $j$ ($i \neq j$). Here, we adopt the atomic units $e = \hbar = c = m_e = 1$ (see Table 4.1) and cgs unit for the Coulomb interaction. If SI unit is adopted, $\mathcal{T}_e + \mathcal{V}_e$

**Table 4.1** Atomic unit (a.u.).

| Symbol | Quantity | a.u. | Value in SI |
|---|---|---|---|
| $t$ | Time | 1 | $2.419 \times 10^{-17}$ s |
| $c\ (1/\alpha)$ | Speed of light | 1 | $2.998 \times 10^{8}$ m/s |
| $\hbar$ | $h/2\pi$ (angular momentum) | 1 | $1.055 \times 10^{-34}$ Js |
| $h$ | Planck's constant | $2\pi$ | $6.626 \times 10^{-31}$ Js |
| Ha ($E_h$) | Hartree (atomic energy) | 1 | $4.360 \times 10^{-18}$ J |
| $m_e$ | Electron mass | 1 | $9.110 \times 10^{-31}$ kg |
| $e$ | Electron charge | 1 | $1.602 \times 10^{-19}$ C |
| $a_0$ | Bohr radius (atomic distance) | 1 | $5.292 \times 10^{-11}$ m |
| $e/a_0^3$ | Charge density | 1 | $1.081 \times 10^{12}$ C/m$^3$ |
| $eE_h/\hbar$ | Current | 1 | $6.623 \times 10^{-3}$ A |
| $E_h/(ea_0^2)$ | Electric field | 1 | $9.717 \times 10^{21}$ V/m$^2$ |
| $\mu_B$ | Bohr magneton | 1/2 | $9.274 \times 10^{-24}$ J/T |
| $4\pi\epsilon_0$ | Vacuum permittivity $\times 4\pi$ | 1 | $1.113 \times 10^{-10}$ C$^2$/Jm |
| $E_h/a_0$ | Force | 1 | $8.238 \times 10^{-8}$ N |
| $E_h/a_0^3$ | Pressure | 1 | $2.942 \times 10^{13}$ Pa |

Helpful conversions: 1 Ha = 27.2114 eV = 2 Ry.

is expressed by

$$-\sum_{i=1}^{N_e} \frac{\hbar^2 \nabla_{\boldsymbol{r}_i}^2}{2m_e} + \frac{1}{2} \sum_{i \neq j}^{N_e} \frac{e^2}{4\pi\epsilon_0 |\boldsymbol{r}_i - \boldsymbol{r}_j|}. \tag{4.3}$$

The Hamiltonian in Eq. (4.2) is considered as a coupled nuclear and electronic problem. However, the nuclei are much heavier than the electrons (e.g., $M_H/m_e = 1,836$ in hydrogen or $M_C/m_e = 21,868$ in carbon). Moreover, the average speed of the nuclei is much smaller than that of the electrons. Therefore, we can assume that the electrons will follow the nuclear motions without any delay, and we can decouple the electronic and nuclear motions to the first approximation, which is known as the **Born-Oppenheimer**

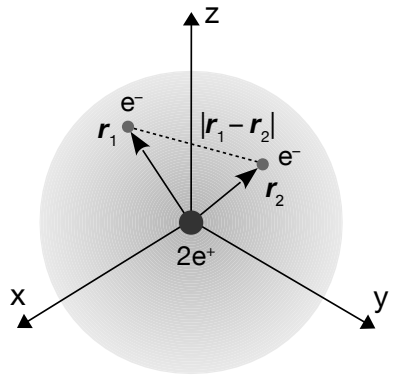


**Figure 4.2** Two electrons in a helium atom, where $\boldsymbol{r}_i$ $(i = 1, 2)$ are the positions of the $i$-th electron, and $|\boldsymbol{r}_1 - \boldsymbol{r}_2|$ is the distance between two electrons.

**approximation (BOA)** [Born and Oppenheimer (1927)]. The nuclei in the material are almost immobile except for hydrogen atoms, and their positions can be determined precisely by X-ray crystallography (see Sec. 5.2). Thus, we can fix the positions of the nuclei in the real space with zero kinetic energy (i.e., $\mathcal{T}_n = 0$) for calculating the electronic energy band. Then $\mathcal{V}_n$ becomes an external potential (or simply a constant). In this case, the problem that we have to solve becomes a purely electronic one as

$$\mathcal{H}_e\psi = (\mathcal{T}_e + \mathcal{V}_e + \mathcal{V}_{en})\psi = E\psi, \tag{4.4}$$

where $E = E_{\text{tot}} - \mathcal{V}_n$ is *the total energy of the electrons* and $\psi$ is a wavefunction of the $N$ electrons, in which $\psi$ is a many-body function of the positions of $N$ electrons $\boldsymbol{r}_i$ $(i = 1, 2, ..., N)$: $\psi(\boldsymbol{r}_1, \boldsymbol{r}_2, ..., \boldsymbol{r}_N)$. Since an electron interacts with the rest of the electrons due to the Coulomb repulsion $\mathcal{V}_e$, the many-body state has to account for all the degrees of freedom of $N$ electrons in the system (or the $3N$-dimensional configuration space).

---

❑ **The Schrödinger equation for a helium atom:** Let us consider the case of a helium (He) atom, which consists of one nucleus with $Z = 2$ and two electrons at $\boldsymbol{r}_1$ and $\boldsymbol{r}_2$, as shown in Fig. 4.2.

Equation (4.4) for a helium atom is given by

$$\left(-\frac{1}{2}\nabla_{\boldsymbol{r}_1}^2-\frac{1}{2}\nabla_{\boldsymbol{r}_2}^2+\frac{1}{|\boldsymbol{r}_1-\boldsymbol{r}_2|}-\frac{2}{|\boldsymbol{r}_1|}-\frac{2}{|\boldsymbol{r}_2|}\right)\psi(\boldsymbol{r}_1,\boldsymbol{r}_2) = E\psi(\boldsymbol{r}_1,\boldsymbol{r}_2). \tag{4.5}$$

Although Eq. (4.5) looks simple, an analytical solution cannot be found because Eq. (4.5) is a six-dimensional partial differential equation (PDE). High-dimensional PDEs are hard to solve in physics, in which they occur not only in quantum mechanics but also in classical mechanics (e.g., the Hamilton-Jacobi equation[1] with a large number of degrees of freedom).

Since the Schrödinger equation is a PDE where all terms are known, one can try to solve it numerically on a grid.[2] This approach can solve Eq. (4.5) for an electron, but it fails for a system with more than two electrons. For example, if we take 3D silicon as an example, it has a unit cell volume of $a^3/4$, where $a = 5.431$ Å is the lattice constant. If we consider a grid of the unit cell with points spaced by $\Delta d \sim 0.2$ Å, this grid consists of $(a^3/4)/(\Delta d^3) \sim 5000$ points. Since two silicon atoms in the unit cell contain 28 electrons, the grid has $28 \times 3 = 84$ coordinates. Therefore, a complete specification of a wavefunction $\psi_{\mathrm{Si}}(\boldsymbol{r}_1, \boldsymbol{r}_2, ..., \boldsymbol{r}_{28})$ requires $5000^{84}$ complex numbers. We need a stack of DVDs from the earth to the sun to store this wavefunction. To overcome this problem, many researchers have been developing methods of approximation since the late 1920s. The most successful method in physics is the density-functional theory (DFT). The DFT is defined by the theory of approximation in which the Coulomb interaction between electrons is expressed by a functional[3] of the electron density. With the DFT, the Schrödinger equation can be reformulated in terms of the electron density. Therefore, the $3N$-dimensional PDE is reduced to $N$ PDE's of 3-dimension, so that we can solve Eq. (4.2) for silicon and store their wavefunction by using a PC.

---

[1] The Hamilton-Jacobi equation is an alternative formulation of classical mechanics, equivalent to other formulations such as the Newton second law.

[2] In a grid approach, functions are represented by their values at certain grid points and derivatives are approximated through differences in these values.

[3] A functional is a function whose variable is another function such as $V(n(\boldsymbol{r}))$.

## 4.3 Systems of non-interacting electrons

Before explaining the DFT, we would like to show some approximations for solving Eq. (4.5), which are regarded as the conceptual origin of the DFT. As discussed in Sec. 4.2, the problem to solve the Schrödinger equation comes from the Coulomb repulsion between electrons $\mathcal{V}_e$. If we assume that the $N_e$ electrons in the system are non-interacting to one another, we can set $\mathcal{V}_e = 0$, and Eq. (4.4) can be rewritten as a function of $\boldsymbol{r}_i$ $(i = 1, ..., N_e)$

$$(\mathcal{T}_e + \mathcal{V}_{en})\psi = \left( -\sum_{i=1}^{N_e} \frac{\nabla_{\boldsymbol{r}_i}^2}{2} + \sum_{i=1}^{N_e}\sum_{I=1}^{N_n} \frac{-Z_I}{|\boldsymbol{r}_i - \boldsymbol{R}_I|} \right) \psi = E\psi. \quad (4.6)$$

Here we define a **single-particle Hamiltonian** of one electron as

$$h(\boldsymbol{r}) = -\frac{\nabla_{\boldsymbol{r}}^2}{2} + \sum_{I=1}^{N_n} \frac{-Z_I}{|\boldsymbol{r} - \boldsymbol{R}_I|}, \quad (4.7)$$

so that Eq. (4.6) can be rewritten as

$$h(\boldsymbol{r}_i)\psi(\boldsymbol{r}_i) = E\psi(\boldsymbol{r}_i), \text{ with } (i = 1, ..., N_e). \quad (4.8)$$

From Eq.(4.8) we can say that, for the case of the non-interacting electrons, the Hamiltonian of the system can be written as $N_e$ independent single-particle Hamiltonian, and the wavefunction is written by $\psi(\boldsymbol{r}_i)$. Eq. (4.8) is used to obtain the energy of electrons for the following two cases: (1) **distinguishable**[4] and (2) **indistinguishable**[5] electrons. For simplicity, we consider the two electrons in a helium atom as follows:

(1) **Two distinguishable electrons**: Let us consider electron 1 in one state $\phi_a(\boldsymbol{r}_1)$ and electron 2 in another state $\phi_b(\boldsymbol{r}_2)$. Since two electrons are independent of each other, the probability of finding (electron 1 at $\boldsymbol{r}_1$) *and* (electron 2 at $\boldsymbol{r}_2$) can be given by the *product* as $|\psi(\boldsymbol{r}_1, \boldsymbol{r}_2)|^2 = |\phi_a(\boldsymbol{r}_1)|^2 |\phi_b(\boldsymbol{r}_2)|^2$. In this case, the wavefunction can

[4] If the electrons are distinguishable, the physical properties of the system are changed by switching the positions of two electrons.
[5] If the electrons are indistinguishable, switching the positions of two electrons makes no physical change.

be expressed by the product of one-body wavefunction, $\psi(\boldsymbol{r}_1, \boldsymbol{r}_2) = \phi_a(\boldsymbol{r}_1)\phi_b(\boldsymbol{r}_2)$, which is known as **one-body approximation**. In this case, Eq. (4.8) can be written as

$$[h(\boldsymbol{r}_1) + h(\boldsymbol{r}_2)]\,\phi_a(\boldsymbol{r}_1)\phi_b(\boldsymbol{r}_2) = E\phi_a(\boldsymbol{r}_1)\phi_b(\boldsymbol{r}_2). \tag{4.9}$$

Since $h(\boldsymbol{r}_i)$ $(i = 1, 2)$ acts only on $\phi_\alpha(\boldsymbol{r}_i)$ $(\alpha = a, b)$ as

$$h(\boldsymbol{r}_i)\phi_\alpha(\boldsymbol{r}_i) = \epsilon_\alpha\phi_\alpha(\boldsymbol{r}_i), \tag{4.10}$$

where $\epsilon_\alpha$ is the energy of one electron, the left-hand side of Eq. (4.9) is rewritten as

$$\begin{aligned} &[h(\boldsymbol{r}_1) + h(\boldsymbol{r}_2)]\,\phi_a(\boldsymbol{r}_1)\phi_b(\boldsymbol{r}_2) \\ &= [h(\boldsymbol{r}_1)\phi_a(\boldsymbol{r}_1)]\phi_b(\boldsymbol{r}_2) + \phi_a(\boldsymbol{r}_1)[h(\boldsymbol{r}_2)\phi_b(\boldsymbol{r}_2)] \\ &= \epsilon_a\phi_a(\boldsymbol{r}_1)\phi_b(\boldsymbol{r}_2) + \phi_a(\boldsymbol{r}_1)\epsilon_b\phi_b(\boldsymbol{r}_2) \\ &= (\epsilon_a + \epsilon_b)\phi_a(\boldsymbol{r}_1)\phi_b(\boldsymbol{r}_2). \end{aligned} \tag{4.11}$$

By substituting Eq. (4.11) into Eq. (4.9), we obtain

$$E = \epsilon_a + \epsilon_b. \tag{4.12}$$

Thus, for the case of the non-interacting system with the distinguishable electrons, the total energy of the electrons is the sum of the energy of each electron.

(2) **Two indistinguishable electrons**: In quantum mechanics, two electrons are indistinguishable (i.e., $\phi_a(\boldsymbol{r}_1)\phi_b(\boldsymbol{r}_2)$ is equivalent to $\phi_a(\boldsymbol{r}_2)\phi_b(\boldsymbol{r}_1)$). Thus, one possible shape of the wavefunction $\psi(\boldsymbol{r}_1, \boldsymbol{r}_2)$ is a **linear combination** of two states as [Kittel (1976)]

$$\psi(\boldsymbol{r}_1, \boldsymbol{r}_2) = \frac{1}{\sqrt{2}}[\phi_a(\boldsymbol{r}_1)\phi_b(\boldsymbol{r}_2) - \phi_b(\boldsymbol{r}_1)\phi_a(\boldsymbol{r}_2)], \tag{4.13}$$

where the prefactor $\frac{1}{\sqrt{2}}$ is for normalizing the wave function, $\int |\psi(\boldsymbol{r}_1, \boldsymbol{r}_2)|^2 \mathrm{d}\boldsymbol{r}_1\boldsymbol{r}_2 = 1$. Eq. (4.13) shows that the wavefunction is anti-symmetric for exchanging $\boldsymbol{r}_1$ and $\boldsymbol{r}_2$ as $\psi(\boldsymbol{r}_1, \boldsymbol{r}_2) = -\psi(\boldsymbol{r}_2, \boldsymbol{r}_1)$. When we put $\boldsymbol{r}_1 = \boldsymbol{r}_2$ for $\psi(\boldsymbol{r}_1, \boldsymbol{r}_2)$, we get $\psi = 0$. It means that two electrons cannot occupy the same position, in accordance with the

**Pauli exclusion principle** [Pauli (1925)]. Eq. (4.13) can also be written by using a matrix determinant as

$$\psi(\boldsymbol{r}_1, \boldsymbol{r}_2) = \frac{1}{\sqrt{2}} \begin{vmatrix} \phi_a(\boldsymbol{r}_1) & \phi_b(\boldsymbol{r}_1) \\ \phi_a(\boldsymbol{r}_2) & \phi_b(\boldsymbol{r}_2) \end{vmatrix}, \tag{4.14}$$

which is known as the **Slater determinant** [Slater (1929)].

By substituting Eq. (4.13) into Eq. (4.8), we get the same energy as the case of two distinguishable electrons (i.e., $E = \epsilon_a + \epsilon_b$). The probability of finding an electron at position $\boldsymbol{r}$, i.e., the **electron density**, is given by

$$n(\boldsymbol{r}) = P_1(\boldsymbol{r}) + P_2(\boldsymbol{r}), \tag{4.15}$$

where $P_1(\boldsymbol{r}) = \int |\psi(\boldsymbol{r}, \boldsymbol{r}_2)|^2 \mathrm{d}\boldsymbol{r}_2$ and $P_2(\boldsymbol{r}) = \int |\psi(\boldsymbol{r}_1, \boldsymbol{r})|^2 \mathrm{d}\boldsymbol{r}_1$ are probabilities of finding first and second electrons at $\boldsymbol{r}$, respectively, while other electrons can exist anywhere except for $\boldsymbol{r}$. Since two electrons are indistinguishable (i.e., $P_1(\boldsymbol{r}) = P_2(\boldsymbol{r})$), Eq. (4.15) can be rewritten as

$$n(\boldsymbol{r}) = 2 \int |\psi(\boldsymbol{r}, \boldsymbol{r}_2)|^2 \mathrm{d}\boldsymbol{r}_2. \tag{4.16}$$

By substituting Eq. (4.13) into Eq. (4.16) and using the normalization and orthogonality conditions, respectively, as

$$\int \phi_a^*(\boldsymbol{r}) \phi_a(\boldsymbol{r}) \mathrm{d}\boldsymbol{r} = \int \phi_b^*(\boldsymbol{r}) \phi_b(\boldsymbol{r}) \mathrm{d}\boldsymbol{r} = 1 \tag{4.17}$$

and

$$\int \phi_b^*(\boldsymbol{r}) \phi_a(\boldsymbol{r}) \mathrm{d}\boldsymbol{r} = \int \phi_a^*(\boldsymbol{r}) \phi_b(\boldsymbol{r}) \mathrm{d}\boldsymbol{r} = 0, \tag{4.18}$$

the electron density is expressed by

$$n(\boldsymbol{r}) = |\phi_a(\boldsymbol{r})|^2 + |\phi_b(\boldsymbol{r})|^2. \tag{4.19}$$

Therefore, the electron density of the non-interacting electrons is simply equal to the sum of the squares of the occupied states.

---

❑ **Electron density and energy of a helium atom without**

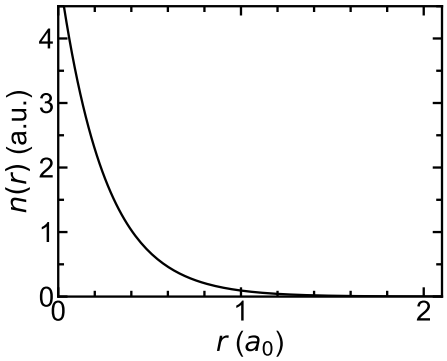


**Figure 4.3** Electron density in atomic unit of a helium atom as a function of $r$ in the approximation of non-interacting electrons.

**Coulomb repulsion:** Let us recall that the wavefunction of $s$-orbital and the energy of a hydrogen-like atom with a nucleus $+Ze$ are given by

$$\phi(\boldsymbol{r}) = \frac{Z^{3/2}}{\sqrt{\pi}} \exp(-Z|\boldsymbol{r}|) \text{ and } \epsilon = -\frac{Z^2}{2}, \tag{4.20}$$

respectively. We note that the hydrogen atom is a special case that contains only one electron and Eq. (4.20) gives an analytical solution for $Z = 1$. By substituting Eq. (4.20) into Eqs. (4.19) and (4.12), the electron density and energy of the helium atom are given by

$$n(\boldsymbol{r}) = \frac{2Z^3}{\pi} \exp(-2Z|\boldsymbol{r}|) \text{ and } E = -Z^2, \tag{4.21}$$

respectively, when we neglect the interaction between two electrons. Since the atomic number of a helium atom is $Z = 2$, the electron density and total energy are

$$n(\boldsymbol{r}) = \frac{16}{\pi} \exp(-4|\boldsymbol{r}|) \tag{4.22}$$

and $E = -4$ Ha, respectively. In Fig. 4.3, we plot $n(\boldsymbol{r})$ of Eq. (4.22) as a function of the distance $r = |\boldsymbol{r}|$ from the nucleus, respectively.

To compare the calculated energy $E$ with the experimental values, we remove two electrons from the helium atom as

$$\mathrm{He} \xrightarrow{I_1} \mathrm{He}^{+} + e^{-} \xrightarrow{I_2} \mathrm{He}^{++} + 2e^{-}, \tag{4.23}$$

where $I_1$ and $I_2$ are the first and second **ionization energies**, respectively. $I_1$ is the minimum energy required to remove the first electron from the helium atom and is experimentally given as 0.9 Ha (24.59 eV) [Sucher (1958)]. $I_2$ can be calculated exactly since $\mathrm{He}^{+}$ is a hydrogen-like ion, thus $I_2 = -\epsilon(\mathrm{He}^{+}) = 2$ Ha. Therefore, the energy of the helium atom is given by $-(I_1 + I_2) = -2.9$ Ha, which is larger than the calculated energy ($-4$ Ha). In other words, the non-interacting electrons approximation gives a large deviation of the total energy. The reason for the deviation is that we do not consider the energy of the Coulomb repulsion between the two electrons.

## 4.4 Hartree potential

In Sec. 4.3, we show that the non-interacting electrons without the Coulomb repulsion give a large deviation of the energy. Here we would like to keep the expression of $n(\boldsymbol{r})$ as the for the non-interacting electrons (Eq. (4.19)), and we will take the Coulomb repulsion into account in the energy $E$. When we consider the Coulomb interaction, Eq. (4.4) can be rewritten as

$$\left[h(\boldsymbol{r}_1) + h(\boldsymbol{r}_2) + \frac{1}{|\boldsymbol{r}_1 - \boldsymbol{r}_2|}\right] \phi_a(\boldsymbol{r}_1)\phi_b(\boldsymbol{r}_2) = E\phi_a(\boldsymbol{r}_1)\phi_b(\boldsymbol{r}_2). \tag{4.24}$$

If we multiply $\phi_b^*(\boldsymbol{r}_2)$ to Eq. (4.24) and integrate both sides of Eq. (4.24) on $\boldsymbol{r}_2$ with using the normalization condition in Eq. (4.17), we can obtain the **single-particle Schrödinger equation** for the first electron as

$$\left[h(\boldsymbol{r}_1) + \int \frac{|\phi_b(\boldsymbol{r}_2)|^2}{|\boldsymbol{r}_1 - \boldsymbol{r}_2|}\mathrm{d}\boldsymbol{r}_2\right] \phi_a(\boldsymbol{r}_1) = \epsilon_a^H \phi_a(\boldsymbol{r}_1), \tag{4.25}$$

where $\epsilon_a^H$ is expressed by

$$\epsilon_a^H = E - \int \phi_b^*(\boldsymbol{r}_2) h(\boldsymbol{r}_2) \phi_b(\boldsymbol{r}_2) \mathrm{d}\boldsymbol{r}_2 = E - \epsilon_b, \tag{4.26}$$

where $\epsilon_b$ is the energy of the second electron in the non-interacting Hamiltonian $h(\boldsymbol{r}_2)$ as defined by Eq. (4.10). The single-particle Schrödinger equation for the second electron also can be written by multiplying $\int \phi_a^*(\boldsymbol{r}_1)\mathrm{d}\boldsymbol{r}_1$ as

$$\left[ h(\boldsymbol{r}_2) + \int \frac{|\phi_a(\boldsymbol{r}_1)|^2}{|\boldsymbol{r}_1 - \boldsymbol{r}_2|} \mathrm{d}\boldsymbol{r}_1 \right] \phi_b(\boldsymbol{r}_2) = \epsilon_b^H \phi_b(\boldsymbol{r}_2), \tag{4.27}$$

with

$$\epsilon_b^H = E - \epsilon_a, \tag{4.28}$$

where $\epsilon_a$ is the energy of the first electron.

The integration in Eq. (4.25) can be rewritten in term of electron density, $n(\boldsymbol{r}_2) = |\phi_a(\boldsymbol{r}_2)|^2 + |\phi_b(\boldsymbol{r}_2)|^2$, as

$$\int \frac{|\phi_b(\boldsymbol{r}_2)|^2}{|\boldsymbol{r}_1 - \boldsymbol{r}_2|} \mathrm{d}\boldsymbol{r}_2 = \underbrace{\int \frac{n(\boldsymbol{r}_2)}{|\boldsymbol{r}_1 - \boldsymbol{r}_2|} \mathrm{d}\boldsymbol{r}_2}_{\mathcal{V}_H(\boldsymbol{r}_1)} - \underbrace{\int \frac{|\phi_a(\boldsymbol{r}_2)|^2}{|\boldsymbol{r}_1 - \boldsymbol{r}_2|} \mathrm{d}\boldsymbol{r}_2}_{\mathcal{V}_H^{\mathrm{sic}}(\boldsymbol{r}_1)}. \tag{4.29}$$

The first term $\mathcal{V}_H$ is called the **Hartree potential** [Hartree (1928)], which describes the Coulomb repulsion potential as a function of $\boldsymbol{r}_1$. The second term $\mathcal{V}_H^{\mathrm{sic}}(\boldsymbol{r}_1)$ is called the *self-interaction correction* of the Hartree potential, which takes into account that the electron at the state $\phi_a$ shall not interact with itself, but with the remaining electrons. When the system has many electrons ($\sim 10^{23}$), $\mathcal{V}_H^{\mathrm{sic}}$ can be neglected since $\mathcal{V}_H^{\mathrm{sic}}$ might contribute negligibly small to the total energy [Parr and Yang (1989)].

From Eq. (4.25), we can write the energy as a functional of the wavefunctions as

$$\begin{aligned} \epsilon_a^H &= \int \phi_a^*(\boldsymbol{r}_1) \left[ h(\boldsymbol{r}_1) + \int \frac{|\phi_b(\boldsymbol{r}_2)|^2}{|\boldsymbol{r}_1 - \boldsymbol{r}_2|} \mathrm{d}\boldsymbol{r}_2 \right] \phi_a(\boldsymbol{r}_1) \mathrm{d}\boldsymbol{r}_1 \\ &= \epsilon_a + \iint \frac{|\phi_a(\boldsymbol{r}_1)|^2 |\phi_b(\boldsymbol{r}_2)|^2}{|\boldsymbol{r}_1 - \boldsymbol{r}_2|} \mathrm{d}\boldsymbol{r}_1 \mathrm{d}\boldsymbol{r}_2. \end{aligned} \tag{4.30}$$

By substituting Eq. (4.26) into Eq. (4.30), the total energy $E$ is given by

$$E = \epsilon_a + \epsilon_b + \iint \frac{|\phi_a(\boldsymbol{r}_1)|^2 |\phi_b(\boldsymbol{r}_2)|^2}{|\boldsymbol{r}_1 - \boldsymbol{r}_2|} \mathrm{d}\boldsymbol{r}_1 \mathrm{d}\boldsymbol{r}_2. \tag{4.31}$$

Now the total energy $E$ is not equal neither to $\epsilon_a + \epsilon_b$ nor to $\epsilon_a^H + \epsilon_b^H$. This is because the positive Coulomb interaction between the two electrons is included twice in $\epsilon_a^H + \epsilon_b^H$ (Eqs. (4.25) and (4.27)). Therefore, only one term from the inter-electron interaction is added to $\epsilon_a + \epsilon_b$ in the expression for $E$ as shown in Eq. (4.31).

## 4.5 Self-consistent field

A difficulty in solving the single-particle Schrödinger equation is that the Hartree potential $\mathcal{V}_H$ in Eq. (4.29) requires the value of the state $\phi$, which is not known before we solve the single-particle Schrödinger equation in Eq. (4.25). This is called a *self-consistent problem*.

The Hartree potential can be expressed in a differential form of the Maxwell equation as $\nabla \cdot \boldsymbol{E} = 4\pi n(\boldsymbol{r})$, where $n(\boldsymbol{r})$ is the electron density at $\boldsymbol{r}$ and $\boldsymbol{E} = -\nabla \mathcal{V}_H(\boldsymbol{r})$, where $\mathcal{V}_H(\boldsymbol{r})$ is generally called the electrostatic potential. Combining the two equations, we get the **Possion equation** [Jackson (1999)]:

$$\nabla^2 \mathcal{V}_H(\boldsymbol{r}) = -4\pi n(\boldsymbol{r}). \tag{4.32}$$

The solution of the Poisson equation is given as follows:

$$\mathcal{V}_H(\boldsymbol{r}) = \int \frac{n(\boldsymbol{r}')}{|\boldsymbol{r} - \boldsymbol{r}'|} \mathrm{d}\boldsymbol{r}'. \tag{4.33}$$

Now let us introduce a **self-consistent field** (SCF) method that can be applied to solve the single-particle Schrödinger equation by using the Poisson equation. As shown in Fig. 4.4, first, guessing an initial electron density $n(\boldsymbol{r})$ for the solution, we put $n(\boldsymbol{r})$ into Eq. (4.33) to get the Hartree potential $\mathcal{V}_H(\boldsymbol{r})$. Then we put the $\mathcal{V}_H$ into the single-particle Schrödinger equation to get eigenstate $\phi(\boldsymbol{r})$ to obtain the new $n(\boldsymbol{r}) = \sum |\phi(\boldsymbol{r})|^2$, where the sum runs over the occupied states. We repeat the procedure until $n(\boldsymbol{r})$ does not change

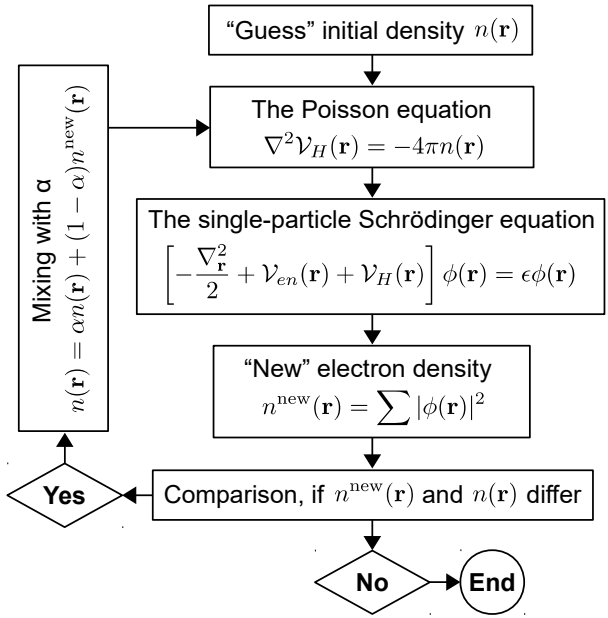


**Figure 4.4** Flow-chart of the self-consistent field method for the solution of the single-particle Schrödinger equation with the Hartree potential $\mathcal{V}_H$.

appreciably, that is, the convergence of the solution. This procedure is called the SCF method. Here, we construct the next guess of $n(\boldsymbol{r})$ by mixing $n^{\mathrm{new}}(\boldsymbol{r})$ with the previous $n(\boldsymbol{r})$. If the mixing parameter $\alpha$ $(0 < \alpha < 1)$ is large, we might find oscillating behavior of $n(\boldsymbol{r})$. We note that the self-interaction term $\mathcal{V}_H^{\mathrm{sic}}$ in Eq. (4.29) is neglected in this procedure.

Let us consider the example of silicon in Sec. 4.2. By using the SCF method, the $3N$-dimensional configuration space of the Schrödinger equation is reduced to an $N$-single-particle Schrödinger equations of three dimensions. In this case, the characteristic size of the arrays needed for describing the wavefunctions becomes $28 \times 5000^3$ for silicon with 28 electrons in a unit cell, instead of $5000^{84}$ in Sec. 4.2. These arrays correspond approximately to a few GB of computer storage.

---

❑ **Hartree potential for helium:** In order to solve the Poisson equation for a helium atom, it is more convenient to use spherical

coordinates $(r, \theta, \varphi)$ rather than Cartesian coordinates $\boldsymbol{r} = (x, y, z)$. These are related to each other by $r = |\boldsymbol{r}|$, $x = r\cos\theta\sin\varphi$, $y = r\sin\theta\cos\varphi$, and $z = r\cos\theta$. Referring back to Eq. (4.33), the Laplacian $\nabla^2$ is expressed in spherical coordinates as follows:

$$\begin{aligned}\nabla^2 =& \frac{1}{r^2}\frac{\partial}{\partial r}\left(r^2\frac{\partial}{\partial r}\right) \\ &+ \frac{1}{r^2\sin\theta}\frac{\partial}{\partial\theta}\left(\sin\theta\frac{\partial}{\partial\theta}\right) + \frac{1}{r^2\sin^2\theta}\frac{\partial^2}{\partial\varphi^2}.\end{aligned} \tag{4.34}$$

When we assume that the Hartree potential $\mathcal{V}_H$ has a spherical symmetry, the derivatives of $\mathcal{V}_H$ with respect to $\theta$ and $\varphi$ become zero. Then the Poisson equation is given by a differential equation on $r$ as follows:

$$\frac{1}{r^2}\frac{\partial}{\partial r}\left(r^2\frac{\partial\mathcal{V}_H}{\partial r}\right) = -4\pi n(r). \tag{4.35}$$

Integrating Eq. (4.35) on $r$ we obtain

$$\mathcal{V}_H(r) = -4\pi\int_0^r \frac{1}{r'^2}\int_0^{r'} r''^2 n(r'')\mathrm{d}r'\mathrm{d}r'' - \frac{C}{r}. \tag{4.36}$$

It is noted that $C/r$ in Eq. (4.36) is a solution of Eq. (4.35) for any value of $C$. Then by substituting the electron density of the helium atom in Eq. (4.21) into Eq. (4.36) and using

$$\int_0^x \frac{1}{x'^2}\int_0^{x'} x''^2\exp(x'')\mathrm{d}x'\mathrm{d}x'' = (1-\frac{2}{x})\exp(x), \tag{4.37}$$

Eq. (4.36) becomes

$$\mathcal{V}_H(r) = -2\left(Z+\frac{1}{r}\right)\exp(-2Zr) - \frac{C}{r}. \tag{4.38}$$

At the limit of $r\to\infty$, from Eq. (4.33), we have $\mathcal{V}_H(r) \xrightarrow{r\to\infty} \frac{1}{r}\int n(r')\mathrm{d}r' = \frac{Z}{r}$. Applying this boundary condition for Eq. (4.38), we obtain $C = -Z$, and Eq. (4.38) can be rewritten for the helium atom

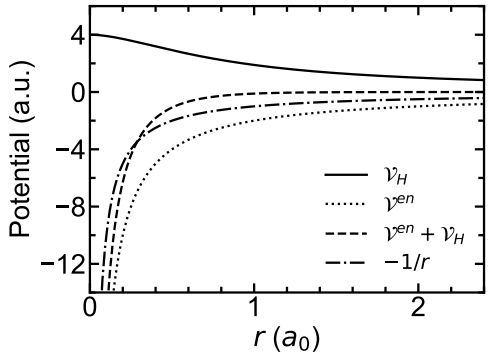


**Figure 4.5** The Hartree potential $\mathcal{V}_H(r)$ (solid line), the Coulomb attraction between electrons and nuclei $\mathcal{V}_{en}$ (dotted line), and the total potential $\mathcal{V}_{en} + \mathcal{V}_H(r)$ (dashed line) of helium atom are plotted in atomic unit as functions of $r$.

as

$$\mathcal{V}_H(r) = -2\left(Z + \frac{1}{r}\right)\exp(-2Zr) + \frac{Z}{r}. \tag{4.39}$$

In Fig. 4.5, we show $\mathcal{V}_H(r)$ with $Z = 2$ (solid line), the Coulomb attractive interaction between electrons and nuclei $\mathcal{V}_{en}(r) = -2/r$ (dotted line), and the total potential $\mathcal{V}_{en}(r) + \mathcal{V}_H(r)$ (dashed line) of the helium atom as functions of $r$. When $r$ increases, the total potential decays exponentially. This trend is incorrect since the total potential of the helium atom decays as $-1/r$ at a large distance [Umrigar and Gonze (1994)]. This is because we neglect some interactions, which will be introduced in the next section.

## 4.6 Exchange potential

In Sec. 4.5, we show that the Schrödinger equation can be solved by using the Hartree approximation and the SCF method. In the Hartree approximation, the Coulomb repulsion between two electrons in the system is approximated by the Hartree potential, in which each individual electron moves independently of each other, only

feeling the averaged electrostatic potential by the other electrons. However, in 1930, Slater pointed out that the Hartree method did not take into account the Pauli exclusion principle for many electrons [Slater (1930b)]. That is, if two electrons have parallel spins to each other, they are not allowed to occupy the same states at the same time. Since the two electrons can not be close to each other by the Pauli principle, the Coulomb repulsion can not be very large. In order to take account of the Pauli exclusion principle, we introduce an **exchange potential**, which is an attractive Coulomb interaction between two electrons with parallel spins. We note that the Hartree potential is a repulsive Coulomb interaction between an electron and electron density of the other electrons ($\mathcal{V}_H > 0$, see Fig. 4.5). Exchange potential is a correction term to $\mathcal{V}_H$, which is over-estimated compared with the real case.

By using the Slater determinant in Eq. (4.14), Eq. (4.8) can be rewritten as

$$\begin{aligned}\left[h(\boldsymbol{r}_1) + h(\boldsymbol{r}_2) + \frac{1}{|\boldsymbol{r}_1 - \boldsymbol{r}_2|}\right][\phi_a(\boldsymbol{r}_1)\phi_b(\boldsymbol{r}_2) - \phi_b(\boldsymbol{r}_1)\phi_a(\boldsymbol{r}_2)] \\ = E[\phi_a(\boldsymbol{r}_1)\phi_b(\boldsymbol{r}_2) - \phi_b(\boldsymbol{r}_1)\phi_a(\boldsymbol{r}_2)].\end{aligned} \tag{4.40}$$

By multiplying $\phi_b^*(\boldsymbol{r}_2)$ in Eq. (4.40) and integrating over $\boldsymbol{r}_2$ with the normalization and orthogonality conditions (Eqs. (4.17) and (4.18)), we obtain:

$$\begin{aligned}h(\boldsymbol{r}_1)\phi_a(\boldsymbol{r}_1) + \phi_a(\boldsymbol{r}_1)\int \frac{\phi_b^*(\boldsymbol{r}_2)\phi_b(\boldsymbol{r}_2)}{|\boldsymbol{r}_1 - \boldsymbol{r}_2|}\mathrm{d}\boldsymbol{r}_2 \\ - \int \frac{\phi_b^*(\boldsymbol{r}_2)\phi_b(\boldsymbol{r}_1)}{|\boldsymbol{r}_1 - \boldsymbol{r}_2|}\phi_a(\boldsymbol{r}_2)\mathrm{d}\boldsymbol{r}_2 = \epsilon_a^{HF}\phi_a(\boldsymbol{r}_1),\end{aligned} \tag{4.41}$$

where $\epsilon_a^{HF}$ is defined by

$$\epsilon_a^{HF} = E - \int \phi_b^*(\boldsymbol{r}_2)h(\boldsymbol{r}_2)\phi_b(\boldsymbol{r}_2)\mathrm{d}\boldsymbol{r}_2 = E - \epsilon_b. \tag{4.42}$$

By substituting Eq. (4.29) into Eq. (4.41), we obtain the single-particle Schrödinger equation for $\phi_a(\boldsymbol{r}_1)$ as

$$[h(\boldsymbol{r}_1) + \mathcal{V}_H(\boldsymbol{r}_1)]\,\phi_a(\boldsymbol{r}_1) - \int \frac{\gamma(\boldsymbol{r}_2, \boldsymbol{r}_1)}{|\boldsymbol{r}_1 - \boldsymbol{r}_2|}\phi_a(\boldsymbol{r}_2)\mathrm{d}\boldsymbol{r}_2 = \epsilon_a^{HF}\phi_a(\boldsymbol{r}_1), \quad (4.43)$$

where $\gamma(\boldsymbol{r}_2, \boldsymbol{r}_1)$ is defined as

$$\gamma(\boldsymbol{r}_2, \boldsymbol{r}_1) = \phi_a^*(\boldsymbol{r}_2)\phi_a(\boldsymbol{r}_1) + \phi_b^*(\boldsymbol{r}_2)\phi_b(\boldsymbol{r}_1). \quad (4.44)$$

The single-particle Schrödinger equation also can be written for $\phi_a(\boldsymbol{r}_2)$ as

$$[h(\boldsymbol{r}_2) + \mathcal{V}_H(\boldsymbol{r}_2)]\,\phi_b(\boldsymbol{r}_2) - \int \frac{\gamma(\boldsymbol{r}_1, \boldsymbol{r}_2)}{|\boldsymbol{r}_1 - \boldsymbol{r}_2|}\phi_b(\boldsymbol{r}_1)\mathrm{d}\boldsymbol{r}_1 = \epsilon_b^{HF}\phi_b(\boldsymbol{r}_2), \quad (4.45)$$

in which $\epsilon_b^{HF}$ is symmetrically given by

$$\epsilon_b^{HF} = E - \epsilon_a. \quad (4.46)$$

Eq. (4.43) or (4.45) is known as the **Hartree-Fock equation** [Fock (1930)], in which the exchange potential $\mathcal{V}_x$ in Eq. (4.43) is defined by

$$\mathcal{V}_x(\boldsymbol{r}_1, \boldsymbol{r}_2) = -\frac{\gamma(\boldsymbol{r}_2, \boldsymbol{r}_1)}{|\boldsymbol{r}_1 - \boldsymbol{r}_2|}. \quad (4.47)$$

$\mathcal{V}_x$ exists only for two electrons at $\boldsymbol{r}_1$ and $\boldsymbol{r}_2$, which have the same quantum state $\phi_a$ or $\phi_b$ including spin, i.e., the exchange potential is the effective Coulomb interaction between the electrons with parallel spins in the system. The origin of $\mathcal{V}_x$ is that two-electrons with the same spin can not exist at the same position ($\boldsymbol{r}_1 = \boldsymbol{r}_2$), in which $\mathcal{V}_H$ should be small by the restriction of the Pauli principle. By considering both $\mathcal{V}_H$ and $\mathcal{V}_x$ in Eq. (4.39), two electrons are interacted not only by their electronic charge but also by their spins. Therefore, the *quantum* behavior of electrons is included by $\mathcal{V}_x$ term in the Hartree-Fock equation. It is important to note that $\mathcal{V}_x$ is a *non-local* potential on $\boldsymbol{r}_1$ since it depends on an integration over the additional variable $\boldsymbol{r}_2$. Therefore, the practical solution of the Hartree-Fock equation becomes more complicated and time-consuming.

Let us discuss the energy that is obtained by the Hartree-Fock equation. From Eq. (4.43), we can write the energy by integrating the wavefunctions as

$$\begin{aligned}\epsilon_a^{HF} =& \int \phi_a^*(\boldsymbol{r}_1)[h(\boldsymbol{r}_1) + \mathcal{V}_H(\boldsymbol{r}_1)]\phi_a(\boldsymbol{r}_1)\mathrm{d}\boldsymbol{r}_1 \\ &+ \iint \phi_a^*(\boldsymbol{r}_1)\frac{\gamma(\boldsymbol{r}_2,\boldsymbol{r}_1)}{|\boldsymbol{r}_1-\boldsymbol{r}_2|}\phi_a(\boldsymbol{r}_2)\mathrm{d}\boldsymbol{r}_1\boldsymbol{r}_2 \\ =& \epsilon_a + J - K,\end{aligned} \tag{4.48}$$

where $J$ and $K$ are called the **Coulomb and exchange integrals**, respectively, which are given by

$$J = \iint \frac{|\phi_a(\boldsymbol{r}_1)|^2|\phi_b(\boldsymbol{r}_2)|^2}{|\boldsymbol{r}_1-\boldsymbol{r}_2|}\mathrm{d}\boldsymbol{r}_1\mathrm{d}\boldsymbol{r}_2 \tag{4.49}$$

and

$$K = \iint \frac{\phi_a^*(\boldsymbol{r}_1)\phi_b(\boldsymbol{r}_1)\phi_b^*(\boldsymbol{r}_2)\phi_a(\boldsymbol{r}_2)}{|\boldsymbol{r}_1-\boldsymbol{r}_2|}\mathrm{d}\boldsymbol{r}_1\mathrm{d}\boldsymbol{r}_2. \tag{4.50}$$

$J$ represents the Coulomb repulsion between the electron at the state $\phi_a(\boldsymbol{r}_1)$ and the other electron at the state $\phi_b(\boldsymbol{r}_2)$. $K$ has a physical interpretation of the overestimate of the Coulomb interaction for two electrons in the case of the parallel spins. It means that with the parallel spins, the two electrons can not be close to each other by the Pauli exclusion principle. It is noted that both values of $J$ and $K$ are the positive values and $J \geq K$, as shown below [Roothaan (1951)]:

By substituting Eq. (4.46) into Eq. (4.48), the total electron energy $E$ in the Hartree-Fock approximation is expressed by

$$E = \epsilon_a + \epsilon_b + J - K. \tag{4.51}$$

On the other hand, from Eq. (4.40), the total electron energy can be obtained, too, as

$$\begin{aligned} E &= \iint \psi^*(\boldsymbol{r}_1,\boldsymbol{r}_2)[h(\boldsymbol{r}_1)+h(\boldsymbol{r}_2)]\psi(\boldsymbol{r}_1,\boldsymbol{r}_2)\mathrm{d}\boldsymbol{r}_1\mathrm{d}\boldsymbol{r}_2 \\ &\quad + \iint \psi^*(\boldsymbol{r}_1,\boldsymbol{r}_2)\frac{1}{|\boldsymbol{r}_1-\boldsymbol{r}_2|}\psi(\boldsymbol{r}_1,\boldsymbol{r}_2)\mathrm{d}\boldsymbol{r}_1\boldsymbol{r}_2 \\ &= \epsilon_a+\epsilon_b+\iint \frac{|\psi(\boldsymbol{r}_2,\boldsymbol{r}_1)|^2}{|\boldsymbol{r}_1-\boldsymbol{r}_2|}\mathrm{d}\boldsymbol{r}_1\boldsymbol{r}_2. \end{aligned} \tag{4.52}$$

By subtracting Eq. (4.52) from Eq. (4.51), we obtain:

$$J-K=\iint \frac{|\psi(\boldsymbol{r}_1,\boldsymbol{r}_2)|^2}{|\boldsymbol{r}_1-\boldsymbol{r}_2|}\mathrm{d}\boldsymbol{r}_1\mathrm{d}\boldsymbol{r}_2 \geq 0. \tag{4.53}$$

Therefore, $J \geq K$ and the total electron energy $E$ is always larger than the sum of the one-electron energies $(\epsilon_a+\epsilon_b)$ because of the net repulsion Coulomb interaction between two electrons.

---

❑ **Total energy of helium atom:** In the case of the helium atom, two electrons at the 1$s$ state $\phi$ must have different spin directions, up $\uparrow$ and down $\downarrow$ because of the Pauli principle. Let us consider the spin states of two electrons, respectively, as

$$\phi_\uparrow(\boldsymbol{r})=\phi(\boldsymbol{r})\begin{pmatrix}1\\0\end{pmatrix} \text{ and } \phi_\downarrow(\boldsymbol{r})=\phi(\boldsymbol{r})\begin{pmatrix}0\\1\end{pmatrix}, \tag{4.54}$$

where $\binom{1}{0}$ and $\binom{0}{1}$ correspond to up- and down-spin wavefunctions, respectively. From Eq. (4.54), we define the product of two spin-functions as follows:

$$\phi^*_\uparrow(\boldsymbol{r})\phi_\uparrow(\boldsymbol{r})=\phi^2(\boldsymbol{r})\begin{pmatrix}1&0\end{pmatrix}\begin{pmatrix}1\\0\end{pmatrix}=\phi^2(\boldsymbol{r}), \tag{4.55}$$

and

$$\phi^*_\uparrow(\boldsymbol{r})\phi_\downarrow(\boldsymbol{r})=\phi^2(\boldsymbol{r})\begin{pmatrix}1&0\end{pmatrix}\begin{pmatrix}0\\1\end{pmatrix}=0. \tag{4.56}$$

By substituting Eqs. (4.55) and (4.56) into Eqs. (4.49) and (4.50), respectively, we obtain:

$$J = \iint \frac{\phi_\uparrow^*(\boldsymbol{r})\phi_\uparrow(\boldsymbol{r})\phi_\downarrow^*(\boldsymbol{r}')\phi_\downarrow(\boldsymbol{r}')}{|\boldsymbol{r}-\boldsymbol{r}'|^2}\mathrm{d}\boldsymbol{r}\mathrm{d}\boldsymbol{r}' = \iint \frac{|\phi(\boldsymbol{r})|^2\,|\phi(\boldsymbol{r}')|^2}{|\boldsymbol{r}-\boldsymbol{r}'|^2}\mathrm{d}\boldsymbol{r}\mathrm{d}\boldsymbol{r}', \tag{4.57}$$

and

$$K = \iint \frac{\phi_\uparrow^*(\boldsymbol{r})\phi_\downarrow(\boldsymbol{r})\phi_\downarrow^*(\boldsymbol{r}')\phi_\uparrow(\boldsymbol{r}')}{|\boldsymbol{r}-\boldsymbol{r}'|^2}\mathrm{d}\boldsymbol{r}\mathrm{d}\boldsymbol{r}' = 0. \tag{4.58}$$

$K = 0$ is consistent with fact that the exchange potential is zero since there are no parallel spins. Since the electronic density is expressed as $n(\boldsymbol{r}') = |\phi_\uparrow(\boldsymbol{r}')|^2 + |\phi_\downarrow(\boldsymbol{r}')|^2 = 2|\phi(\boldsymbol{r}')|^2$, the Coulomb integral in Eq. (4.57) can be rewritten as

$$J = \frac{1}{2}\iint \frac{|\phi(\boldsymbol{r})|^2 n(\boldsymbol{r}')}{|\boldsymbol{r}-\boldsymbol{r}'|^2}\mathrm{d}\boldsymbol{r}\mathrm{d}\boldsymbol{r}' = \frac{1}{2}\int |\phi(\boldsymbol{r})|^2 \mathcal{V}_H(\boldsymbol{r})\mathrm{d}\boldsymbol{r}. \tag{4.59}$$

By substituting $J$ in Eq. (4.59) and $K = 0$ in Eq. (4.58) into Eq. (4.51), the total electron energy $E$ is expressed as

$$E = 2\epsilon + \frac{1}{2}\int |\phi(\boldsymbol{r})|^2 \mathcal{V}_H(\boldsymbol{r})\mathrm{d}\boldsymbol{r}. \tag{4.60}$$

In order to apply Eq. (4.60) for the helium atom, we define an *effective* atomic number $Z$, i.e., $\phi(\boldsymbol{r}, Z)$, which gives minimized $E$ when subject to the Hartree potential $\mathcal{V}_H(\boldsymbol{r})$. Eq. (4.60) can be obtained by the following steps:

- Step 1: Using a beginning value $Z = 2$, from Eq. (4.39), the Hartree potential $\mathcal{V}_H(\boldsymbol{r})$ is given by

$$\mathcal{V}_H(r) = -2\left(2 + \frac{1}{r}\right)\exp(-4r) + \frac{2}{r}. \tag{4.61}$$

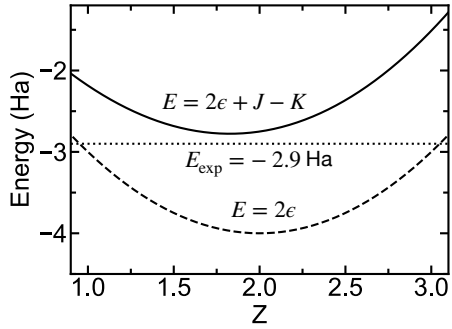


**Figure 4.6** Total electron energy of helium atom as a function of effective atomic number $Z$. $E = 2\epsilon$ and $E = 2\epsilon + J - K$ are corresponding to the cases of non-interacting electrons and Hartree-Fock approximation, respectively. Experimental value $E_{\text{exp}}$ of the helium atom is $-2.9$ Ha [Sucher (1958)].

- Step 2: By substituting Eq. (4.61) and $\phi(\boldsymbol{r}, Z) = \frac{Z^{3/2}}{\sqrt{\pi}} \exp(-Z|\boldsymbol{r}|)$ in Eq. (4.20) into Eq. (4.60), we obtain:

$$\begin{aligned} E &= \underbrace{Z^2 - 4Z}_{2\epsilon} + 2\pi \int r^2 |\phi(\boldsymbol{r}, Z)|^2 \mathcal{V}_H(r) \mathrm{d}r \\ &= Z^2 - 3Z + \frac{Z^3(Z+4)}{(Z+2)^3}. \end{aligned} \tag{4.62}$$

- Step 3: According to the variational principle,[6] we minimize $E$ with respect to the variational parameter $Z$, i.e., $\mathrm{d}E/\mathrm{d}Z = 0$ for $E$ in Eq. (4.62). We can obtain the effective atomic number $Z_{\text{eff}} = 1.826$ and the value of $E$ at $Z = Z_{\text{eff}}$ is about $-2.777$ Ha.

In Fig. 4.6, we show the energies for the two cases of the non-interacting electrons, $E = 2\epsilon$, and the Hartree-Fock approximation, $E = 2\epsilon + J - K$, as functions of the effective atomic number $Z$. For $E = 2\epsilon$, the electrons feel a potential corresponding to the nucleus with a charge $Z = 2$, but it makes the error for $E$ as discussed in Sec. 4.3. For $E = 2\epsilon + J - K$, the electrons feel a potential with a reduced charge $Z = 1.826$. Eq. (4.60) can also be solved by the SCF method. This

[6] The variational principle states that the energy of any approximate wavefunction is higher than or equal to the energy of ground-state wavefunction. The lower the energy is the better the approximation to the ground state.

could be done by recalculating the Hartree potential with new state $\phi(\boldsymbol{r}, Z_{\text{eff}} = 1.826)$ in Step 1, then we recalculate Steps 2 and 3 until the value of $Z_{\text{eff}}$ does not change significantly. Finally, we can obtain the $E_{\text{eff}} = -2.85$ Ha, which is not too far from the exact value from the experiment about $-2.9$ Ha. Slater derived a formula to determine $Z_{\text{eff}}$ as $Z_{\text{eff}} = Z - S$, where $S$ is the shielding constant, which is known as **Slater's rule** [Slater (1930a)]. For the $1s$ state in the helium atom, $S = 0.3$ and $Z_{\text{eff}} = 1.7$, which is close to the result of the SCF method ($Z_{\text{eff}} = 1.826$).

## 4.7 Correlation potential

In Sec. 4.6, we show that due to the Pauli exclusion principle, the electrons with parallel spins have an exchange term of the Coulomb interaction $\mathcal{V}_x$. The two electrons with the parallel spin move to avoid each other because the electrons can not overlap. Avoiding picture should exist for the two electrons with anti-parallel spins because these electrons also move with keeping apart to lower the Coulomb repulsion. This behavior of the electrons with anti-parallel spins is missing in the Hartree approximation as well as in the Hartree-Fock approximation. A complete picture of the motion of an electron in a system is shown in Fig. 4.7. In general, the correlation interaction, $\mathcal{V}_c$, is defined by the remaining term that is missing in the Hartree-Fock method.[7] Thus, an **effective potential** in the single-particle Schrödinger equation is defined by

$$\mathcal{V}_{\text{eff}} = \mathcal{V}_{en} + \mathcal{V}_H + \mathcal{V}_{xc}, \tag{4.63}$$

where $\mathcal{V}_{xc} \equiv \mathcal{V}_x + \mathcal{V}_c$ is called the **exchange-correlation potential**.

Since $\mathcal{V}_H$ is obtained by the total electron density $n(\boldsymbol{r})$, it suggests that if $\mathcal{V}_{xc}$ can be expressed by a functional of $n(\boldsymbol{r})$, the single-particle Schrödinger equation can be written as

$$\left\{ -\frac{\nabla_{\boldsymbol{r}}^2}{2} + \mathcal{V}_{\text{eff}}[n(\boldsymbol{r})] \right\} \phi(\boldsymbol{r}) = \epsilon \phi(\boldsymbol{r}). \tag{4.64}$$

[7] The correlation interaction is defined in the field of the density-functional theory.

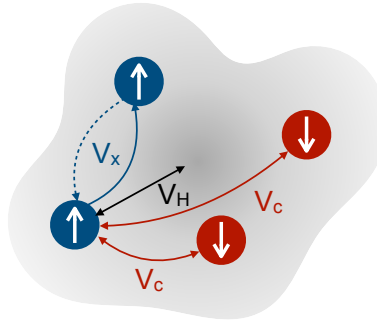


**Figure 4.7** The motion of an electron with up-spin in a system is affected by three interactions, including the Hartree $\mathcal{V}_H$, exchange $\mathcal{V}_x$, and correlation $\mathcal{V}_c$ potentials. $\mathcal{V}_H$ is the Coulomb interaction between one electron and the total charge density, which is generated by all electrons in the system. $\mathcal{V}_x$ arises due to the Pauli exclusion principle, in which the electrons with parallel spins can not exist at the same position at the same time. $\mathcal{V}_c$ arises due to the fact that the electrons with anti-parallel spins also keep apart to lower their mutual Coulomb repulsion.

When we know the value of $\mathcal{V}_{xc}[n(\boldsymbol{r})]$, Eq. (4.64) can be solved by using the SCF method as discussed in Sec. 4.5. However, we do not know the exact shape of $\mathcal{V}_{xc}[n(\boldsymbol{r})]$. Many people proposed the many functionals for $\mathcal{V}_{xc}[n(\boldsymbol{r})]$ over the past few decades. The efforts to develop the accurate approximations for $\mathcal{V}_{xc}[n(\boldsymbol{r})]$ led to a theory, the so-called density-functional theory (DFT). We will discuss these approximations in the next section.

## 4.8 Early DFT for free-electron gas

Let us consider how to obtain $\mathcal{V}_{xc}[n(\boldsymbol{r})]$ for a free-electron gas, where the contribution of ions is treated as a uniform-positive-charge background, which is called the Jellium model [Brack (1993)], as shown in Fig. 4.8. Since the potential is uniform, the electronic states are expressed by plane waves as (see Sec. 5.3)

$$\phi_{\boldsymbol{k},\sigma}(\boldsymbol{r}) = \frac{1}{\sqrt{V}} \exp(i\boldsymbol{k}\boldsymbol{r})\chi_\sigma, \tag{4.65}$$

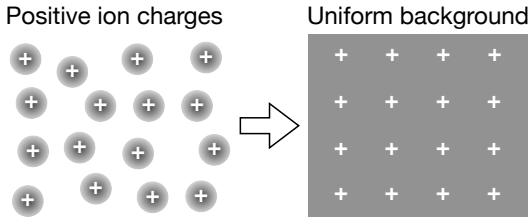


**Figure 4.8** A free-electron gas, where the contribution of nuclear ions is treated as a uniform-positive-charge background.

where $V$ is the volume of the system, $\boldsymbol{k}$ is the wavevector, and $\chi_\sigma$ is the spin function, in which $\binom{1}{0}$ for spin-up and $\binom{0}{1}$ for spin-down. Since the unit cell can not be defined by the uniform background, the value of $\boldsymbol{k}$ is taken not from the Brillouin zone but all the $\boldsymbol{k}$ space. Since $\phi_{\boldsymbol{k},\sigma}(\boldsymbol{r})$ is a one-electron wavefunction, $\phi_{\boldsymbol{k},\sigma}(\boldsymbol{r})$ can be a solution of the Hartree-Fock equation in Eq. (4.43). Moreover, in the free-electron gas, the electron density of the ground state is also a uniform-negative-charge background. Therefore, the electron density cancels the positive charge background, i.e., $\mathcal{V}_{en} + \mathcal{V}_H = 0$ and only the exchange term $\mathcal{V}_x$ survives in Eq. (4.43). Thus, the single-particle Schrödinger equation of a free-electron gas can be written as

$$-\frac{\nabla_{\boldsymbol{r}}}{2}\phi_{\boldsymbol{k},\sigma}(\boldsymbol{r}) + \underbrace{\int \mathcal{V}_x(\boldsymbol{r}',\boldsymbol{r})\phi_{\boldsymbol{k},\sigma}(\boldsymbol{r}')\mathrm{d}\boldsymbol{r}'}_{I_x} = \epsilon_{\boldsymbol{k}}\phi_{\boldsymbol{k},\sigma}(\boldsymbol{r}), \tag{4.66}$$

where the integral $I_x$ is given by

$$\begin{aligned} I_x &= -\sum_{\sigma'}\sum_{\boldsymbol{k}'}\int \frac{\phi^*_{\boldsymbol{k}',\sigma'}(\boldsymbol{r}')\phi_{\boldsymbol{k}',\sigma'}(\boldsymbol{r})}{|\boldsymbol{r}-\boldsymbol{r}'|}\phi_{\boldsymbol{k},\sigma}(\boldsymbol{r}')\mathrm{d}\boldsymbol{r}' \\ &= -\sum_{\sigma'}\sum_{\boldsymbol{k}'}\phi_{\boldsymbol{k}',\sigma'}(\boldsymbol{r})\int \frac{\phi^*_{\boldsymbol{k}',\sigma'}(\boldsymbol{r}')\phi_{\boldsymbol{k},\sigma}(\boldsymbol{r}')}{|\boldsymbol{r}-\boldsymbol{r}'|}\mathrm{d}\boldsymbol{r}'. \end{aligned} \tag{4.67}$$

By substituting the electronic states in Eq. (4.65) into Eq. (4.67), we obtain:

$$\begin{aligned} I_x &= -\sum_{\boldsymbol{k}'} \frac{1}{V^{3/2}} \exp(i\boldsymbol{k}'\boldsymbol{r})\chi_\sigma \int \frac{\exp\big(-i(\boldsymbol{k}'-\boldsymbol{k})\boldsymbol{r}'\big)}{|\boldsymbol{r}-\boldsymbol{r}'|}\mathrm{d}\boldsymbol{r}' \\ &= \left[-\sum_{\boldsymbol{k}'} \frac{1}{V} \int \frac{\exp\big(-i(\boldsymbol{k}'-\boldsymbol{k})(\boldsymbol{r}'-\boldsymbol{r})\big)}{|\boldsymbol{r}-\boldsymbol{r}'|}\mathrm{d}\boldsymbol{r}'\right] \phi_{\boldsymbol{k},\sigma}(\boldsymbol{r}) \\ &= \left[-\sum_{\boldsymbol{k}'} f(\boldsymbol{k}'-\boldsymbol{k})\right] \phi_{\boldsymbol{k},\sigma}(\boldsymbol{r}), \end{aligned} \tag{4.68}$$

where the function $f$ is defined as

$$f(\boldsymbol{q}) = \frac{1}{V}\int \frac{\exp(-i\boldsymbol{q}\boldsymbol{x})}{|\boldsymbol{x}|}\mathrm{d}\boldsymbol{x} = \frac{1}{V}\frac{4\pi}{\boldsymbol{q}^2}, \tag{4.69}$$

with $\boldsymbol{q} = \boldsymbol{k}' - \boldsymbol{k}$ and $\boldsymbol{x} = \boldsymbol{r}' - \boldsymbol{r}$. By substituting Eq. (4.69) into Eq. (4.68), we obtain:

$$\begin{aligned} I_x &= \left[-\frac{1}{V}\sum_{\boldsymbol{k}'} \frac{4\pi}{|\boldsymbol{k}'-\boldsymbol{k}|^2}\right] \phi_{\boldsymbol{k},\sigma}(\boldsymbol{r}) \\ &= \left[-\frac{1}{(2\pi)^3}\int_0^{k_F} \frac{4\pi}{|\boldsymbol{k}'-\boldsymbol{k}|^2}\mathrm{d}\boldsymbol{k}'\right] \phi_{\boldsymbol{k},\sigma}(\boldsymbol{r}) \\ &= -\frac{k_F}{\pi} F\left(\frac{k}{k_F}\right) \phi_{\boldsymbol{k},\sigma}(\boldsymbol{r}), \end{aligned} \tag{4.70}$$

where $k = |\boldsymbol{k}|$, $k_F$ is the Fermi wavevector, and $F$ is called the **Lindhard function**:

$$F(x) = 1 + \frac{1-x^2}{2x}\ln\left|\frac{1+x}{1-x}\right|, \text{ with } x = \frac{k}{k_F}. \tag{4.71}$$

The function $F(x)$ is shown in Fig. 4.9. $F(x)$ monotonically decreases from 2 at $x = 0$ (or $k = 0$) to 1 at $x = 1$ (or $k = k_F$).

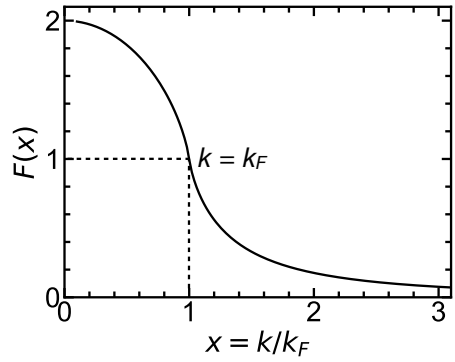


**Figure 4.9** The Lindhard function $F(x)$ is plotted as a function of the dimensionless $x = k/k_F$.

By substituting Eq. (4.70) into Eq. (4.66), Eq. (4.66) can be rewritten as

$$\left[-\frac{\nabla_{\boldsymbol{r}}}{2} - \frac{k_F}{\pi} F\left(\frac{k}{k_F}\right)\right] \phi_{\boldsymbol{k},\sigma}(\boldsymbol{r}) = \epsilon_{\boldsymbol{k}} \phi_{\boldsymbol{k},\sigma}(\boldsymbol{r}). \tag{4.72}$$

Then we can obtain the energy as a function of wavevector $\boldsymbol{k}$ as

$$\epsilon_{\boldsymbol{k},\sigma} = \frac{k^2}{2} - \frac{k_F}{\pi} F\left(\frac{k}{k_F}\right). \tag{4.73}$$

By taking the sum of all occupied states, we obtain the total energy as

$$\begin{aligned} E &= \sum_{\sigma} \sum_{|\boldsymbol{k}| < k_F} \frac{k^2}{2} - \frac{1}{2} \sum_{\sigma} \sum_{|\boldsymbol{k}| < k_F} \frac{k_F}{\pi} F\left(\frac{k}{k_F}\right) \\ &= \frac{2V}{(2\pi)^3} \int_0^{k_F} \frac{k^2}{2} \mathrm{d}\boldsymbol{k} - \frac{k_F}{\pi} \frac{V}{(2\pi)^3} \int_0^{k_F} F\left(\frac{k}{k_F}\right) \mathrm{d}\boldsymbol{k} \\ &= \frac{V}{4\pi^3} 4\pi \int_0^{k_F} \frac{k^4}{2} \mathrm{d}k - \frac{k_F V}{8\pi^4} 4\pi \int_0^{k_F} k^2 F\left(\frac{k}{k_F}\right) \mathrm{d}k \\ &= \frac{V}{10\pi^2} k_F^5 - \frac{V}{2\pi^3} k_F^4 \underbrace{\int_0^1 x^2 F(x) \mathrm{d}x}_{=1/2} \\ &= \frac{V}{10\pi^2} k_F^5 - \frac{V}{4\pi^3} k_F^4, \end{aligned} \tag{4.74}$$

with the factor of 1/2 in the second term of the right-hand side in the first line of Eq. (4.74) is needed to compensate for double counting of the exchange interaction.

For the free-electron gas, the number of electrons $N_e$ is equal to the number of occupied states in the systems:

$$N_e = \sum_{\sigma}\sum_{\boldsymbol{k}} = 2V\int_0^{k_F}\frac{\mathrm{d}\boldsymbol{k}}{(2\pi)^3} = \frac{V}{\pi^2}\int_0^{k_F}k^2\mathrm{d}k = V\frac{k_F^3}{3\pi^2}. \quad (4.75)$$

Therefore, the electron density $n$ is expressed by

$$n = \frac{N_e}{V} = \frac{k_F^3}{3\pi^2}. \quad (4.76)$$

By substituting Eqs. (4.75) and (4.76) into Eq. (4.74), the total energy per electron is expressed by

$$\frac{E}{N_e} = C_1 n^{2/3} + C_2 n^{1/3}, \quad (4.77)$$

where $C_1$ and $C_2$ are constants given by

$$C_1 = \frac{3}{10}(3\pi^2)^{2/3} = 2.871 \text{ and } C_2 = -\frac{3}{4}\left(\frac{3}{\pi}\right)^{1/3} = -0.738. \quad (4.78)$$

The first term ($C_1 n^{2/3}$) in Eq. (4.77) represents the kinetic energy, and the second term ($C_2 n^{1/3}$) represents the effective electron-electron interaction due to exchange potential. We can see that the exchange potential reduces the total energy of the system from the kinetic energy.

For a system with the free electron gas, $n$ is a constant. However, for a system with the non-uniform-electron charge, $n$ becomes a function of $\boldsymbol{r}$. Slater [Slater (1951)] introduced the exchange potential as a function of $n(\boldsymbol{r})$ as

$$\mathcal{V}_x[n(\boldsymbol{r})] = 2C_2 n^{1/3}(\boldsymbol{r}) = -\frac{3}{2}\left(\frac{3}{\pi}\right)^{1/3} n^{1/3}(\boldsymbol{r}), \quad (4.79)$$

where an extra factor of 2 is introduced to account in Eq. (4.79) because the $\mathcal{V}_x$ term in the single-particle equation (Eq. (4.64)) is

twice as large as the corresponding term in the total energy per particle (Eq. (4.77)).

For an approximation to include the correlation effects, Slater and Johnson [Slater and Johnson (1972)] introduced a *"fudge factor"* $\alpha$ in Eq. (4.79) as

$$\mathcal{V}_{xc}[n(\boldsymbol{r})] = 2\alpha C_2 n^{1/3}(\boldsymbol{r}), \tag{4.80}$$

where $\alpha$ usually taken in the range $2/3 < \alpha < 1$. For example, $\alpha = 0.772$ and 0.978 [Schwarz (1972)] for He and H atoms, respectively. Eq. (4.80) is called the $\boldsymbol{X\alpha}$ **potential**.

## 4.9 Thomas-Fermi-Dirac theory

In Sec. 4.8, we consider a free-electron gas with a uniform-positive background. However, the ions are not represented by a uniform-positive background in the real materials. The Thomas-Fermi-Dirac theory gives a first approximation to calculate the total energy of non-uniform systems. It is important to note that both papers [Thomas (1927), Fermi (1928)] published by Thomas and Fermi in 1927 and 1928, respectively, before the development of the Hartree-Fock theory in 1930. Although Thomas and Fermi neglected exchange and correction potentials, the approximation was extended by Dirac [Dirac (1930)] in 1930 based on the Hartree-Fock theory.

Let us consider an atom with $N_e$ electrons, and thus the atomic number is $Z = N_e$. We assume that the presence of the non-uniform-positive charge does not change the Hartree-Fock results significantly (in Sec. 4.8) for kinetic and exchange energies of the uniform background. In this case, the total energy per atom in Eq. (4.77) is modified by adding two terms as follows:

$$\frac{E}{N_e} = C_1 n^{2/3} + C_2 n^{1/3} - \frac{Z}{|\boldsymbol{r}|} + \frac{1}{2}\int \frac{n(\boldsymbol{r}')}{|\boldsymbol{r} - \boldsymbol{r}'|}\mathrm{d}\boldsymbol{r}', \tag{4.81}$$

where $Z/|\boldsymbol{r}|$ is the external potential that each electron feels the presence of the ions and the last term is the Coulomb repulsion between an electron at position $\boldsymbol{r}$ and all other electrons at $\boldsymbol{r}'$, which is expressed by the density $n(\boldsymbol{r}')$. The factor of 1/2 of the last term

is given by avoiding the double-counting of the Coulomb interaction. For the non-uniform systems, $N_e$ is defined by

$$N_e = \int n(\boldsymbol{r}) \mathrm{d}\boldsymbol{r}. \tag{4.82}$$

By substituting Eq. (4.82) into Eq. (4.81), the total energy of the system is expressed as

$$\begin{aligned} E[n(\boldsymbol{r})] = C_1 \int n^{5/3}(\boldsymbol{r}) \mathrm{d}\boldsymbol{r} + C_2 \int n^{4/3}(\boldsymbol{r}) \mathrm{d}\boldsymbol{r} \\ - Z \int \frac{n(\boldsymbol{r})}{|\boldsymbol{r}|} \mathrm{d}\boldsymbol{r} + \frac{1}{2} \iint \frac{n(\boldsymbol{r}) n(\boldsymbol{r}')}{|\boldsymbol{r} - \boldsymbol{r}'|} \mathrm{d}\boldsymbol{r}' \mathrm{d}\boldsymbol{r}, \end{aligned} \tag{4.83}$$

where the first and second terms of the right-hand side are the kinetic and exchange energies of the free-electron gas, respectively, the third term is the Coulomb attraction between the ions and the electron density, and the last term describes Coulomb repulsion between the electrons. $n(\boldsymbol{r})$ for the ground-state and the total energy of the system can be obtained by minimizing the energy functional $E[n(\boldsymbol{r})]$. Although the Thomas-Fermi-Dirac approximation is not accurate good-enough compared with the present electronic structure calculation, the approach shows a prototype expression of the DFT, in which $n(\boldsymbol{r})$ is a crucial physical quantity to calculate the ground-state properties of a many-electron system.

## 4.10 DFT: Hohenberg-Kohn-Sham

The DFT is established by two papers by Hohenberg and Kohn in 1964 [Hohenberg and Kohn (1964)] and Kohn and Sham [Kohn and Sham (1965)] in 1965. The original formulation discussed in the first paper of Hohenberg and Kohn, which is known as **the Hohenberg-Kohn theorem**. The second paper of Kohn and Sham developed a method to apply the Hohenberg-Kohn theorem, which is referred to as **the Kohn-Sham equation**.

### 4.10.1 Hohenberg-Kohn theorem

**Theorem:** There is a one-to-one correspondence between an external potential $\mathcal{V}_{en}(\boldsymbol{r})$ and an electron density $n(\boldsymbol{r})$ [Hohenberg and Kohn (1964)].

*Proof:* To prove the theorem, we suppose that two different external potentials, $\mathcal{V}_{en}(\boldsymbol{r})$ and $\mathcal{V}'_{en}(\boldsymbol{r})$, give the same electron density $n(\boldsymbol{r})$. We will show that this situation is not possible. Let us consider the two Hamiltonians $\mathcal{H}$ and $\mathcal{H}'$, which contain $\mathcal{V}_{en}$ and $\mathcal{V}'_{en}$, respectively, as follows:

$$\mathcal{H} = \mathcal{F} + \mathcal{V}_{en} \text{ and } \mathcal{H}' = \mathcal{F} + \mathcal{V}'_{en}, \tag{4.84}$$

where $\mathcal{F}$ includes all the terms in the Hamiltonian except for the external potential. That means that $\mathcal{F}$ contains the kinetic energy and electron-electron interaction terms. Therefore, $\mathcal{F}$ has the same shape for all $N_e$-electrons systems with any external potentials.

The total energies of the ground states of the Hamiltonians is given by

$$E = \langle\psi|\mathcal{H}|\psi\rangle \text{ and } E' = \langle\psi'|\mathcal{H}'|\psi'\rangle, \tag{4.85}$$

where $\psi$ and $\psi'$ are the wavefunctions of the ground states of $\mathcal{H}$ and $\mathcal{H}'$, respectively. Here we can say that $E \neq E'$ and $\psi \neq \psi'$ because the potentials are not the same. According to the variational principle, we have:

$$\begin{aligned} E < \langle\psi'|\mathcal{H}|\psi'\rangle &= \langle\psi'|\mathcal{H}' - \mathcal{V}'_{en} + \mathcal{V}_{en}|\psi'\rangle \\ &= E' + \langle\psi'|\mathcal{V}_{en} - \mathcal{V}'_{en}|\psi'\rangle, \end{aligned} \tag{4.86}$$

and

$$\begin{aligned} E' < \langle\psi|\mathcal{H}'|\psi\rangle &= \langle\psi|\mathcal{H} - \mathcal{V}_{en} + \mathcal{V}'_{en}|\psi\rangle \\ &= E - \langle\psi|\mathcal{V}_{en} - \mathcal{V}'_{en}|\psi\rangle. \end{aligned} \tag{4.87}$$

By adding Eqs. (4.86) and (4.87), we obtain:

$$(E + E') < (E + E') + \langle \psi' | \mathcal{V}_{en} - \mathcal{V}'_{en} | \psi' \rangle - \langle \psi | \mathcal{V}_{en} - \mathcal{V}'_{en} | \psi \rangle. \quad (4.88)$$

If the both $\mathcal{V}_{en}$ and $\mathcal{V}'_{en}$ gave the same electron density $n(\boldsymbol{r})$, the two terms on the right-hand side of Eq. (4.88) would be expressed by

$$\langle \psi' | \mathcal{V}_{en} - \mathcal{V}'_{en} | \psi' \rangle = \int [\mathcal{V}_{en}(\boldsymbol{r}) - \mathcal{V}'_{en}(\boldsymbol{r})]\, n(\boldsymbol{r}) \mathrm{d}\boldsymbol{r} \quad (4.89)$$

and

$$\langle \psi | \mathcal{V}_{en} - \mathcal{V}'_{en} | \psi \rangle = \int [\mathcal{V}_{en}(\boldsymbol{r}) - \mathcal{V}'_{en}(\boldsymbol{r})]\, n(\boldsymbol{r}) \mathrm{d}\boldsymbol{r}. \quad (4.90)$$

Eqs. (4.88), (4.89), and (4.90) lead to the contradictory relation $E + E' < E + E'$. Therefore, our assumption that $n(\boldsymbol{r})$ is the same with the different external potentials is not correct. This proves the Hohenberg-Kohn theorem.

**Corollary 1:** *The electron density $n(\boldsymbol{r})$ uniquely specifies the external potential $\mathcal{V}_{en}(\boldsymbol{r})$ and hence the Hamiltonian $\mathcal{H}$.* Because the ground-state wavefunction $\psi$ is obtained by solving the Schrödinger equation for $\mathcal{H}$, $\psi$ must be a unique functional of $n(\boldsymbol{r})$. Therefore, we obtain the following equation:

$$\langle \psi | \mathcal{H} - \mathcal{V}_{en} | \psi \rangle = \langle \psi | \mathcal{F} | \psi \rangle = \mathcal{F}[n(\boldsymbol{r})], \quad (4.91)$$

which tells us that $\mathcal{F}$ must be a functional of $n(\boldsymbol{r})$.

We can also conclude that the total energy $E$ is a functional of $n(\boldsymbol{r})$, and $E$ is given by

$$E[n(\boldsymbol{r})] = \langle \psi | \mathcal{H} | \psi \rangle = \mathcal{F}[n(\boldsymbol{r})] + \int \mathcal{V}_{en}(\boldsymbol{r}) n(\boldsymbol{r}) \mathrm{d}\boldsymbol{r}. \quad (4.92)$$

According to the variational principle, we can deduce that for a given $\mathcal{V}_{en}(\boldsymbol{r})$, Eq. (4.92) gives the global minimum value for the correct electron density $n(\boldsymbol{r})$. This is because that for any other density $n'(\boldsymbol{r})$,

we get a larger $E[n'(\boldsymbol{r})]$:

$$\begin{aligned} E[n'(\boldsymbol{r})] &= \mathcal{F}\big(n'(\boldsymbol{r})\big) + \int \mathcal{V}_{en}(\boldsymbol{r}) n'(\boldsymbol{r}) \mathrm{d}\boldsymbol{r} \\ &= \langle \psi' | \mathcal{H} | \psi' \rangle > \langle \psi | \mathcal{H} | \psi \rangle = E[n(\boldsymbol{r})]. \end{aligned} \tag{4.93}$$

**Corollary 2:** *If the functional $\mathcal{F}[n(\boldsymbol{r})]$ was known, then by minimizing the total energy in Eq.* (4.92)*, with respect to variations in the electron density $n(\boldsymbol{r})$, the ground state of the electron density and the total energy are obtained.* Therefore, it is important to develop adequate approximations for the functional $\mathcal{F}[n(\boldsymbol{r})]$ that will be discussed in Sec. 4.10.2. It is noted that the functional $\mathcal{F}[n(\boldsymbol{r})]$ determines only non-degenerated ground state, and thus the Hohenberg-Kohn theorem does not provide any guidance concerning excited states.

### 4.10.2 Kohn-Sham equation

In Sec. 4.10.1, we discussed the Hohenberg-Kohn theorem, which guarantees to give the ground-state energy. However, the theorem does not provide any analytical solution of the ground state since the functional $\mathcal{F}[n(\boldsymbol{r})]$ of Eq. (4.92) is not explicitly given. Kohn and Sham [Kohn and Sham (1965)] provided an explicit form for $\mathcal{F}[n(\boldsymbol{r})]$ and constructing the Schrödinger-like equation based on $\mathcal{F}[n(\boldsymbol{r})]$ with the SCF method (see Sec. 4.5), which allows the implementation to computer codes.

Let us write the functional $\mathcal{F}[n(\boldsymbol{r})]$ for the single-particle states $\phi_i(\boldsymbol{r})$ as

$$\mathcal{F}[n(\boldsymbol{r})] = \mathcal{K}_e[n(\boldsymbol{r})] + \frac{1}{2} \iint \frac{n(\boldsymbol{r}) n(\boldsymbol{r}')}{|\boldsymbol{r} - \boldsymbol{r}'|} \mathrm{d}\boldsymbol{r} \mathrm{d}\boldsymbol{r}' + \mathcal{E}_{xc}[n(\boldsymbol{r})], \tag{4.94}$$

where electron density $n(\boldsymbol{r})$ is given by Eq. (4.19) as

$$n(\boldsymbol{r}) = \sum_i |\phi_i(\boldsymbol{r})|^2, \tag{4.95}$$

$\mathcal{K}_e[n(\boldsymbol{r})]$ represents the kinetic energy of single-particle states:

$$\mathcal{K}_e[n(\boldsymbol{r})] = \sum_i \left\langle \phi_i \left| -\frac{\nabla_{\boldsymbol{r}}^2}{2} \right| \phi_i \right\rangle, \tag{4.96}$$

the second term of the right-hand side represents the electrostatic Coulomb repulsion between electrons, with a factor of 1/2 due to the double counting, and $\mathcal{E}_{xc}[n(\boldsymbol{r})]$ is the **exchange-correlation functional**, which contains all other contributions to the many-body energy of electrons. It is noted that $\mathcal{K}_e[n(\boldsymbol{r})]$ is not the exact kinetic energy of the many-body system of electrons; thus $\mathcal{E}_{xc}[n(\boldsymbol{r})]$ is needed to reproduce the correct functional $\mathcal{K}_e[n(\boldsymbol{r})]$.

When we apply the Hohenberg-Kohn theorem by substituting Eq. (4.94) into Eq. (4.92), the total energy is given by

$$\begin{aligned} E[n(\boldsymbol{r})] = \mathcal{K}_e[n(\boldsymbol{r})] + \frac{1}{2} \iint \frac{n(\boldsymbol{r})n(\boldsymbol{r}')}{|\boldsymbol{r} - \boldsymbol{r}'|} \mathrm{d}\boldsymbol{r}\mathrm{d}\boldsymbol{r}' \\ + \mathcal{E}_{xc}[n(\boldsymbol{r})] + \int \mathcal{V}_{en}(\boldsymbol{r})n(\boldsymbol{r})\mathrm{d}\boldsymbol{r}, \end{aligned} \tag{4.97}$$

that we need to minimize with respect to $n(\boldsymbol{r})$ in order to obtain the ground-state energy. We consider a variation in the electron density with the constraint that the total number of electrons does not change:

$$\int \delta n(\boldsymbol{r})\mathrm{d}\boldsymbol{r} = 0. \tag{4.98}$$

By using the Lagrange multiplier, $\epsilon_i$, with the constraint in Eq. (4.98), we obtain the **Kohn-Sham equation** as

$$\left\{ -\frac{\nabla_{\boldsymbol{r}}^2}{2} + \mathcal{V}_{\mathrm{eff}}[n(\boldsymbol{r})] \right\} \phi_i(\boldsymbol{r}) = \epsilon_i \phi_i(\boldsymbol{r}), \tag{4.99}$$

where the effective potential $\mathcal{V}_{\mathrm{eff}}[n(\boldsymbol{r})]$ is given by

$$\mathcal{V}_{\mathrm{eff}}[n(\boldsymbol{r})] = \mathcal{V}_{en}(\boldsymbol{r}) + \int \frac{n(\boldsymbol{r}')}{|\boldsymbol{r} - \boldsymbol{r}'|} \mathrm{d}\boldsymbol{r}' + \frac{\delta \mathcal{E}_{xc}[n(\boldsymbol{r})]}{\delta n(\boldsymbol{r})}, \tag{4.100}$$

where the first term $\mathcal{V}_{en}(\boldsymbol{r})$ is the external potential due to the ions, the second term is the Hartree potential $\mathcal{V}_H$ (see Eq. (4.33)) and the

last term is the variational functional derivative of the exchange-correlation interaction $\mathcal{E}_{xc}[n(\boldsymbol{r})]$. The last term in Eq. (4.100) is defined as the **exchange-correlation potential**:

$$\mathcal{V}_{xc}[n(\boldsymbol{r})] = \frac{\delta \mathcal{E}_{xc}[n(\boldsymbol{r})]}{\delta n(\boldsymbol{r})}. \tag{4.101}$$

By assuming that one knows $\mathcal{E}_{xc}[n(\boldsymbol{r})]$ or at least an adequate approximation, the Kohn-Sham equation in Eq. (4.99) can be solved by the SCF method (see Sec. 4.5) by the following steps:

1. Make an initial guess of $n^{\text{in}}(\boldsymbol{r})$.
2. Calculate $\mathcal{V}_{xc}[n^{\text{in}}(\boldsymbol{r})]$ in Eq. (4.101) and therewith $\mathcal{V}_{\text{eff}}[n^{\text{in}}(\boldsymbol{r})]$ in Eq. (4.100).
3. Solve Eq. (4.99) to get $\phi_i(\boldsymbol{r})$.
4. Calculate the new electron density $n^{\text{new}}(\boldsymbol{r})$ via Eq. (4.95).
5. If $n^{\text{new}}(\boldsymbol{r})$ is not equal to $n^{\text{in}}(\boldsymbol{r})$, we go back to step (1).
6. If $n^{\text{new}}(\boldsymbol{r})$ is equal to $n^{\text{in}}(\boldsymbol{r})$, we calculate the total energy by using Eq. (4.97).

The SCF calculation is an essential step in Quantum ESPRESSO. The run-time tutorial for the SCF calculation is shown in Sec. 3.1.1.

### 4.10.3 Relationship between Kohn-Sham energy and total energy

Multiplying the Kohn-Sham equation in Eq. (4.99) by $\phi_i^*(r)$ from the left and summing over all occupied states, we obtain **the Kohn-Sham energy** as

$$\sum_i \epsilon_i = \mathcal{K}_e[n(\boldsymbol{r})] + \int \mathcal{V}_{\text{eff}}(\boldsymbol{r}) n(\boldsymbol{r}) \mathrm{d}\boldsymbol{r}. \tag{4.102}$$

By substituting $\mathcal{V}_{\text{eff}}(\boldsymbol{r})$ from Eq. (4.100) into Eq. (4.102), then subtracting the total energy $E[n(\boldsymbol{r})]$ in Eq. (4.97), we find:

$$\begin{aligned} E[n(\boldsymbol{r})] &= \sum_i \epsilon_i - \frac{1}{2}\iint \frac{n(\boldsymbol{r})n(\boldsymbol{r}')}{|\boldsymbol{r}-\boldsymbol{r}'|}\mathrm{d}\boldsymbol{r}\mathrm{d}\boldsymbol{r}' - \Delta\mathcal{E}_{\text{xc}}[n(\boldsymbol{r})] \\ &= \sum_i \epsilon_i - \frac{1}{2}\int \mathcal{V}_H(\boldsymbol{r})n(\boldsymbol{r})\mathrm{d}\boldsymbol{r} - \Delta\mathcal{E}_{\text{xc}}[n(\boldsymbol{r})], \end{aligned} \tag{4.103}$$

where $\Delta\mathcal{E}_{\text{xc}}[n(\boldsymbol{r})]$ is the difference between exchange and correlation potentials as

$$\Delta\mathcal{E}_{\text{xc}}[n(\boldsymbol{r})] = \int \mathcal{V}_{\text{xc}}(\boldsymbol{r})n(\boldsymbol{r})\mathrm{d}\boldsymbol{r} - \mathcal{E}_{\text{xc}}[n(\boldsymbol{r})]. \tag{4.104}$$

## 4.11 Exchange-correlation functional

In Sec. 4.10, we show that how the ground-state properties are calculated by the Kohn-Sham equation. Unfortunately, the exact form of the exchange-correlation functional $\mathcal{E}_{xc}[n(\boldsymbol{r})]$ is not known, and we should take an approximation from many proposed approximations. The most common approximations are the **local-density approximation** (LDA) and the **generalized gradient approximation** (GGA), which will be discussed in Sec. 4.11.1 and Sec. 4.11.2, respectively. We also discuss the **hybrid functionals** in Sec. 4.11.3, which is beyond the LDA and GGA.

### 4.11.1 Local-density approximation

The LDA is an approximation of $\mathcal{E}_{xc}[n(\boldsymbol{r})]$ based on the uniform-electron system as discussed in Sec. 4.8. As shown in Eq. (4.77), the contribution of exchange interaction to the total energy for the uniform-electron charge is:

$$E_x(n) = N_e C_2 n^{1/3}, \tag{4.105}$$

with $C_2 = -0.738$ (see Eq. (4.78)).

Now, let us consider Eq. (4.105) for the case of the non-uniform-electron charge, in which $n$ is a function of $\boldsymbol{r}$. If $n(\boldsymbol{r})$ is a slowly varying function, the exchange functional $\mathcal{E}_x[n(\boldsymbol{r})]$ is approximated as

$$\mathcal{E}_x^{\mathrm{LDA}}[n(\boldsymbol{r})] \approx N_e C_2 n^{1/3}(\boldsymbol{r}). \tag{4.106}$$

By substituting the number of electrons $N_e$ in Eq. (4.82) into Eq. (4.83), we obtain:

$$\mathcal{E}_x^{\mathrm{LDA}}[n(\boldsymbol{r})] = \int \epsilon_x(\boldsymbol{r}) n(\boldsymbol{r}) \mathrm{d}\boldsymbol{r}, \tag{4.107}$$

where $\epsilon_x(\boldsymbol{r})$ is the exchange energy, which is defined by

$$\epsilon_x(\boldsymbol{r}) = C_2 n^{1/3}(\boldsymbol{r}). \tag{4.108}$$

Eq. (4.108) allows to calculate the exchange potential $\mathcal{V}_x[n(\boldsymbol{r})]$ as

$$\mathcal{V}_x[n(\boldsymbol{r})] = \frac{\delta \mathcal{E}_x^{\mathrm{LDA}}[n(\boldsymbol{r})]}{\delta n(\boldsymbol{r})} = \frac{\partial[\epsilon_x(\boldsymbol{r}) n(\boldsymbol{r})]}{\partial n(\boldsymbol{r})} = \frac{4}{3} C_2 n^{1/3}(\boldsymbol{r}). \tag{4.109}$$

Note that the ratio of the exchange potential in Eq. (4.109) to the Slater exchange potential in Eq. (4.79) is 2/3.

Since Eq. (4.107) is based on the free-electron gas (see Sec. 4.8), the correlation interaction is needed to capture accurately the many-body system. Therefore, the energy of correlation interaction $\epsilon_c(\boldsymbol{r})$ is added to Eq. (4.107) as

$$\mathcal{E}_{xc}^{\mathrm{LDA}}[n(\boldsymbol{r})] = \int [\epsilon_x(\boldsymbol{r}) + \epsilon_c(\boldsymbol{r})] n(\boldsymbol{r}) \mathrm{d}\boldsymbol{r}. \tag{4.110}$$

When we consider two limit cases of high-density limit ($n \to \infty$) and low-density limit ($n \to 0$), $\epsilon_c(\boldsymbol{r})$ is proposed in analytic forms by many groups as follows:

*For the high-density limit*:

$$\epsilon_c(r_s) = \sum_{i=0}^{\infty} [a_i \ln r_s + b_i] r_s^i = a_0 \ln r_s + b_0 + \ldots \ (r_s \ll 1), \tag{4.111}$$

where $r_s$ is the radius of a sphere containing a single electron in the atomic unit, which is defined by

$$\frac{4\pi r_s^3}{3} = \frac{1}{n(\boldsymbol{r})}, \text{ or } r_s = \left[\frac{3}{4\pi n(\boldsymbol{r})}\right]^{1/3}, \tag{4.112}$$

and $a_0 = 0.0311$ and $b_0 = -0.048$ are given by Gell-Mann and Brueckner [Gell-Mann and Brueckner (1957)] with neglecting contributions to the coefficients of higher order terms ($i \geq 1$).

*For the low-density limit*:

$$\epsilon_c(r_s) = \sum_{i=0}^{\infty} \frac{c_i}{r_s^{i/2+1}} = \frac{c_0}{r_s} + \frac{c_1}{r_s^{3/2}} + \frac{c_2}{r_s^2} + \ldots \ (r_s \gg 1), \tag{4.113}$$

where $c_0 = -1.792$, $c_1 = 2.65$, and $c_2 = -0.73$ are given by Carr *et al.* [Carr Jr *et al.* (1961)] for a body-centered-cubic lattice system, in which the higher order terms $i \geq 2$ are neglected.

The more accurate numerical calculation of $\epsilon_c(r_s)$ is given by Ceperley and Alder [Ceperley and Alder (1980)]. They calculated the total energy for the uniform-electron system for different values of $r_s$ by using the quantum Monte Carlo method.[8] Then the correlation energy was obtained by subtracting the corresponding kinetic and exchange energies from the total energy. Based on fitting functions to the numerical results of Ceperley and Alder, several forms of $\epsilon_c(r_s)$ are proposed by Vosko, Wilk, and Nusair (VWN) [Vosko *et al.* (1980)], Perdew and Zunger (PZ) [Perdew and Zunger (1981)], and Perdew and Wang (PW) [Perdew and Wang (1992)], which are listed in Table 4.2. Although the expressions of $\epsilon_c(r_s)$ do not depend on the spin, the parameters of $\epsilon_c(r_s)$ depend on the relative spin polarization, which is defined by

$$\zeta = \frac{n_\uparrow(\boldsymbol{r}) - n_\downarrow(\boldsymbol{r})}{n(\boldsymbol{r})}, \tag{4.114}$$

[8] The quantum Monte Carlo method is a set of computational methods to provide a reliable solution (or an accurate approximation) of the quantum many-body problem, in which the anti-commutation relation of two electrons are taken into account.

**Table 4.2** Correlation energy $\epsilon_c(r_s)$ in various models (VWN = Vosko-Wilk-Nusair, PZ = Perdew-Zunger, and PW = Perdew-Wang). $r_s$ is in atomic unit ($a_0 = 1$) and $\epsilon_c(r_s)$ is in units of Ry. $\zeta = [n_\uparrow(\boldsymbol{r}) - n_\downarrow(\boldsymbol{r})]/n(\boldsymbol{r})$ is the relative spin polarization. Parameters are set for $\zeta = 0$ and $\zeta = 1$ in units of a.u.

| **Model** | **Correlation energy** $\epsilon_c(r_s)$ | **for** $\zeta = 0$ | **for** $\zeta = 1$ |
|---|---|---|---|
| VWN | $A\left\{ \ln \frac{x^2}{X(x)} + \frac{2b}{Q} \arctan \frac{Q}{2x+b} - \frac{bx_0}{X(x_0)} \left[ \ln \frac{(x-x_0)^2}{X(x)} + \frac{2(b+2x_0)}{Q} \arctan \frac{Q}{2x+b} \right] \right\}$, where $x = \sqrt{r_s}$, $Q = \sqrt{4c - b^2}$, and $X(x) = x^2 + bx + c$ | $A = 0.031091$<br>$b = 3.72744$<br>$c = 12.9352$<br>$x_0 = -0.10498$ | 0.015545<br>7.06042<br>18.0578<br>−0.32500 |
| PZ | $A\ln(r_s) + B + Cr_s\ln(r_s) + Dr_s$, where $r_s < 1$ and $\gamma/(1 + \beta_1\sqrt{r_s} + \beta_2 r_s)$ with $r_s \geq 1$ | $A = 0.0311$<br>$B = -0.048$<br>$C = 0.0020$<br>$D = -0.0116$<br>$\gamma = -0.1423$<br>$\beta_1 = 1.0529$<br>$\beta_2 = 0.3334$ | 0.0311<br>−0.048<br>0.0007<br>−0.0048<br>−0.0843<br>1.3981<br>0.2611 |
| PW | $-2A(1 + \alpha_1 r_s)\ln\left[1 + \frac{1}{2A\left(\beta_1 r_s^{1/2} + \beta_2 r_s + \beta_3 r_s^{3/2} + \beta_4 r_s^{p+1}\right)}\right]$ | $A = 0.031091$<br>$\alpha_1 = 0.21370$<br>$\beta_1 = 7.5957$<br>$\beta_2 = 3.5876$<br>$\beta_3 = 1.6382$<br>$\beta_4 = 0.49294$<br>$p = 1.0$ | 0.015545<br>0.20548<br>14.1189<br>6.1977<br>3.3662<br>0.6251)<br>1.0 |

where $n_\uparrow(\boldsymbol{r})$ and $n_\downarrow(\boldsymbol{r})$ are the electron densities of up-spin and down-spin states. $\zeta = 0$ and 1 are the spin-unpolarized and spin-polarized systems, respectively.

In Fig. 4.10, we show $-\epsilon_c$ by VWN, PZ, and PW parameters as a function of $r_s$ for the uniform electron system with both the spin-unpolarized and spin-polarized systems by using the parameters in Table 4.2. All functions fit very well with the numerical results (the circles and diamonds symbols for the spin-unpolarized and spin-polarized cases, respectively) of Ceperley and Alder [Ceperley and Alder (1980)]. For $r_s < 5$, which is relevant for condensed metals, the correlation energy becomes more important. On the other hand, the correlation energy becomes a small

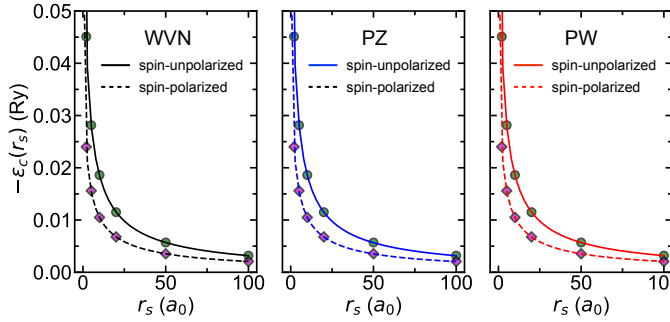


**Figure 4.10** The Vosko-Wilk-Nusair (VWN), Perdew-Zunger (PZ), and Perdew-Wang (PW) correlation energies $-\epsilon_c(r_s)$ are plotted as functions of $r_s$ for both spin-unpolarized (solid lines) and spin-polarized (dashed lines) systems. The expressions and parameters of $\epsilon_c(r_s)$ are given in Table 4.2. The circle and diamond symbols are the accurate numerical results (by Ceperley and Alder) of the uniform electron system with the spin-unpolarized and spin-polarized systems, respectively.

contribution for $r_s > 10$, which are relevant for semiconductors or insulators. Although all functions give the same results in the case of the uniform electron system, for a specific material, they can give somewhat different results of the total energy. Among these functions, the PZ function is often used in Quantum ESPRESSO.

### 4.11.2 Generalized gradient approximation

As discussed in Sec. 4.11.1, the LDA is an approximation in the case that $n(\boldsymbol{r})$ is a slowly varying function. However, $n(\boldsymbol{r})$ often changes rapidly in the real material. Moreover, $n(\boldsymbol{r})$ is generally spin-dependent. There are many attempts to improve the accuracy of the LDA for the real systems where $n(\boldsymbol{r})$ varies rapidly. The most successful one is the **generalized gradient approximation** (GGA). In the GGA, for the exchange term, an **enhancement factor** $F_x$ is added in Eq. (4.107) by Perdew, Burke, and Ernzerhof (PBE) [Perdew *et al.* (1996a)] as

$$\mathcal{E}_x^{\mathrm{GGA}}[n(\boldsymbol{r})] = \int \epsilon_x(\boldsymbol{r}) n(\boldsymbol{r}) F_x(s) \mathrm{d}\boldsymbol{r} = C_2 \int n^{4/3}(\boldsymbol{r}) F_x(s) \mathrm{d}\boldsymbol{r}, \quad (4.115)$$

where $s$ is the dimensionless gradient of $n(\boldsymbol{r})$, which is defined by

$$s = \frac{|\nabla n(\boldsymbol{r})|}{2k_F n(\boldsymbol{r})}, \text{ with } k_F = \left[3\pi^2 n(\boldsymbol{r})\right]^{1/3}, \tag{4.116}$$

and the enhancement factor $F_x(s)$ is expressed by

$$F_x(s) = 1 + \kappa - \frac{\kappa}{1 + \mu s^2/\kappa}, \tag{4.117}$$

where $\kappa = 0.804$ and $\mu = 0.21951$ are constants. Note that the range of $s$ for the real systems is $0 \leq s \leq 3$. Eqs. (4.115) and (4.117) show that

$$\mathcal{E}_x^{\mathrm{GGA}}[n(\boldsymbol{r})] \geq \mathcal{E}_x^{\mathrm{LDA}}[n(\boldsymbol{r})] \text{ with } s \geq 0. \tag{4.118}$$

Therefore, $\mathcal{E}_x^{\mathrm{GGA}}[n(\boldsymbol{r})]$ satisfies the Lieb-Oxford lower bound[9] [Lieb and Oxford (1981)] as shown in Eq. (4.118).

For the correlation term, $\mathcal{E}_c^{\mathrm{GGA}}[n(\boldsymbol{r})]$ is expressed by $\epsilon_c(\boldsymbol{r})$ of the uniform electron system (see Table 4.2) plus an additional term $H[n(\boldsymbol{r}), \zeta]$, which depends on both the gradient $\nabla n(\boldsymbol{r})$ and the spin polarization $\zeta$. The $\mathcal{E}_c^{\mathrm{GGA}}[n(\boldsymbol{r})]$ functional is given by PBE as

$$\mathcal{E}_c^{\mathrm{GGA}}[n(\boldsymbol{r})] = \int \left\{\epsilon_c(\boldsymbol{r}) + H[n(\boldsymbol{r}), \zeta]\right\} n(\boldsymbol{r}) \mathrm{d}\boldsymbol{r}, \tag{4.119}$$

where $H[n(\boldsymbol{r}), \zeta]$ is given by

$$H[n(\boldsymbol{r}), \zeta] = \gamma\phi^3 \ln\left[1 + \frac{\beta}{\gamma} t^2 \left(\frac{1 + At^2}{1 + At^2 + A^2 t^4}\right)\right]. \tag{4.120}$$

Here the function $A$ in Eq. (4.120) is given by

$$A = \frac{\beta}{\gamma}\left\{\exp\left[-\frac{\epsilon_c(\boldsymbol{r})}{\gamma\phi^3}\right] - 1\right\}^{-1}, \tag{4.121}$$

where $\beta = 0.066725$ and $\gamma = 0.031091$ are non-empirical constants, and $\phi(\zeta) = \left[(1+\zeta)^{2/3} + (1-\zeta)^{2/3}\right]/2$ is the spin-scaling factor.

[9] The repulsive Coulomb energy (exchange plus correlation energy) has a lower bound of the form $C_2 \int n^{4/3}(\boldsymbol{r}) \mathrm{d}\boldsymbol{r}$, where $n(\boldsymbol{r})$ is the single-particle electron density.

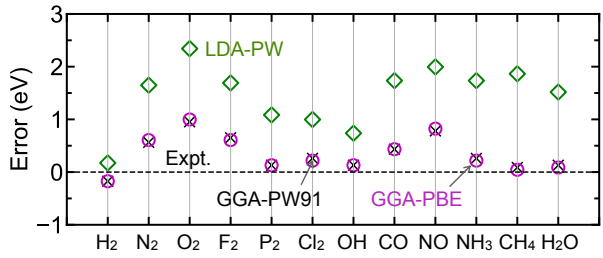


**Figure 4.11** Errors of atomization energies of several molecules in units of eV. The dashed line at zero error corresponds to the experimental values. The square, cross, and circle symbols are the LDA-PW functional, the GGA-PW91 functional, and the GGA-PBE functional, respectively. All numerical data are taken from Ref. [Perdew *et al.* (1996a)].

The function $t$ in Eq. (4.120) is given by $t = |\nabla n(\boldsymbol{r})|/2\phi k_s \nabla n(\boldsymbol{r})$, which is another dimensionless gradient of $n(\boldsymbol{r})$, where $k_s = \sqrt{4k_F/\pi}$ is the Thomas-Fermi screening wave number. The $F(s)$ and $H[n(\boldsymbol{r}), \zeta]$ functions in Eqs. (4.115) and (4.119), respectively, are also developed by Perdew and Wang (PW91) [Perdew *et al.* (1992)] with the slightly different forms and parameters. Although both PBE and PW91 are available in Quantum ESPRESSO, the PBE functional is often used for many materials (see Sec. 3.1.6).

In Fig. 4.11, we show the error of atomization energies for small molecules, in which the experimental values are set to zero error. The atomization energies are calculated by the LDA-PW, GGA-PW91, and GGA-PBE. Both GGA-PW91 and GGA-PBE give almost the same results, and they are closer to the experimental values than LDA-PW. Although LDA-PW overestimates the atomization energies of molecules and solids, LDA-PW remains a popular approximation for realistic solid-state calculations since it has a simple form of the functional compared with GGA.

### 4.11.3 Hybrid functionals

Hybrid functional is a functional that combines the GGA functional with a fraction of the non-local Hartree-Fock exchange interaction. The hybrid functionals are developed for solving the famous "band-gap problem" [Sham and Schlüter (1983)], in which *the LDA and*

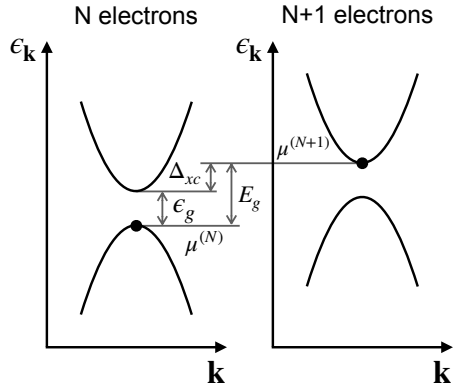


**Figure 4.12** Illustration of the contribution of $\Delta_{xc}$, the discontinuity in $\mathcal{V}_{xc}[n(\boldsymbol{r})]$. The energies $\epsilon$ of the Kohn-Sham equation are shown in the form of a band structure for the $(N)$- and $(N+1)$- electron systems. The two differ in a uniform increase of the eigenvalues by $\Delta_{xc}$. The quasiparticle band-gap $E_g$ is the difference between the two eigenvalues as $E_g = \epsilon_{N+1}^{(N+1)} - \epsilon_N^{(N)}$, which leads to $E_g = \epsilon_g + \Delta_{xc}$, where the Kohn-Sham gap is given by $\epsilon_g = \epsilon_{N+1}^{(N)} - \epsilon_N^{(N)}$.

*GGA always underestimate the band gap*. First, let us explain the reason why both the LDA and GGA underestimate the band gaps for semiconductors and insulators even though they are the basis of good approximations for the ground-state properties.

The origin of the band-gap problem is the discontinuity of chemical potential in the exchange-correlation potential $\mathcal{V}_{xc}$ [Sham and Schlüter (1985)]. This is because the density is given by the summation up to the chemical potential $\mu$ as $n(\boldsymbol{r}) = \sum_i \Theta(\mu - \epsilon_i)|\phi_i|^2$, where $\Theta$ is the Heaviside step function.[10] Therefore, a change $\delta n(\boldsymbol{r})$ leads to a discontinuous jump of $\mu$ from the top of valence band to the bottom of conduction band when we change from $(N)$ to $(N+1)$-electron systems. Since $\mathcal{V}_{xc}[n(\boldsymbol{r})] = \delta\mathcal{E}_{xc}[n(\boldsymbol{r})]/\delta n(\boldsymbol{r})$ in Eq. (4.101) is given by derivative on $\delta n(\boldsymbol{r})$, we also expect a discontinuity $\Delta_{xc}$ (positive value) in $\mathcal{V}_{xc}[n(\boldsymbol{r})]$. Thus, the quasiparticle band-gap $E_g$ can be divided into

[10] The Heaviside step function $\Theta(x)$ is a discontinuous function, whose value is zero for negative arguments $x < 0$ and one for positive arguments $x > 0$.

two components as follows [Perdew and Levy (1983)]

$$E_g = \epsilon_g + \Delta_{xc}, \tag{4.122}$$

where $\epsilon_g$ is the gap obtained from the Kohn-Sham equation for the ground state. In Fig. 4.12, we show the contribution of $\Delta_{xc}$ to $E_g = \epsilon_{N+1}^{(N+1)} - \epsilon_N^{(N)}$, where $\epsilon_J^{(N)}$ denotes $J$-th energy for $(N)$-electron system. As shown in Secs. 4.11.1 and 4.11.2, both the LDA and GGA do not consider the discontinuity in $\mathcal{V}_{xc}[n(\boldsymbol{r})]$ since they are the *smooth* and *local* functions of $n(\boldsymbol{r})$. Therefore, the LDA and GGA would give zero $\Delta_{xc}$, which is the reason why they always underestimate the value of $E_g$ even they give a good approximation to $\epsilon_g$.

Several hybrid functionals have been proposed to obtain non-zero value of $\Delta_{xc}$. The idea of the hybrid functional is based on a *non-local* functional to the exchange-correlation functional $\mathcal{E}_{xc}[n(\boldsymbol{r})]$. As discussed in Sec. 3.6, the exchange potential of the Hartree-Fock equation is a *non-local* potential (see Eq. (4.47)). The exchange energy can be obtained from the Hartree-Fock exchange potential as

$$\mathcal{E}_x^{\mathrm{HF}} = -\frac{1}{2}\sum_{ij}\iint \frac{\phi_i^*(\boldsymbol{r}_1)\phi_j^*(\boldsymbol{r}_2)\phi_j(\boldsymbol{r}_1)\phi_i(\boldsymbol{r}_2)}{|\boldsymbol{r}_1 - \boldsymbol{r}_2|}\mathrm{d}\boldsymbol{r}_1\mathrm{d}\boldsymbol{r}_2, \tag{4.123}$$

where a factor of 1/2 accounts for double counting of the exchange interactions. Here, the exchange potential as a function of $\boldsymbol{r}_1$ is given by as a function of $\boldsymbol{r}_2$, which is the origin of non-local potential. By using $\mathcal{E}_x^{\mathrm{HF}}$ in Eq. (4.123), the expressions of the hybrid functionals are given in Table 4.3, which are usually constructed as a linear combination of a *non-local* term $\mathcal{E}_x^{\mathrm{HF}}$ and the *local* terms from the LDA or GGA. The most popular hybrid functional is B3LYP (B = Becke, 3 = three coefficients, LYP = Lee-Yang-Parr) [Becke (1993), Stephens *et al.* (1994)]. For B3LYP, $\mathcal{E}_x^{\mathrm{GGA}}$ and $\mathcal{E}_c^{\mathrm{GGA}}$ are the exchange functional of Becke (B88) [Becke (1988)] and the correlation functional of Lee, Yang, and Parr [Lee *et al.* (1988)], respectively, and the coefficients $a_o$, $a_x$, and $a_c$ are empirically fitted to atomic and molecular data. The next hybrid functional is PBE0 [Perdew *et al.* (1996b)] (PBE = Perdew-Burke-Ernzerhof, 0 = no empirical coefficient), in which the coefficient $a = 1/4$ is determined by fourth-order perturbation theory [Adamo and Barone (1999)].

**Table 4.3** Hybrid functionals of B3LYP (Becke, 3-parameter, Lee-Yang-Parr), PBE0 (Perdew-Burke-Ernzerhof), and HSE (Heyd-Scuseria-Ernzerhof).

| **Model** | **Exchange-correlation functional** $\mathcal{E}_{xc}$ | **Mixing coefficients** |
|---|---|---|
| B3LYP | $\mathcal{E}_{xc}^{\mathrm{VWN}} + a_0\left(\mathcal{E}_x^{\mathrm{HF}} - \mathcal{E}_x^{\mathrm{VWN}}\right) + a_x\mathcal{E}_x^{\mathrm{GGA}} + a_c\left(\mathcal{E}_c^{\mathrm{GGA}} - \mathcal{E}_c^{\mathrm{VWN}}\right)$ | $a_0 = 0.20$, $a_x = 0.72$, $a_c = 0.81$ |
| PBE0 | $a\mathcal{E}_x^{\mathrm{HF}} + (1-a)\mathcal{E}_x^{\mathrm{PBE}} + \mathcal{E}_c^{\mathrm{PBE}}$ | $a = 1/4$ |
| HSE | $a\mathcal{E}_x^{\mathrm{HF,SR}}(\eta) + (1-a)E_x^{\mathrm{PBE,SR}}(\eta) + \mathcal{E}_x^{\mathrm{PBE,LR}}(\eta) + \mathcal{E}_c^{\mathrm{PBE}}$ | $a = 1/4$, $\eta = 0.106$ |

Although B3LYP and PBE0 are very successful for quantitative calculations in molecules, they might not be suitable for solids. This is because the Hartree-Fock approximation is problematic for delocalized electrons such as metals. As discussed in Sec. 4.8, the Hartree-Fock equation leads to the Lindhard function $F(k/k_F)$ in the energy $\epsilon_{\boldsymbol{k}}$ of a uniform-electron system (see Eq. (4.73)). Therefore, the velocity $\mathrm{d}\epsilon_{\boldsymbol{k}}/\mathrm{d}\boldsymbol{k}$ diverges at the Fermi surface, which contradicts the experiment. The singularity of the Lindhard function at the Fermi surface, which was pointed out by Bardeen [Bardeen (1936)], is a consequence of long-range Coulomb interaction. However, the divergence of $\mathrm{d}\epsilon_{\boldsymbol{k}}/\mathrm{d}\boldsymbol{k}$ can be avoided by either if there is a finite gap (i.e., in an insulator) or if the Coulomb interaction is screened to be effectively short range, which is explained below.

The Coulomb interaction can be divided into short-range (SR) and long-range (LR) parts by using the Ewald summation [Ewald (1921)] as

$$\frac{1}{r} = \underbrace{\frac{1-\mathrm{erf}(\eta r)}{r}}_{\mathrm{SR}} + \underbrace{\frac{\mathrm{erf}(\eta r)}{r}}_{\mathrm{LR}}, \tag{4.124}$$

where erf is the error function[11] and $\eta$ is an adjustable parameter. Applying Eq. (4.124), the HSE (Heyd-Scuseria-

[11] The error function is a function of a variable $x$, which is defined as $\mathrm{erf}(x) = \frac{2}{\sqrt{\pi}}\int_0^x \exp(-t^2)\mathrm{d}t$.

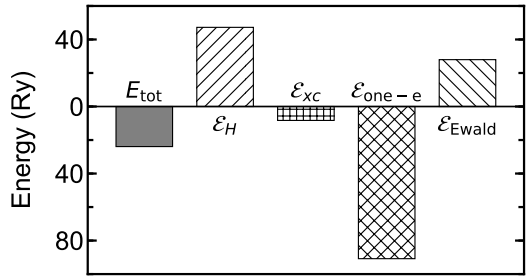


**Figure 4.13** Contributions of the Hartree energy $\mathcal{E}_H$, the exchange-correlation energy $\mathcal{E}_{xc}$, the one-electron energy $\mathcal{E}_{\text{one-e}}$, and the Ewald energy $\mathcal{E}_{\text{Ewald}}$ to total energy $E_{\text{tot}}$ of graphene.

Ernzerhof) [Heyd *et al.* (2003)] hybrid functional (the expression is given in Table. 4.3) is obtained from the PBE0 functional. The form of HSE has the advantage that it can be applied to metals, and it reduces to the PBE functional for $\eta \to \infty$ and the PBE0 hybrid functional for $\eta \to 0$. All B3LYP, PBE0, and HSE options are available in Quantum ESPRESSO. Although the hybrid functionals give a better value, they are significantly time-consuming compared with the LDA and GGA.

## 4.12 Total energy calculation

In the discussion up to now, we only consider the total energy of the electrons by solving the Kohn-Sham equation (see Sec. 4.10.2). However, in Quantum ESPRESSO, the total energy of a solid contains both the electron and ion contributions as

$$E_{\text{tot}} = \underbrace{\mathcal{E}_H + \mathcal{E}_{xc} + \mathcal{E}_{\text{one-e}}}_{\text{electrons}} + \underbrace{\mathcal{E}_{\text{Ewald}}}_{\text{ions}}, \tag{4.125}$$

where $\mathcal{E}_H$ is the Hartree energy, $\mathcal{E}_{xc}$ is the exchange-correlation energy, $\mathcal{E}_{\text{one-e}}$ is the kinetic energy of the electrons plus the pseudopotential energy, and $\mathcal{E}_{\text{Ewald}}$ is the Coulomb repulsion between pairs of ions. These values of the energies can be found on the output file of the Quantum ESPRESSO calculation, as shown in Fig. 4.13 for graphene (see output file in Sec. 3.1.1). In this section, we will explain each energy by using the **plane wave expansion** (Sec. 5.3). With the

plane waves, the convergence of physical properties is controlled by the **cut-off energy**, which can be tested (see Sec. 3.1.2).

### 4.12.1 Hartree contribution

First, let us discuss the Hartree energy $\mathcal{E}_H$, which is expressed as

$$\mathcal{E}_H[n(\boldsymbol{r})] = \frac{1}{2}\int \mathcal{V}_H(\boldsymbol{r})n(\boldsymbol{r})\mathrm{d}\boldsymbol{r}, \tag{4.126}$$

where a factor of 1/2 takes into account the double counting and $\mathcal{V}_H(\boldsymbol{r})$ is the Hartree potential, which is given in Eq. (4.33).

For a periodic solid, the total electron density and the potentials can be expressed in the terms of the plane waves, $e^{i\boldsymbol{G}\boldsymbol{r}}$, with $\boldsymbol{G}$ is the reciprocal lattice vectors (see Sec. 5.3) as

$$n(\boldsymbol{r}) = \sum_{\boldsymbol{G}} e^{i\boldsymbol{G}\boldsymbol{r}} n(\boldsymbol{G}), \text{ and } \mathcal{V}_H(\boldsymbol{r}) = \sum_{\boldsymbol{G}} e^{i\boldsymbol{G}\boldsymbol{r}} \mathcal{V}_H(\boldsymbol{G}), \tag{4.127}$$

where $n(\boldsymbol{G})$ and $\mathcal{V}_H(\boldsymbol{G})$ are, respectively, given by

$$n(\boldsymbol{G}) = \int n(\boldsymbol{r})e^{-i\boldsymbol{G}\boldsymbol{r}}\mathrm{d}\boldsymbol{r}, \text{ and } \mathcal{V}_H(\boldsymbol{G}) = \int \mathcal{V}_H(\boldsymbol{r})e^{-i\boldsymbol{G}\boldsymbol{r}}\mathrm{d}\boldsymbol{r}. \tag{4.128}$$

For the neutral case, the total negative charge of the electrons is canceled by the total positive charge of the ions. Therefore, the average potential is zero. Since $\boldsymbol{G} = 0$ in Eq. (4.127) corresponds to the average potential over all the space, we can omit $\boldsymbol{G} = 0$ in the summation due to charge neutrality.[12] Then, by substituting

[12] There might be a contribution from the $\boldsymbol{G} = 0$ term if the systems have an intrinsic electric dipole moment.

Eq. (4.127) into Eq. (4.126), we obtain

$$\begin{aligned}\mathcal{E}_H[n(\boldsymbol{r})] &= \frac{1}{2}\sum_{\boldsymbol{G}\boldsymbol{G}'}\int e^{i(\boldsymbol{G}+\boldsymbol{G}')\boldsymbol{r}}\mathcal{V}_H(\boldsymbol{G})n(\boldsymbol{G}')\mathrm{d}\boldsymbol{r} \\ &= \frac{\Omega}{2}\delta_{\boldsymbol{G}+\boldsymbol{G}',0}\mathcal{V}_H(\boldsymbol{G})n(\boldsymbol{G}') \\ &= \frac{\Omega}{2}\sum_{\boldsymbol{G}\neq 0}\mathcal{V}_H(\boldsymbol{G})n(-\boldsymbol{G}) \\ &= \frac{\Omega}{2}\sum_{\boldsymbol{G}\neq 0}\mathcal{V}_H(\boldsymbol{G})n(\boldsymbol{G}),\end{aligned} \tag{4.129}$$

where $\Omega$ is the volume of the unit cell. Here we assume that $n(+\boldsymbol{G}) = n(-\boldsymbol{G})$. On the other hand, by substituting Eq. (4.127) into the Poisson equation (see Sec. 4.5), we have

$$\nabla^2\mathcal{V}_H(\boldsymbol{r}) = -4\pi n(\boldsymbol{r}) \iff \mathcal{V}_H(\boldsymbol{G}) = 4\pi\frac{n(\boldsymbol{G})}{|\boldsymbol{G}|^2}. \tag{4.130}$$

By substituting Eq. (4.130) into Eq. (4.129), we obtain

$$\mathcal{E}_H = 2\pi\Omega\sum_{\boldsymbol{G}\neq 0}\frac{n^2(\boldsymbol{G})}{|\boldsymbol{G}|^2}. \tag{4.131}$$

### 4.12.2 Exchange-correlation contribution

From Eq. (4.110), the exchange-correlation energy is defined by

$$\mathcal{E}_{xc}[n(\boldsymbol{r})] = \int \epsilon_{xc}(\boldsymbol{r})n(\boldsymbol{r})\mathrm{d}\boldsymbol{r}, \tag{4.132}$$

where $\epsilon_{xc}(\boldsymbol{r}) = \epsilon_x(\boldsymbol{r}) + \epsilon_c(\boldsymbol{r})$ can be expressed in the terms of the plane waves as

$$\epsilon_{xc}(\boldsymbol{r}) = \sum_{\boldsymbol{G}\neq 0} e^{i\boldsymbol{G}\boldsymbol{r}}\epsilon_{xc}(\boldsymbol{G}). \tag{4.133}$$

By substituting Eqs. (4.133) and (4.127) into Eq. (4.132), we obtain

$$\mathcal{E}_{xc}[n(\boldsymbol{r})] = \Omega \sum_{\boldsymbol{G}\neq 0} \epsilon_{xc}(\boldsymbol{G}) n(\boldsymbol{G}). \tag{4.134}$$

### 4.12.3 One-electron contribution and pseudopotential

In Quantum ESPRESSO, $\mathcal{E}_{\text{one-e}}$ defined in Eq. (4.125) is the sum of the kinetic energy $\mathcal{K}_e$ and the external energy $\mathcal{E}_{\text{ext}}$ of the electrons in the potential of the atom cores:

$$\mathcal{E}_{\text{one-e}}[n(\boldsymbol{r})] = \mathcal{K}_e[n(\boldsymbol{r})] + \mathcal{E}_{\text{ext}}[n(\boldsymbol{r})]. \tag{4.135}$$

The expression of $\mathcal{K}_e[n(\boldsymbol{r})]$ is given by Eq. (4.96), which can be rewritten in the terms of the plane waves as

$$\mathcal{K}_e[n(\boldsymbol{r})] = \frac{\Omega}{2} \sum_i \sum_{\boldsymbol{k}} \sum_{\boldsymbol{G}} |\boldsymbol{k}+\boldsymbol{G}|^2 |C_{i,\boldsymbol{k}}(\boldsymbol{G})|^2, \tag{4.136}$$

where $C_{i,\boldsymbol{k}}(\boldsymbol{G})$ are the coefficients of the wavefunctions $\phi_i$.

The expression of $\mathcal{E}_{\text{ext}}[n(\boldsymbol{r})]$ is given by

$$\mathcal{E}_{\text{ext}}[n(\boldsymbol{r})] = \int \mathcal{V}_{en}(\boldsymbol{r}) n(\boldsymbol{r}) \mathrm{d}\boldsymbol{r}. \tag{4.137}$$

Since the external potential term $\mathcal{V}_{en}(\boldsymbol{r})$ in Eq. (4.137) is costly computation with the plane waves, $\mathcal{V}_{en}(\boldsymbol{r})$ is replaced by a **pseudopotential** $\mathcal{V}_{\text{ps}}(\boldsymbol{r})$, which is related to replacing the effects of the core electrons with an effective potential.

A local form of the pseudopotential of a single ion, $v_{\text{ps}}(\boldsymbol{r})$, is proposed by Ashcroft-Heine-Abarenkov [Ashcroft (1966), Heine and Abarenkov (1964)] as

$$v_{\text{ps}}(\boldsymbol{r}) = \begin{cases} v_0 & r < r_{\text{cut}} \\ -\frac{Z}{r} & r > r_{\text{cut}} \end{cases}, \tag{4.138}$$

where $Z$ is the charge of the ionic core and $r_{\text{cut}}$ is the effective radius, which is determined by the radius of core electrons, as shown in Fig. 4.14. The constants $r_{\text{cut}}$ and $v_0$ are chosen such that the energy levels

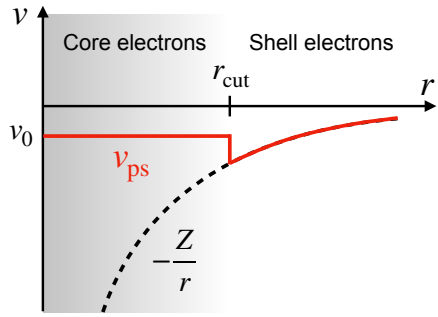


**Figure 4.14** The Ashcroft-Heine-Abarenkov pseudopotential for a single ion.

of the shell electrons are reproduced for the single-atom calculations. For example, let us consider 1*s*- and 2*s*-electrons of the C atom as core electrons. Then, $r_{\rm cut}$ and $v_0$ are adjusted by solving the one-particle equation to reproduce the observed ionization energy of the 2*p*-electron.

A global form of the pseudopotential can be obtained by taking into account the contribution of the individual atoms of a unit cell as

$$\mathcal{V}_{\rm ps}(\boldsymbol{r}) = \sum_I \sum_{\boldsymbol{T}} v_{\rm ps}^I(|\boldsymbol{r} - \boldsymbol{T} - \boldsymbol{R}_I|), \tag{4.139}$$

where $\boldsymbol{T}$ are the lattice translation vectors, $\boldsymbol{R}_I$ denotes the relative positions of the $I$-th atom in the unit cell, and $v_{\rm ps}^I$ is the pseudopotential of the $I$-th atom. Eq. (4.139) can be expressed by the Fourier transform as

$$\begin{aligned}
\mathcal{V}_{\rm ps}(\boldsymbol{G}) &= \frac{1}{V}\int \sum_I \sum_{\boldsymbol{T}} v_{\rm ps}^I(|\boldsymbol{r} - \boldsymbol{T} - \boldsymbol{R}_I|)e^{-i\boldsymbol{G}\boldsymbol{r}}\mathrm{d}\boldsymbol{r} \\
&= \frac{N_{\rm cell}}{V}\sum_I e^{-i\boldsymbol{G}\boldsymbol{R}_I}\int v_{\rm ps}^I(|\boldsymbol{r}|)e^{-i\boldsymbol{G}\boldsymbol{r}}\mathrm{d}\boldsymbol{r} \\
&= \sum_I e^{-i\boldsymbol{G}\boldsymbol{R}_I}\frac{1}{\Omega}\int v_{\rm ps}^I(|\boldsymbol{r}|)e^{-i\boldsymbol{G}\boldsymbol{r}}\mathrm{d}\boldsymbol{r} \\
&= \sum_I S_I(\boldsymbol{G})F_I(\boldsymbol{G}),
\end{aligned} \tag{4.140}$$

in which $S_I(\boldsymbol{G})$ and $F_I(\boldsymbol{G})$ are defined by

$$S_I(\boldsymbol{G}) = e^{-i\boldsymbol{G}\boldsymbol{R}_I}, \text{ and } F_I(\boldsymbol{G}) = \frac{1}{\Omega}\int v_{\text{ps}}^I(|\boldsymbol{r}|)e^{-i\boldsymbol{G}\boldsymbol{r}}\mathrm{d}\boldsymbol{r}, \tag{4.141}$$

where $N_{\text{cell}}$ is the number of unit cells in the crystal, $V = N_{\text{cell}}\Omega$ is the crystal volume, and $\sum_I S_I(\boldsymbol{G})$ and $F_I(\boldsymbol{G})$ are called the **structure factor**[13] and the **atomic form factor**[14] of the $I$-th atom, respectively.

For a given pseudopotential such as Eq. (4.138), the external energy can be expressed as

$$\mathcal{E}_{\text{ext}}[n(\boldsymbol{r})] = \int \mathcal{V}_{\text{ps}}(\boldsymbol{r})n(\boldsymbol{r})\mathrm{d}\boldsymbol{r} = \Omega\sum_{\boldsymbol{G}}\mathcal{V}_{\text{ps}}(\boldsymbol{G})n(\boldsymbol{G}). \tag{4.142}$$

Then by substituting Eq. (4.140) into Eq. (4.142), we obtain

$$\mathcal{E}_{\text{ext}}[n(\boldsymbol{r})] = \Omega\sum_{\boldsymbol{G}}\sum_{I} S_I(\boldsymbol{G})F_I(\boldsymbol{G})n(\boldsymbol{G}). \tag{4.143}$$

For Quantum ESPRESSO, the $\mathcal{V}_{\text{ps}}$ is often used with norm-conserving or ultra-soft (non-local) pseudopotentials (see Sec. 5.4). In the case of non-local pseudopotential, however, the expression of the external energy is rather complicated and needs special treatment for an efficient implementation [Pickett (1989)].

### 4.12.4 The Ewald contribution

Finally, we will discuss the last term $\mathcal{E}_{\text{Ewald}}$ in Eq. (4.125). In Quantum ESPRESSO, $\mathcal{E}_{\text{Ewald}}$ denotes the ion-ion Coulomb energy, which is given by

$$\mathcal{E}_{\text{Ewald}} = \frac{1}{2}\sum_{I\neq J}^{N_n}\frac{Z_I Z_J}{|\boldsymbol{R}_I - \boldsymbol{R}_J|}. \tag{4.144}$$

[13] The structure factor contains all the information about the lattice structure. The structure factor gives the extinction rule for X-ray diffraction (see Sec. 5.2).
[14] The atomic form factor contains the information of each atom, which can be calculated or obtained by fitting experimental data. The form factor is important for obtaining the intensity of X-ray scattering.

This sum converges slowly since the potentials of the Coulomb interaction is a long-range function of $|\boldsymbol{R}_I - \boldsymbol{R}_J|$. Thus, in order to converge Eq. (4.144) rapidly, we can apply the **Ewald summation** [Ewald (1921)], which splits the potential into short-range (SR) and long-range (LR) parts. As shown in Eq. (4.124), the Ewald summation of the ionic potential can be expressed as

$$\begin{aligned}\sum_J^{N_n} \frac{Z_J}{|\boldsymbol{R} - \boldsymbol{R}_J|} = &\underbrace{\sum_J^{N_n} Z_I \frac{1 - \mathrm{erf}(\eta|\boldsymbol{R} - \boldsymbol{R}_J|)}{|\boldsymbol{R} - \boldsymbol{R}_J|}}_{\mathrm{SR}} \\ &+ \underbrace{\sum_J^{N_n} Z_J \frac{\mathrm{erf}(\eta|\boldsymbol{R} - \boldsymbol{R}_J|)}{|\boldsymbol{R} - \boldsymbol{R}_J|}}_{\mathrm{LR}},\end{aligned} \tag{4.145}$$

in which, the LR part can be expressed in reciprocal space as [Marder (2010)]

$$\sum_J^{N_n} Z_J \frac{\mathrm{erf}(\eta|\boldsymbol{R} - \boldsymbol{R}_J|)}{|\boldsymbol{R} - \boldsymbol{R}_J|} = \frac{4\pi}{V} \sum_J^{N_n} \sum_{\boldsymbol{G}\neq 0} Z_J \frac{e^{-|\boldsymbol{G}|^2/(4\eta)^2} e^{i\boldsymbol{G}(\boldsymbol{R} - \boldsymbol{R}_J)}}{|\boldsymbol{G}|^2}. \tag{4.146}$$

Then the both SR and LR parts can converge quickly with increasing $|\boldsymbol{G}|$ and $|\boldsymbol{R}|$ for a given value of $\eta$. Therefore, the ion-ion Coulomb energy can be obtained by a few terms in the summations over $|\boldsymbol{G}|$ and $J$.

When we insert Eqs. (4.145) and (4.146) into Eq. (4.144), we must subtract separately the term for $\boldsymbol{R} = \boldsymbol{R}_J$ in Eq. (4.146), to avoid the divergence. If we adopt the following equation:

$$\lim_{\boldsymbol{R}\to\boldsymbol{R}_J} \left[ \frac{\mathrm{erf}(\eta|\boldsymbol{R} - \boldsymbol{R}_J|)}{|\boldsymbol{R} - \boldsymbol{R}_J|} \right] = 2\frac{\eta}{\sqrt{\pi}}, \tag{4.147}$$

Eq. (4.144) can be rewritten as

$$\begin{aligned}\mathcal{E}_{\text{Ewald}} =& \frac{1}{2}\sum_{I\neq J}^{N_n} Z_I Z_J \frac{1-\text{erf}(\eta|\boldsymbol{R}_I-\boldsymbol{R}_J|)}{|\boldsymbol{R}_I-\boldsymbol{R}_J|} \\ &+ \frac{2\pi}{V}\sum_{I,J}^{N_n}\sum_{\boldsymbol{G}\neq 0} Z_I Z_J \frac{e^{-|\boldsymbol{G}|^2/(4\eta)^2} e^{i\boldsymbol{G}(\boldsymbol{R}_I-\boldsymbol{R}_J)}}{|\boldsymbol{G}|^2} \\ &- \sum_{J}^{N_n} Z_J^2 \frac{\eta}{\sqrt{\pi}}.\end{aligned} \tag{4.148}$$

Thus, we can avoid the divergence, too.

## 4.13 Ionic forces

The ionic forces are used to study the dynamics of ions such as optimizing ionic positions (see Sec. 3.1.4). Using the total energy in Sec. 4.12, we can calculate the forces that act to the ion $I$, which is given by taking the derivative of the total energy with respect to individual ionic position $\boldsymbol{R}_I$ as

$$F_I = -\frac{\partial E_{\text{tot}}}{\partial \boldsymbol{R}_I} = -\frac{\partial \mathcal{E}_{\text{Ewald}}}{\partial \boldsymbol{R}_I} - \frac{\partial \mathcal{E}_{\text{ext}}}{\partial \boldsymbol{R}_I}. \tag{4.149}$$

There are two contributions to the ionic forces, one from the ion-ion interaction energy $\mathcal{E}_{\text{Ewald}}$ in Eq. (4.148), and one from the ion-electron interaction energy $\mathcal{E}_{\text{ext}}$ in Eq. (4.142). For the ion-ion interaction energy, the force of ion $I$ is given by Eq. (4.148) as follows:

$$F_I^{\text{ion}} = -\frac{\partial \mathcal{E}_{\text{Ewald}}}{\partial \boldsymbol{R}_I} = \sum_{J\neq I}^{N_n} \frac{Z_I Z_J}{|\boldsymbol{R}_I-\boldsymbol{R}_J|^3}(\boldsymbol{R}_I-\boldsymbol{R}_J), \tag{4.150}$$

which can be solved by a method analogous to the Ewald summation that is used in Sec. 4.12.4.

As for the ion-electron interaction energy, the force is calculated by adopting the **Hellmann-Feynman theorem**[15] [Feynman (1939), Hellmann (1937)] as

$$F_I^{\text{ion-e}} = -\frac{\partial \mathcal{E}_{\text{ext}}}{\partial \boldsymbol{R}_I} = -\sum_i \left\langle \phi_i \left| \frac{\partial \mathcal{V}_{\text{ps}}}{\partial \boldsymbol{R}_I} \right| \phi_i \right\rangle. \tag{4.151}$$

For the $I$-th pseudopotential $\mathcal{V}_{\text{ps}}^I(\boldsymbol{r}) = \sum_{\boldsymbol{T}} v_{\text{ps}}^I(|\boldsymbol{r} - \boldsymbol{T} - \boldsymbol{R}_I|)$ (see Eq. (4.139)), Eq. (4.151) is rewritten in term of $n(\boldsymbol{r})$ as

$$F_I^{\text{ion-e}} = -\int \frac{\partial \mathcal{V}_{\text{ps}}(\boldsymbol{r})}{\partial \boldsymbol{R}_I} n(\boldsymbol{r}) \mathrm{d}\boldsymbol{r}. \tag{4.152}$$

Eq. (4.152) tells us that $F_I^{\text{ion-e}}$ does not depend on any derivative of $n(\boldsymbol{r})$. The Hellmann-Feynman force is straightforwardly calculated by the calculated $n(\boldsymbol{r})$ once the self-consistent electronic density is obtained.

## 4.14 A simple DFT-LDA program for an atom

This section shows a step-by-step calculation of the ground-state energy of a helium atom for understanding the DFT for an atom. The DFT calculation of an atom is also important since Quantum ESPRESSO does not support the package for an atom. We use Python language (version 3) to write the simplest DFT code for the LDA (see Sec. 4.11.1). The present tutorial contains three main calculations: (1) to solve the radial Schrödinger equation by using the Numerov algorithm, (2) to solve the radial Possion equation by using the Verlet algorithm, and (3) incorporating to calculate the ground-state energy of the helium atom by using the LDA with PZ parameters. This tutorial requires the basic Python programming and Jupyter notebook, which are given in Chapter 6.

[15] The Hellmann-Feynman theorem states that the forces are given by the expectation value of the derivative of the external potential.

### 4.14.1 Radial Schrödinger equation

❑ **Purpose:** The purpose of the first step is to calculate the electron density of the helium atom by solving a **radial Schrödinger equation**, which is the Schrödinger equation in spherical coordinates.
❑ **Background:** In spherical coordinates, the wavefunction $\phi(\boldsymbol{r}) = \phi(r,\theta,\varphi)$ can be written as the product of a radial function $R(r)$ and an angular function $Y(\theta,\varphi)$:

$$\phi(r,\theta,\varphi) = R(r)Y(\theta,\varphi). \tag{4.153}$$

Then we obtain the radial Schrödinger equation for $R(r)$ as follows [Kittel (1976)]

$$\left[-\frac{1}{2r^2}\frac{\mathrm{d}}{\mathrm{d}r}\left(r^2\frac{\mathrm{d}}{\mathrm{d}r}\right) + \frac{\ell(\ell+1)}{2r^2} + \mathcal{V}(r)\right] R(r) = \epsilon R(r), \tag{4.154}$$

where $\ell$ is azimuthal quantum number $\ell = 0, 1, 2, \ldots$ . Let us define a *reduced radial wavefunction* $u(r)$ as

$$u(r) = rR(r). \tag{4.155}$$

By substituting Eq. (4.155) into Eq. (4.154), we obtain the *reduced radial equation* for 1*s* orbital by substituting $\ell = 0$ as

$$\left[-\frac{1}{2}\frac{\mathrm{d}^2}{\mathrm{d}r^2} + \mathcal{V}(r)\right] u(r) = \epsilon u(r). \tag{4.156}$$

Eq. (4.156) can be rewritten in the form of a second-order differential equation as

$$\frac{\mathrm{d}^2 u}{\mathrm{d}r^2} = -k(r)u(r), \tag{4.157}$$

where $k(r)$ is defined by

$$k(r) = 2\left[\epsilon - \mathcal{V}(r)\right]. \tag{4.158}$$

A method to solve Eq. (4.157) is the **Numerov algorithm**.[16] In the Numerov algorithm, the reduced radial wavefunction $u(r)$ is expressed as

$$u_{n+1}(r) = \frac{2c_0 u_n(r) - c_1 u_{n-1}(r)}{c_2}, \tag{4.159}$$

where $c_0$, $c_1$, and $c_2$ are defined by

$$\begin{cases} c_0 = 1 - \frac{5}{12}h^2 k_n^2(r) \\ c_1 = 1 + \frac{1}{12}h^2 k_{n-1}^2(r) \\ c_2 = 1 + \frac{1}{12}h^2 k_{n+1}^2(r) \end{cases}, \tag{4.160}$$

where $h = r_{n+1} - r_n$. By given two initial values, $u_0(r)$ and $u_1(r)$, Eq. (4.159) can be used to determine $u_n(r)$ for $n = 2, 3, 4, \ldots$ with an error in the order of $h^6$.

We normalize $u(r)$ as

$$\int u^2(r)\mathrm{d}r = 1. \tag{4.161}$$

Then, the electron density $n(r)$ of a single electron for the $1s$ state ($Y(\theta, \varphi) = 1/\sqrt{4\pi}$) is given by

$$n(r) = \frac{R^2(r)}{4\pi} = \frac{u^2(r)}{4\pi r^2}. \tag{4.162}$$

Note that, for the helium atom, the total electron density is $2n(r)$ since we have two electrons.

❏ **How to run:** To run this tutorial, the readers will do the following command lines:

```
$ cd ~/SSP-QE/dft-he
$ jupyter-lab check-schrodinger.ipynb
```

- Line 1: Go to the `dft-he` directory that includes the input files.
- Line 2: Run `check-schrodinger.ipynb` by JupyterLab.

[16] The Numerov algorithm is a numerical method to solve ordinary differential equations of second order in which the first-order term does not appear.

❑ **Input file:** The input files include a subroutine file (`schrodinger.py`) and a main file (`check-schrodinger.ipynb`). The subroutine contains the Numerov algorithm in Eq. (4.159) and the radial Schrödinger equation in Eq. (4.157), and the main file calculates the ground-states energy and wavefunction for the helium atom.

**SSP-QE/dft-he/schrodinger.py**

```
# Import the numpy modules
import numpy as np
# The Numerov algorithm for equation:
# u"(r) = -k(r)u(r) with k(r)=2(eps-V)
# Input: k(r), two initial values u0(r) and u1(r)
# Output: u(r)
def numerov(k, u0, u1, dr):
    u = np.zeros_like(k)
    u[0] = u0
    u[1] = u1
    for i in range(2, len(k)):
        dr_sqr = dr**2
        c0 = (1 + 1/12.*dr_sqr*k[i-2])
        c1 = 2*(1 - 5/12.*dr_sqr*k[i-1])
        c2 = (1 + 1/12.*dr_sqr*k[i])
        u[i] = (c1*u[i-1] - c0*u[i-2])/c2
    return u
# Solve the reduced radial Schrodinger equation:
# u"(r) = -2(eps-V)u(r)
# Inputs: r and V(r)
# Outputs: eigen energy eps and u(r)
def solve_schrodinger(r, V, eps_min=-4, eps_max=0,
    maxiter=100, stoptol = 0.0001):
    dr = r[1] - r[0]
    for i in range(maxiter):
        eps = (eps_min + eps_max)/2.
        k = 2*(eps - V)
        # starting from r*exp(-r)
        u0 = r[-1]*np.exp(-r[-1])
        u1 = r[-2]*np.exp(-r[-2])
        # call the Numerov algorithm
        u = numerov(k[::-1], u0, u1, dr)
        u = u[::-1]
        num_nodes = np.sum(u[1:]*u[:-1] < 0)
        if num_nodes == 0 and np.abs(u[0]) <=
            stoptol:
            return (eps, u)
        if num_nodes == 0 and u[0] > 0:
            eps_min = eps
```

```
38          else:
39              assert num_nodes > 0, 'expect #nodes>0
                    since u[0]<0 while u[infty]>0'
40              eps_max = eps
41      raise Exception('Not converged after %d
            iterations.' %(maxiter))
```

**SSP-QE/dft-he/check-schrodinger.ipynb**

```
# Import the necessary packages and modules
# sci.mplstyle is customized Matplotlib style
import matplotlib.pyplot as plt
plt.style.use('../matplotlib/sci.mplstyle')
import numpy as np
from schrodinger import solve_schrodinger

# Set r from 0 to 15 bohr with 50000 steps
r, dr = np.linspace(0, 15, 50001, retstep=True)
r = r[1:]  # Skip r = 0
# Set kinetic energy of helium
Z = 2
V_en = -Z/r

# Solve the reduced radial equation:
# u"(r) = -2(eps-V_en)u(r)
eps, u = solve_schrodinger(r, V_en)
# Normalize u(r)
u /= np.linalg.norm(u)*np.sqrt(dr)

# Total electron density of helium
n = 2*(u**2/4/np.pi/r**2)
# Compare with exact density of helium
n_exact = (2*Z**3/np.pi)*np.exp(-2*Z*r)

# Plot the comparison
plt.figure()
plt.plot(r, n, label='numerov')
plt.plot(r, n_exact, ':', lw=4, label='exact')
plt.xlabel('$r$ ($a_0$)')
plt.ylabel('$n(r)$ (a.u.)')
plt.title('Electron density of helium')
plt.legend(loc='best')
plt.xlim(0, 5)
plt.show()
```

❑ **Output data:** In main work area of the JupyterLab interface, the readers can see the plot as shown in Fig. 4.15. We can see

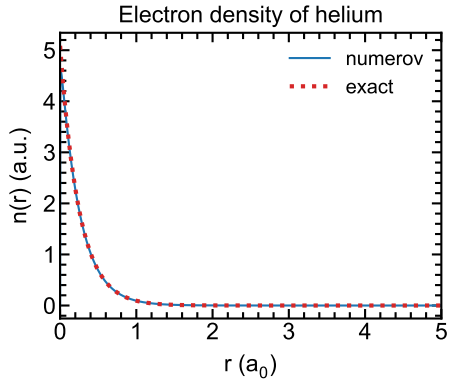


**Figure 4.15** Electron density of helium. Solid and dashed lines denote the electron densities, which are obtained by the Numerov algorithm and analytical methods, respectively.

that the electron density from the numerical method (the Numerov algorithm) reproduces the exact electron density of the helium atom given by Eq. (4.21).

### 4.14.2 The Poisson equation

❑ **Purpose:** Next, let us calculate the Hartree potential from the reduced radial wavefunction $u(r)$.
❑ **Background:** Let us define a Hartree potential as a function of $r$, $U_H(r) = r\mathcal{V}_H(r)$, then the Poisson equation in Eq. (4.32) reduces to the following differential equation:

$$\nabla^2 U_H(r) = -4\pi r n(r). \tag{4.163}$$

Eq. (4.163) is an ordinary second-order differential equation which can be solved by using the **Verlet algorithm**.[17] By substituting Eq. (4.162) into Eq. (4.163), we have

$$\nabla^2 U_H(r) = -\frac{u^2(r)}{r}. \tag{4.164}$$

[17] The Verlet algorithm is a simple method for integrating second order differential equations of the form $x''(t) = f[x(t), t]$.

The Verlet algorithm for Eq. (4.164) is expressed as following:

$$U_H(r+\delta r) = 2U_H(r) - U_H(r-\delta r) + \delta r^2 \nabla^2 U_H(r). \tag{4.165}$$

The boundary conditions are also applied to solve Eq. (4.164). For the hydrogen, the conditions are $U_H(0) = 0$ and $U_H(r_{\max}) = 1$. Note that, for the helium case, the Hartree potential is $2U_H(r)/r$ since the electron density is $2n(r)$.

❏ **How to run:** To run this tutorial, the readers will do the following command lines:

```
$ cd ~/SSP-QE/dft-he
$ jupyter-lab check-poisson.ipynb
```

- Line 1: Go to the `dft-he` directory that includes the input files.
- Line 2: Run `check-poisson.ipynb` by JupyterLab.

❏ **Input file:** The input files include two subroutine files (`schrodinger.py` and `poisson.py`) and a main file (`check-poisson.ipynb`). The subroutine `poisson.py` contains the Verlet algorithm in Eq. (4.165) and the Poisson equation in Eq. (4.164), and the main file calculates the Hartree potential for the helium atom.

**SSP-QE/dft-he/poisson.py**

```
1  # Import the numpy modules
2  import numpy as np
3  # The Verlet algorithm
4  def verlet(f, U0, U1, dr):
5      dr_sqr = dr**2
6      U_H = np.zeros_like(f)
7      U_H[0] = U0
8      U_H[1] = U1
9      for i in range(2, len(f)):
10         U_H[i] = 2*U_H[i-1] - U_H[i-2] + f[i-1]*
               dr_sqr
11     return U_H
12 # Solve the Poisson equation
13 # Inputs: r and u(r)
14 # Outputs: U_H(r)
15 def solve_poisson(r, u):
16     # start the Verlet algorithm
17     dr = r[1]-r[0]
```

```
    f = -u**2/r
    U0, U1 = r[0], r[1]
    U_H = verlet(f, U0, U1, dr)
    # fix the boundary condition
    U_H = U_H - (U_H[-1]-1)/r[-1]*r
    return U_H
```

**SSP-QE/dft-he/check-poisson.ipynb**

```
# Import the necessary packages and modules
# sci.mplstyle is customized Matplotlib style
import matplotlib.pyplot as plt
plt.style.use('../matplotlib/sci.mplstyle')
import numpy as np
from schrodinger import solve_schrodinger
from poisson import solve_poisson

# Set r from 0 to 15 bohr with 50000 steps
r, dr = np.linspace(0, 15, 50001, retstep=True)
r = r[1:]  # Skip r = 0
# Set kinetic energy of helium
Z = 2
V_en = -Z/r

# Solve the radial Schrodinger equation
eps, u = solve_schrodinger(r, V_en)
# Normalize the radial wave function u(r)
u /= np.linalg.norm(u)*np.sqrt(dr)

# Solve the Poisson equation
U_H = solve_poisson(r, u)
# Convert U_H(r) to the Hartree potential V_H(r)
# The factor of 2 since helium has two electrons
V_H = 2*U_H/r
# Compare with the exact Hartree potential
V_exact = -2*(Z + 1/r)*np.exp(-2*Z*r) + Z/r

# Plot the comparison
plt.plot(r, V_H, label='verlet')
plt.plot(r, V_exact, ':', lw=4, label='exact')
plt.xlabel('r (bohr)')
plt.ylabel('$\mathcal{V}_H(r)$ (a.u.)')
plt.title('Hartree potential of helium')
plt.legend(loc='best')
plt.xlim(0, 5)
plt.show()
```

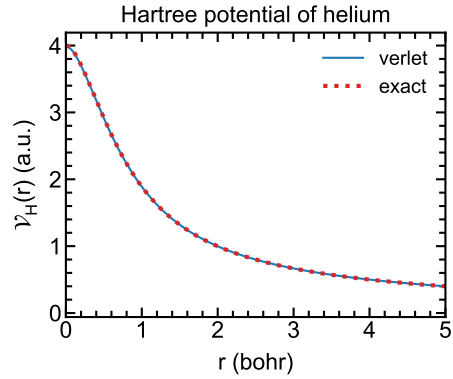


**Figure 4.16** The Hartree potential of helium. Solid and dashed lines denote the Hartree potential, which are obtained by the Verlet algorithm and analytical methods, respectively.

❏ **Output data:** In the main work area of the JupyterLab interface, the readers can see the plot as shown in Fig. 4.16. We can see that the Hartree potential from the numerical method (the Verlet algorithm) reproduces the exact Hartree potential of the helium atom given by Eq. (4.39), too.

### 4.14.3 DFT-LDA for helium

❏ **Purpose:** Finally, we calculate the ground-state energy of the helium atom within LDA.

❏ **Background:** For the LDA, the exchange function $\epsilon_x(\boldsymbol{r})$ and the exchange potential $\mathcal{V}_x[n(\boldsymbol{r})]$ are defined by (see Sec. 4.11.1):

$$\epsilon_x(\boldsymbol{r}) = C_2 n^{1/3}(\boldsymbol{r}) \text{ and } \mathcal{V}_x[n(\boldsymbol{r})] = \frac{4}{3} C_2 n^{1/3}(\boldsymbol{r}), \tag{4.166}$$

respectively, where $C_2 = -0.738$.

We adopt the PZ correlation function $\epsilon_c(r_s)$, which is defined by (see Table 4.2):

$$\epsilon_c(r_s) = \begin{cases} A\ln(r_s) + B + Cr_s\ln(r_s) + Dr_s & \text{if } r_s < 1 \\ \gamma/(1 + \beta_1\sqrt{r_s} + \beta_2 r_s) & \text{if } r_s \geq 1 \end{cases}, \tag{4.167}$$

where the parameters $A, B, C, D, \gamma, \beta_1, \beta_2$ are given in Table 4.2, too. Then, the correlation potential is given by

$$\mathcal{V}_c[n(\boldsymbol{r})] = \frac{\partial[\epsilon_c(\boldsymbol{r})n(\boldsymbol{r})]}{\partial n(\boldsymbol{r})}. \tag{4.168}$$

By substituting the electron density $n(\boldsymbol{r}) = 3/(4\pi r_s^3)$ from Eq. (4.112) into Eq. (4.168), we obtain:

$$\mathcal{V}_c(r_s) = \left(1 - \frac{r_s}{3}\frac{\mathrm{d}}{\mathrm{d}r_s}\right)\epsilon_c(r_s). \tag{4.169}$$

By substituting Eq. (4.167) into Eq. (4.169), we obtain [Thijssen (2007)]:

$$\mathcal{V}_c(r_s) = \begin{cases} A\ln(r_s) + B - \frac{A}{3} + \frac{2}{3}Cr_s\ln(r_s) + \frac{2D-C}{3}r_s, & \text{for } r_s < 1 \\ \gamma(1 + \frac{7}{6}\beta_1\sqrt{r_s} + \beta_2 r_s)/(1 + \beta_1\sqrt{r_s} + \beta_2 r_s)^2, & \text{for } r_s \geq 1 \end{cases}. \tag{4.170}$$

With the presence of the exchange-correlation potential, Eq. (4.156) becomes:

$$\left\{-\frac{1}{2}\frac{\mathrm{d}^2}{\mathrm{d}r^2} + \mathcal{V}_{en}(r) + \mathcal{V}_H(r) + \mathcal{V}_{xc}[n(\boldsymbol{r})]\right\}u(r) = \epsilon u(r), \tag{4.171}$$

where $\mathcal{V}_{xc}[n(\boldsymbol{r})] = \mathcal{V}_x[n(\boldsymbol{r})] + \mathcal{V}_c(r_s)$. Then, the total energy of the helium atom in Eq. (4.103) can be rewritten by

$$E = 2\epsilon - \int \mathcal{V}_H(r)u^2(r)\mathrm{d}r - \Delta\mathcal{E}_{\mathrm{xc}}[n(\boldsymbol{r})], \tag{4.172}$$

where $\Delta\mathcal{E}_{\mathrm{xc}}[n(\boldsymbol{r})]$ is expressed by

$$\begin{aligned} \Delta\mathcal{E}_{\mathrm{xc}}[n(\boldsymbol{r})] &= \int \mathcal{V}_{xc}[n(\boldsymbol{r})]n(\boldsymbol{r})\mathrm{d}\boldsymbol{r} - \mathcal{E}_{xc}[n(\boldsymbol{r})] \\ &= \int \{\mathcal{V}_{xc}[n(\boldsymbol{r})] - \epsilon_{xc}[n(\boldsymbol{r})]\}n(\boldsymbol{r})\mathrm{d}\boldsymbol{r} \\ &= 2\int \{\mathcal{V}_{xc}[n(\boldsymbol{r})] - \epsilon_{xc}[n(\boldsymbol{r})]\}u^2(\boldsymbol{r})\mathrm{d}r, \end{aligned} \tag{4.173}$$

where $\epsilon_{xc}[n(\boldsymbol{r})] = \epsilon_x[n(\boldsymbol{r})] + \epsilon_c(r_s)$. Note that we have to use the electron density $n(r)$ and $\mathcal{V}_H(r)$ for the helium atom.

❏ **How to run:** To run this tutorial, the readers will do the following command lines:

```
$ cd ~/SSP-QE/dft-he
$ jupyter-lab dft-lda-he.ipynb
```

- Line 1: Go to the `dft-he` directory that includes the input files.
- Line 2: Run `dft-lda-he.ipynb` with JupyterLab.

❏ **Input file:** The input files include two subroutine files (`schrodinger.py` and `poisson.py`) and a main file (`dft-lda-he.ipynb`). The main file calculates the total energy of the helium atom.

**SSP-QE/dft-he/dft-lda-he.ipynb**

```
# Import the necessary packages and modules
import numpy as np
from schrodinger import solve_schrodinger
from poisson import solve_poisson

# Set r from 0 to 15 bohr with 50000 steps
r, dr = np.linspace(0, 15, 50001, retstep=True)
r = r[1:]  # Skip r = 0
# Parameter for exchange potential Vx
C2 = -0.738;
# PZ parameters for correlation functional Vc
Aa = 0.0311; B= -0.048; C= 0.002; D= -0.0116; gamma=
     -0.1423; beta1= 1.0529; beta2= 0.3334;

# Define the exchange potential
def exc(n):
    V_x = (4/3)*C2*n**(1/3)
    e_x = C2*n**(1/3)
    return (V_x, e_x)

# Define the correlation potential
def cor(n):
    rs = (3/4/np.pi/n)**(1/3)
    V_c = np.piecewise(rs,[rs<1,rs>=1],[lambda rs:
        Aa*np.log(rs)+B-Aa/3+2/3*C*rs*np.log(rs)+(2*
        D-C)*rs/3, lambda rs: gamma/(1+beta1*rs
        **(1/2)+beta2*rs)*(1+7/6*beta1*rs**(1/2)+
        beta2*rs)/(1+beta1*rs**(1/2)+beta2*rs)])
```

```
24      e_c = np.piecewise(rs,[rs<1,rs>=1],[lambda rs:
            Aa*np.log(rs)+B+C*rs*np.log(rs)+D*rs, lambda
             rs: gamma/(1+beta1*rs**(1/2)+beta2*rs)])
25      return (V_c, e_c)
26
27  # The main DFT for helium with the LDA
28  def dft(V_en, maxiter=100, stop=0.001, correlation=
        False, verbose=False):
29      V_H = np.zeros_like(V_en)
30      V_x = np.zeros_like(V_en)
31      V_c = np.zeros_like(V_en)
32      e_x = np.zeros_like(V_en)
33      e_c = np.zeros_like(V_en)
34      eps = None
35      for i in range(maxiter):
36          eps_old = eps
37          V = V_en + V_H + V_x + V_c
38          V_xc = V_x + V_c
39          e_xc = e_x + e_c
40          # eigen energy and u(r)
41          eps, u = solve_schrodinger(r, V)
42          # normalize u(r)
43          u /= np.linalg.norm(u)*np.sqrt(dr)
44          # convergence of eigen energy
45          if eps_old is not None:
46              if verbose:
47                  print('Step %02d: eps = %f, |eps -
                        eps_old| = %f' %(i, eps, abs(eps
                         - eps_old)))
48              if abs(eps - eps_old) < stop:
49                  return 2*eps - dr*np.dot(V_H, u**2)
                        - 2*dr*np.dot(V_xc - e_xc, u**2)
50          elif verbose:
51              print
52          # update Hartree potential
53          U_H = solve_poisson(r, u)
54          V_H = 2*U_H/r
55          # total electron density
56          n = 2*(u**2/4/np.pi/r**2)
57          # update exchange potential
58          V_x, e_x = exc(n)
59          # update correlation potential
60          if correlation:
61              V_c, e_c = cor(n)
62          elif correlation:
63              V_c = 0
64              e_c = 0
```

```
    raise Exception('Not converged after %d
        iterations; |eps - eps_old| = %f' %(maxiter,
         abs(eps - eps_old)))

print('Total energy of He without correlation')
print('JOB DONE: total energy E = %f Ha' %(dft(-2/r,
     correlation=False,verbose=True)))
print('--------------------------------------')
print('Total energy of He with correlation')
print('JOB DONE: total energy E = %f Ha' %(dft(-2/r,
     correlation=True, verbose=True)))
```

❑ **Output data:** In main work area of the JupyterLab interface, the readers can see the total energy of the helium atom as follows:

```
Total energy of He without correlation
Step 01: eps = -0.320312, |eps - eps_old| = 1.674937
Step 02: eps = -0.625862, |eps - eps_old| = 0.305550
Step 03: eps = -0.470276, |eps - eps_old| = 0.155586
Step 04: eps = -0.537201, |eps - eps_old| = 0.066925
Step 05: eps = -0.505615, |eps - eps_old| = 0.031586
Step 06: eps = -0.519958, |eps - eps_old| = 0.014343
Step 07: eps = -0.513306, |eps - eps_old| = 0.006653
Step 08: eps = -0.516357, |eps - eps_old| = 0.003052
Step 09: eps = -0.514954, |eps - eps_old| = 0.001404
Step 10: eps = -0.515625, |eps - eps_old| = 0.000671
JOB DONE: total energy E = -2.716883 Ha
--------------------------------------
Total energy of He with correlation
Step 01: eps = -0.376953, |eps - eps_old| = 1.618296
Step 02: eps = -0.661568, |eps - eps_old| = 0.284615
Step 03: eps = -0.528656, |eps - eps_old| = 0.132912
Step 04: eps = -0.582932, |eps - eps_old| = 0.054276
Step 05: eps = -0.559113, |eps - eps_old| = 0.023819
Step 06: eps = -0.569275, |eps - eps_old| = 0.010162
Step 07: eps = -0.564880, |eps - eps_old| = 0.004395
Step 08: eps = -0.566772, |eps - eps_old| = 0.001892
Step 09: eps = -0.565948, |eps - eps_old| = 0.000824
JOB DONE: total energy E = -2.826743 Ha
```

The total energy without the correlation energy is $-2.716$ Ha, which is close to the reported value ($-2.72$ Ha [Thijssen (2007)]). However, it is less accurate than the Hartree-Fock method ($-2.85$ Ha, see Sec. 4.6). This is because the exchange potential by the LDA is an approximation for the uniform-electron charge. Therefore, the total energy can be improved by considering the correlation potential. As a result, we obtain the total energy with the PZ correlation functional is $-2.827$ Ha, which is close to the reported value ($-2.83$ Ha [Thijssen (2007)]). Although $-2.827$ Ha is still worse than the

Hartree-Fock result, it is an important improvement with respect to $-2.716$ Ha. The experimental value of the total energy of the helium atom is $-2.9$ Ha [Sucher (1958)].

# Chapter 5

# Solid-State Physics for Quantum ESPRESSO

In order to understand the input and output files of Quantum ESPRESSO, the readers need to know the meaning of technical words in solid-state physics. Here we give minimum information of solid-state physics for Quantum ESPRESSO. The authors wish that the readers take interest in solid-state physics even though their major is not physics.

## 5.1 Unit cell and Brillouin zone

**Unit cell:** In Quantum ESPRESSO, we consider a crystal. A crystal is solid with a periodic structure on the position of atoms in the solid. Thus, in order to express the structure of a crystal, it is sufficient to show a minimum block of the periodicity, which is called a unit cell. The unit cell is a box or a parallelepiped,[1] which can be represented by three vectors, each of which is called a **unit vector**, $\boldsymbol{a}_i$ $(i = 1, 3)$. The angles between the unit vectors can be 90°, 120°, or any value

[1] A parallelepiped is a box in which consists of three pairs of parallel faces.

*Quantum ESPRESSO Course for Solid-State Physics*
Nguyen T. Hung, Ahmad R. T. Nugraha, and Riichiro Saito

ISBN 978-981-4968-37-9 (Hardcover), 978-1-003-29096-4 (eBook)
www.jennystanford.com

depending on the symmetry of the crystal. In three-dimensional materials, we have 230 distinct crystal shapes, which are defined in the space group. The 230 kinds of crystals are classified by (A) 5 crystal families, (B) 14 Bravais lattices, or (C) 32 point groups of the unit cell. Here the Bravais lattice is defined by the nonequivalent translational symmetry of the lattice. In the input file of Quantum ESPRESSO, we input the information of $\boldsymbol{a}_i$ $(i = 1, 3)$. The relative coordinate of the $j$-th atom in the unit cell, $\boldsymbol{r}_j$ is given by fractional numbers $s_{ij}$ $(i = 1, 3, 0 \leq s_{ij} < 0)$ in the input file:

$$\boldsymbol{r}_j = \sum_i^3 s_{ij} \boldsymbol{a}_i. \tag{5.1}$$

It should be careful to set $s_{ij}$ in the unit cell when the unit cell is not cubic or cuboid. A **lattice vector** which is defined by

$$\boldsymbol{R} = p\boldsymbol{a}_1 + q\boldsymbol{a}_2 + r\boldsymbol{a}_3, \qquad (p, q, r; \text{integers}), \tag{5.2}$$

where $\boldsymbol{R}$ represents a position of the unit cell in the crystal. Thus, the coordinate of any atom in a crystal is given by the sum of $\boldsymbol{R} + \boldsymbol{r}_j$.

**Reciprocal lattice vector:** Any wave in the crystal[2] that propagates in the direction of $\boldsymbol{k}$ is expressed by $f(\boldsymbol{k}, \boldsymbol{r}) \equiv \exp(i\boldsymbol{k} \cdot \boldsymbol{r})$ which we call a plane wave. The product of $\boldsymbol{k} \cdot \boldsymbol{r}$ in $\exp(i\boldsymbol{k} \cdot \boldsymbol{r})$ is called a phase of the wave that has a periodicity of $2\pi$. If we take $\boldsymbol{r} = \boldsymbol{a}_i$ and $\boldsymbol{k} = \boldsymbol{b}_i$ so that $\boldsymbol{a}_i \cdot \boldsymbol{b}_i = 2\pi$, we get the same amplitude of $f$ for $\boldsymbol{r}$ and $\boldsymbol{r} + \boldsymbol{a}_i$, that is $f(\boldsymbol{b}_i, \boldsymbol{r}) = f(\boldsymbol{b}_i, \boldsymbol{r} + \boldsymbol{a}_i)$. Further, if we take $\boldsymbol{r} = \boldsymbol{a}_i$, we get $f(\boldsymbol{k}, \boldsymbol{a}_i) = f(\boldsymbol{k} + \boldsymbol{b}_i, \boldsymbol{a}_i)$. It means that the wave has a periodicity not only in the real space but also in the $\boldsymbol{k}$ space, which we call **reciprocal lattice**.[3] The vector $\boldsymbol{b}_i$ is a reciprocal lattice vector. The unit box in the $\boldsymbol{k}$ space which consists of the three $\boldsymbol{b}_i$ is called the **Brillouin zone**. Similar to the lattice vector $\boldsymbol{R}$, we can define **reciprocal lattice vector**, $\boldsymbol{G}$,

$$\boldsymbol{G} = \ell\boldsymbol{b}_1 + m\boldsymbol{b}_2 + n\boldsymbol{b}_3 \equiv (\ell, n, m), (\ell, n, m; \text{integers}), \tag{5.3}$$

[2] In quantum mechanics, electron behaves as a wave. Lattice oscillation is a wave like earthquake in the earth. X-ray propagates in the lattice as electro-magnetic wave.

[3] If you know the Fourier transform, you can imagine that the $\boldsymbol{r}$ and $\boldsymbol{k}$ can be converted to each other. In physics, we call the extended 6 dimensional space of $\{\boldsymbol{r}, \boldsymbol{k}\}$ as a phase space. Any motion of a particle is expressed by a curve in the phase space.

where $\boldsymbol{G}$ represents the position of the Brillouin zone in the $\boldsymbol{k}$ space. The integers of $(\ell, n, m)$ are called **the Miller indices** which are used in X-ray analysis (Sec. 5.2).

The $\boldsymbol{b}_i$ is obtained in the output file of Quantum ESPRESSO since $\boldsymbol{b}_i$ can be calculated by the $\boldsymbol{a}_i$ in the input file as follows:

$$\boldsymbol{a}_i \cdot \boldsymbol{b}_j = 2\pi\delta_{ij}, \qquad \delta_{ij} \equiv \begin{cases} 1 & \text{if } i = j \\ 0 & \text{if } i \neq j \end{cases}. \tag{5.4}$$

In fact, we have the following formula for $\boldsymbol{b}_i$ which satisfies Eq. (5.4):

$$\boldsymbol{b}_1 = \frac{2\pi(\boldsymbol{a}_2 \times \boldsymbol{a}_3)}{\boldsymbol{a}_1 \cdot (\boldsymbol{a}_2 \times \boldsymbol{a}_3)}, \boldsymbol{b}_2 = \frac{2\pi(\boldsymbol{a}_3 \times \boldsymbol{a}_1)}{\boldsymbol{a}_2 \cdot (\boldsymbol{a}_3 \times \boldsymbol{a}_1)}, \boldsymbol{b}_3 = \frac{2\pi(\boldsymbol{a}_1 \times \boldsymbol{a}_2)}{\boldsymbol{a}_3 \cdot (\boldsymbol{a}_1 \times \boldsymbol{a}_2)}, \tag{5.5}$$

where $\times$ denotes a vector product or cross product. Because of the properties of the vector product that the vector $\boldsymbol{a}_2 \times \boldsymbol{a}_3$ is perpendicular to the both $\boldsymbol{a}_2$ and $\boldsymbol{a}_3$, we can check that Eq. (5.5) satisfies Eq. (5.4). The Brillouin zone is given by six vertical bisectors[4] of $\boldsymbol{b}_i$ and $-\boldsymbol{b}_i$, $(i = 1, 3)$.

## 5.2 X-ray analysis

Once we define the unit vectors $\boldsymbol{a}_i$ in the input file of Quantum ESPRESSO, we can plot the 3D picture of the unit cell and lattice, Brillouin zone (see Sec. 5.1) by XCrySDen (see Sec. 3.1.1). Experimentally the lattice structure of a crystal is observed by X-ray spectroscopy. The most popular X-ray analysis is the Debye-Scherrer method in which the incident X-ray is scattered in the direction of an angle so-called $2\theta$ from the propagating direction of incident X-ray ($\boldsymbol{k}_i n$ in Fig. 5.1 (b)).[5] Thus, if we measure the intensity of the scattered X-ray as a function of $2\theta$ for calculating the lattice, we can directly compare the calculated results with the experimental results, which can also be automatically calculated by XCrySDen. The X-ray spectra

[4] A vertical or perpendicular bisector for a given vector is a plane that is perpendicular to the vector and that intersects at the center of a vector.
[5] $2\theta$ is called diffraction angle. The factor 2 of $2\theta$ can be understood by Fig. 5.1.

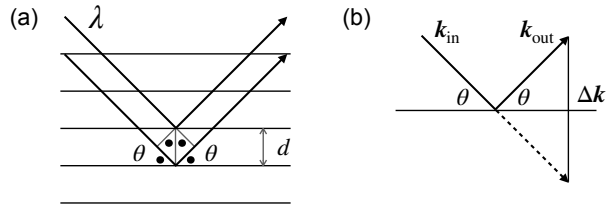


**Figure 5.1** (a) Bragg's condition in the real space. (b) Bragg's condition is the $\boldsymbol{k}$ space.

have one peak at a $2\theta$, which we can label by a Miller index $(\ell, n, m)$ (see Sec. 5.1), which we explain below.

**Bragg's condition:** For a periodic lattice, we can define a **crystal plane** as is shown by thin lines in Fig. 5.1 (a) on which many atoms exist. Since the lattice is periodic, we have many equivalent crystal planes parallel to the crystal plane. In Fig. 5.1 (a), we show the side-view of the crystal planes as parallel lines. When the incident X-ray with the wavelength $\lambda$ enters the crystal with an angle $\theta$ (solid dots in Fig. 5.1 (a)) measured from the plane, the diffracted X-ray that propagates in the direction of $\theta$, too, interfere to each other from two adjacent planes as shown in Fig. 5.1 (a). The condition of the constructive interference of the diffracted light is given by

$$2d \sin\theta = n\lambda, \qquad \sin\theta = \frac{n\lambda}{2d}, \tag{5.6}$$

where $d$ denotes the distance between two adjacent planes and $n = 1, 2, \ldots$ is an integer. Since $d$ and $\lambda$ are given, respectively, by the crystal and incident X-ray, only $\theta$'s for a given $n$ are possible direction of diffracted light. It is noted that the constructive interference occurs not only for the two planes but also for all (say $10^8$) parallel crystal planes in the crystal, which gives a strong X-ray intensity.[6] In Fig. 5.1 (b), we show that the diffraction angle of the scattered X-ray becomes $2\theta$ which is the reason why we use $2\theta$ in the horizontal axis of X-ray intensity plot. Since $|\boldsymbol{k}_{\rm in}| = |\boldsymbol{k}_{\rm out}| = k = 2\pi/\lambda$, the change of the

[6] If you know diffraction grating, the concept of the diffracting grating comes from the Bragg condition of one-dimensional periodicity.

wavevector $\Delta k$ is given by

$$\Delta k = 2k \sin\theta = 2k \cdot \frac{n\lambda}{2d} = \frac{2\pi}{d} \cdot n, \tag{5.7}$$

where we use Eq. (5.6). The value of $2\pi/d$ corresponds to a reciprocal lattice vector for a given $d$, which should be one of $\boldsymbol{G}$ defined by Eq. (5.3) for being $d$ as a distance of crystal plane. In fact, a crystal plane is defined by three points in the space, which is given by the end point of the three vectors of $\ell^{-1}\boldsymbol{a}_1$, $m^{-1}\boldsymbol{a}_2$, $n^{-1}\boldsymbol{a}_3$. The normal vector of the crystal plane is given by $\boldsymbol{G}$ with the Miller index $(\ell, m, n)$. Thus, $d$ ($2\theta$) for a given Miller index $(\ell, m, n)$ is expressed by

$$d = \frac{2\pi}{|\boldsymbol{G}|} = \frac{2\pi}{\sqrt{(\ell\boldsymbol{b}_1 + m\boldsymbol{b}_2 + n\boldsymbol{b}_3)^2}}. \tag{5.8}$$

When we plot X-ray intensity as a function of $2\theta$, we do the following procedure:

1. We assign the shape of the unit cell by $\boldsymbol{a}_i$, $(i = 1, 2, 3)$.
2. We get the reciprocal lattice vector $\boldsymbol{b}_i$, $(i = 1, 2, 3)$ by Eq. (5.5).
3. For a given Miller index, $(\ell, m, n)$, we calculate $d$ by Eq. (5.8).
4. From the calculated $d$, we get $\theta$ by Eq. (5.7) by putting $n = 1$ and $\lambda = 1.54$ Å.[7]
5. Then we calculated X-ray intensity at $2\theta$.

For calculation of X-ray intensity, we need to know the concepts of "structure factor" and "atomic form factor". However, we will not explain in detail those words for simplicity. Since the software or database gives the X-ray intensity automatically, it is sufficient for the reader to know the meaning of $2\theta$. If you wish to know how to calculate the two factors, please take a look at the solid-state textbook.

Nevertheless, we should comment on an important concept of the "structure factor" for assigning the crystal symmetry. The scattering amplitude of solid is given by the sum of the scattering

[7] This wavelength of X-ray is called for Cu K$\alpha$ line. If there is no specification of the wavelength in the experiment, you can use this value for comparison.

amplitude of atoms in the unit cell. The intensity of the X-ray is calculated by taking the square of the sum of scattering amplitudes of atoms in the unit cell. When the number of atoms in the unit cell is more than one, the destructive interface of the scattering amplitude occurs for two in-equivalent atoms in a unit cell. In this case, the X-ray intensity for some $(\ell, m, n)$ becomes zero, which is known as **X-ray extinction law**. The extinction law is calculated by calculating the structure factor. Since the extinct $(\ell, m, n)$ values depend on the lattice symmetry, the extinction law is important for identifying the symmetry of the lattice.

## 5.3 Plane wave expansion

The main results of Quantum ESPRESSO are energy dispersion or simply energy bands. The energy band is a function of electronic energy for an electron in the solid as a function of the wavevector (or crystal momentum) of the electron. The energy band is obtained by solving the Schrödinger equation in quantum mechanics (or more precisely the Kohn-Sham equation of the density-functional theory (Sec. 4.10.2)), $\mathcal{H}\Psi = E\Psi$, where $\mathcal{H}$ is the Hamiltonian operator, $\Psi$ denote the wavefunction and $E$ is energy. For a given $\mathcal{H}$, we solve $\mathcal{H}\Psi = E\Psi$ to obtain an eigenvalue $E$ and an eigenfunction $\Psi$.[8]

When there is a periodicity of the unit cell in the real space, we have another periodicity of the reciprocal lattice vector $\boldsymbol{G}$ in the $\boldsymbol{k}$ space (Sec. 5.1). In this case, the wavevector $\boldsymbol{k}$ is a conserved variable and thus a good quantum number for expressing both $E(\boldsymbol{k})$ and $\Psi_{\boldsymbol{k}}(\boldsymbol{r})$. For the energy $E(\boldsymbol{k})$, we have the periodicity of $E(\boldsymbol{k}) = E(\boldsymbol{k} + \boldsymbol{G})$ for any $\boldsymbol{G}$. For the wavefunction $\Psi$, using the periodicity of $\boldsymbol{G}$, we can expand $\Psi_{\boldsymbol{k}}(\boldsymbol{r})$ as follows:

$$\Psi_{\boldsymbol{k}}(\boldsymbol{r}) = \sum_{\boldsymbol{G}} C_{\boldsymbol{G}}(\boldsymbol{k}) e^{i(\boldsymbol{k}+\boldsymbol{G})\boldsymbol{r}}, \tag{5.9}$$

where $C_{\boldsymbol{G}}(\boldsymbol{k})$ is the coefficient to be solved for each $\boldsymbol{k}$ and the summation on $\boldsymbol{G}$ is taken for many $\boldsymbol{G}$. This expansion is called **plane**

[8] The Schrödinger equation is given by the differential equation, and thus we solve the eigenvalue problem of the differential equation.

**wave expansion**. The plane expansion is one of the Fourier series expansion[9] for a periodic function and thus if we take more number of $\boldsymbol{G}$, we get more precise value of the function.

Let us explain how to solve the Schrödinger equation by using the plane wave expansion. The Hamiltonian $\mathcal{H}$ is given by

$$\mathcal{H}(\boldsymbol{r}) = -\frac{\hbar^2}{2m}\Delta + \mathcal{V}(\boldsymbol{r}), \tag{5.10}$$

where $-\frac{\hbar^2}{2m}\Delta$ and $\mathcal{V}(\boldsymbol{r})$ are kinetic and potential energy operators, respectively, that satisfy the periodicity of the unit cell.[10] Thus, we can expand $\mathcal{V}$ by the reciprocal lattice vector $\boldsymbol{G}$ as follows:

$$\mathcal{V}(\boldsymbol{r}) = \sum_{\boldsymbol{G}} \mathcal{V}_{\boldsymbol{G}} e^{i\boldsymbol{G}\boldsymbol{r}}, \text{ where } \mathcal{V}_{\boldsymbol{G}} = \frac{1}{N_{\mathrm{u}}} \int \mathrm{d}\boldsymbol{r}' \mathcal{V}(\boldsymbol{r}') e^{-i\boldsymbol{G}\boldsymbol{r}'}. \tag{5.11}$$

Here integration on $\boldsymbol{r}'$ is taken over the crystal and $N_u$ denotes the number of the unit cells in the crystal. By substituting Eqs. (5.9), (5.10), and (5.11) into $\mathcal{H}\Psi = E\Psi$, we get

$$\begin{aligned} &\sum_{\boldsymbol{G}} \frac{\hbar^2}{2m}(\boldsymbol{k}+\boldsymbol{G})^2 C_{\boldsymbol{G}} e^{i(\boldsymbol{k}+\boldsymbol{G})\boldsymbol{r}} + \sum_{\boldsymbol{G}',\boldsymbol{G}''} \mathcal{V}_{\boldsymbol{G}'} C_{\boldsymbol{G}''} e^{i(\boldsymbol{k}+\boldsymbol{G}'+\boldsymbol{G}'')\boldsymbol{r}} \\ &\quad = E \sum_{\boldsymbol{G}} C_{\boldsymbol{G}} e^{i(\boldsymbol{k}+\boldsymbol{G})\boldsymbol{r}}. \end{aligned} \tag{5.12}$$

---

[9] For a periodic function $f(x)$ with a period $L$, we can express

$$f(x) = \sum_{p=0}^{\infty} f_p e^{i2\pi px/L}$$

which is called the Fourier series expansion. Here $2\pi/L$ is the reciprocal lattice vector for $L$.

[10] The Laplacian $\Delta$ are invariant for transformation of $x' = x + a$ and $\mathcal{V}(\boldsymbol{r}+\boldsymbol{a}) = \mathcal{V}(\boldsymbol{r})$.

In the second term, we put $\boldsymbol{G}' + \boldsymbol{G}'' = \boldsymbol{G}$ and take the term of $e^{i(\boldsymbol{k}+\boldsymbol{G})\boldsymbol{r}}$, we get the following equation,[11]

$$\frac{\hbar^2}{2m}(\boldsymbol{k}+\boldsymbol{G})^2 C_{\boldsymbol{G}} + \sum_{\boldsymbol{G}''} \mathcal{V}_{\boldsymbol{G}-\boldsymbol{G}''} C_{\boldsymbol{G}''} = E C_{\boldsymbol{G}}. \tag{5.13}$$

Eq. (5.13) is simultaneous equation for obtaining $C_{\boldsymbol{G}}$. In the real calculation, when we define $N \times N$ Hamiltonian matrix

$$\mathcal{H}_{\boldsymbol{G}\boldsymbol{G}'} = \begin{cases} \dfrac{\hbar^2}{2m}(\boldsymbol{k}+\boldsymbol{G})^2, & \text{if } (\boldsymbol{G} = \boldsymbol{G}') \\ \mathcal{V}_{\boldsymbol{G}-\boldsymbol{G}'}, & \text{if } (\boldsymbol{G} \neq \boldsymbol{G}') \end{cases}. \tag{5.14}$$

Eq. (5.13) is expressed by a matrix equation $\mathcal{H}\boldsymbol{C} = E\boldsymbol{C}$ from which we can obtain eigenvalue $E$ and eigenvector $\boldsymbol{C}$ by diagonalizing the matrix by numerical calculation.[12]

## 5.4 Cut-off energy and pseudopotential

The size of the Hamiltonian matrix, $N$, is given by the number of reciprocal lattice vectors $\boldsymbol{G}$. Although the accuracy of calculation monotonically increases with increasing $N$, the memory size and computational time of the computer quickly increases with increasing $N$. Thus, we must find a reasonable $N$ by plotting the total energy and computational time as a function of $N$.

**Cut-off energy**: In the first-principles calculation, we do not usually compare $N$ for different calculations but **cut-off energy** in units of atomic unit (see Table 4.1) which is defined by

$$E_{\text{cut-off}} = \frac{\hbar^2}{2m}\boldsymbol{G}_{\text{max}}^2, \tag{5.15}$$

where $\boldsymbol{G}_{\text{max}}$ is the largest reciprocal lattice vector. We use the cut-off energy because the values of $N$ depend on the size of the unit

[11] Since $e^{i(\boldsymbol{k}+\boldsymbol{G})\boldsymbol{r}}$ are independent functions for different values of $\boldsymbol{G}$, the coefficients of the both-hand sides should be identical. Further, we change the summation on $\boldsymbol{G}'$ and $\boldsymbol{G}''$ to the sum on $\boldsymbol{G}$ and $\boldsymbol{G}''$. Note that $\boldsymbol{G}' = \boldsymbol{G} - \boldsymbol{G}''$.

[12] LAPACK is the name of a famous software package for linear algebra calculation including diagonalizing a matrix (zheev).

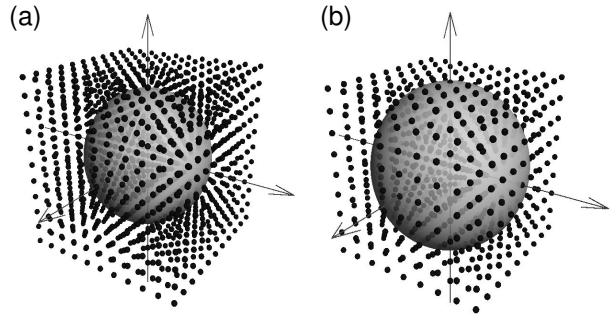


**Figure 5.2** Cut-off energy. Dots in the $k$ space represent the reciprocal lattice vectors $\boldsymbol{G}$. When we define a sphere whose diameter is $|\boldsymbol{G}_{\max}|$, we will use $\boldsymbol{G}$'s in the sphere. Then cut-off energy is given by Eq. (5.15). (a) When the unit cell is large, $\boldsymbol{G}$ becomes small, and thus we have more $\boldsymbol{G}$'s in the sphere. (b) When the unit cell is relatively small, the number of $\boldsymbol{G}$'s becomes small even for the same cutting energy. Reprinted with permission from Asakura Publishing Co. Ltd.

cell. When the size of the unit cell is relatively large because of many atoms in the unit cell, the corresponding absolute value of $\boldsymbol{G}$ becomes small as shown in Fig. 5.2 (a). In order to obtain the same accuracy for calculating the atomic potentials in the smaller unit cell (Fig. 5.2 (b)), a larger $\boldsymbol{G}_{\max}$ is needed. On the other hand, when we use the same cut-off energy for two different sizes of unit cells, we expect the accuracy of the calculation to be similar to each other.

The selection of cut-off energy also depends on the selection of **pseudopotential** for each atom, which we explain below. As shown in Eq. (5.12), the off-diagonal matrix element of the Hamiltonian matrix is the Fourier transform of the crystal potential $V$, which is given by the sum of atomic potentials. If we adopt the real atomic potential for an atom, we expect a large Coulomb potential, $-Ze^2/(4\pi\epsilon_0 r)$ ($Z$ is the atomic number of the atom). Fourier transform of $1/r$ is $1/|\boldsymbol{G}|^2$ which is a slowly decreasing function of $|\boldsymbol{G}|$ compared with $\exp(-C|\boldsymbol{G}|)$ ($C$ is a constant) in three dimensions. Thus, it is not a good idea that we do not adopt the real atomic potential in the plane wave expansion.

**Pseudopotential**: For discussing most of the solid-state properties, inner-core electrons in the $1s$, $2s$, $2p$ atomic orbitals for a heavy element are not so important. Only the valence electrons near the highest occupied orbitals contribute to the properties. The valence

electrons feel screened Coulomb potentials by core electrons except for the core region of the atom. **Pseudopotential** is a potential in which the core region of an atom is artificially smoothed out near $\boldsymbol{r} = 0$ so that we do not need many $\boldsymbol{G}$ (or $N$) for obtaining $\mathcal{V}_{\boldsymbol{G}}$ with the same numerical accuracy.

In history, pseudopotentials have been proposed by many researchers, which we select from the list of pseudopotentials on the web pages as input files of Quantum ESPRESSO. The pseudopotential is given as a function of distance from the center of atom $r$ and the density of electrons based on the density-functional theory (Sec. 4.12.3).

**Norm-conserving pseudopotential**: Although we will not go to in detail of the selection of pseudopotential, it is important to point out that the readers should select so-called **norm-conserving pseudopotential** if they want to use the wavefunction for calculating some matrix elements such as for calculating optical absorption spectra. For norm-conserving pestilential, (1) the pseudo wavefunction that is obtained by solving the Kohn-Sham (or the Schrödinger equation in the DFT) equation coincides with the real wavefunction for a larger $r$ than a cut-off radius, $r_{\rm cut}$. (2) At $r_{\rm cut}$, the values and derivative of the pseudo wavefunction and real wavefunction should be the same. (3) For $r < r_{\rm cut}$, the norms of the pseudo wavefunction and real wavefunction are selected to be the same, though the pseudo wavefunction does not have a node as a function of $r$. (4) The eigenvalues or energies for pseudopotentials are the same as those by real potentials. The solid-state properties calculated by norm-conserving pseudopotentials can be compared with experimental results with reasonably high accuracy. On the other hand, **ultra-soft pseudopotential** is another direction of pseudopotentials in which the number of plane waves can be reduced significantly by neglecting the norm-conserving conditions. If one wants to obtain the energy band of many atoms in a large unit-cell, the selection of ultra-soft pseudopotential is important.

## 5.5 Energy bands and density of states

**Energy bands**: By selecting $k$ points on high symmetry lines in the Brillouin zone in the input file of `bands.x` (see Sec. 3.2.2), we can

obtain the energy as a function of $k$, $E(k)$, which we call **energy dispersion** or simply **energy bands**. The name of energy bands comes from the fact that the energy dispersion exists in a finite energy region. For a given energy dispersion, two electrons with the up- and down-spin of electron per unit cell can be occupied. As far as two energy dispersion does not cross each other, we can occupy two electrons per energy band from the lowest bands to the **valence band** which is the highest occupied energy band. Suppose two energy bands cross each other before filling the lower energy band fully. In that case, the electron starts to occupy the higher energy band with keeping the common highest occupied energies of the two energy bands, which is called the **Fermi energy**, $E_F$.

**Density of states**: For a given energy dispersion $E(k)$, when we denote d$N$ for the number of states in the energy region from $E$ to $E + \mathrm{d}E$, we define **density of states (DOS)**, $D(E)$, as $D(E) \equiv \mathrm{d}N/\mathrm{d}E$. The unit of DOS can be "states/eV/unit cell". DOS becomes large when $E(k)$ is flat in the energy dispersion.

Since the wavevector of a crystal in one direction is given by $k = 2\pi p/Na$, $(p = 0, 1, 2, ..., N-1)$, where $N$ is the number of the unit cell in the direction and $a$ is the lattice constant. In a single crystal with a size of 1 cm, since $N$ is large $N(\sim 10^8)$, the wavevector $k$ exists almost continuously, which is why energy dispersion $E(k)$ is generally given a function of $k$. For each $k$ state, we can put two electrons with up-spin and down-spin, and thus in total, we can put $2N$ electrons for $N$ $k$ states. Since there are $N$ unit cells in the direction, we can say that we can occupy two electrons per unit cell, whose situation is the same as the case of three dimensions.

In Quantum ESPRESSO, DOS is calculated by making a mesh of $k$ in the Brillouin zone. For a given $E$ and for a given three-dimensional box made of mesh, if there is an equi-energy surface of $E(k) = E$, the area of the surface in the mesh is proportional to DOS. The number of mesh specified by the input file of DOS (see Sec. 3.2.3) is about 10 $\times$ 10 $\times$ 10 since we can interpolate $E(k)$ in the box of the mesh. This method is called the "tetrahedron method", from which you can learn more about the tetrahedron method for obtaining DOS.

**Metal, semimetal, semiconductor, insulator**: Using the output values of the energy bands, the Fermi energy, and density of states, we classify the materials. When the Fermi energy is located in the middle energy of the energy band, electrons in the energy band can

easily excite the unoccupied states within the same energy band. This situation is called "**metal**". We can say that metal is defined by a finite density of states at the Fermi energy, $D(E_{\rm F}) \neq 0$. When the valence band is fully occupied, and the next higher energy band, that is **conduction band** is unoccupied, we usually have an **energy gap**. An energy gap, $E_g$, is defined by an energy difference between the highest energy of valence band and the lowest energy of conduction bands.[13] Since there are no states in the energy gap region, the occupied electron in the valence band needs at least $E_g$ for exciting the electron. This situation corresponds to "semiconductor" or "insulator". The difference between "semiconductor" or "insulator" is the value of $E_g$. If $E_g < 3$eV, we can say that the material is semiconductor, while $E_g > 5$ eV, we call "insulator".[14]

When $E_g = 0$ or $E_g$ is a small value compared with the thermal energy $k_B T$ ($k_B$ is the Boltzmann constant), part of electrons in the valence band can be excited at the finite temperature. In this situation, if the density of states at the Fermi energy is much smaller than $D(E_F)$ of three-dimensional metal, the number of carriers for flowing an electric current[15] becomes small, too. Such material is called **semimetal**. A typical example of semimetal is graphene in which $E_g = 0$ and $D(E_F) = 0$.

**k sampling points**: It is noted that Quantum ESPRESSO calculation of a metal takes more computational time than that of a semiconductor in the SCF calculation (Sec. 4.5). In the SCF calculation, we evaluate the charge density $\rho(r)$ by occupying electrons in the energy bands, which require more $k$ points in the case of metal. When we evaluate $\rho(r)$ for a semiconductor, we can use a few numbers of sampling $k$ points in the Brillouin zone. When all energy bands are fully occupied or unoccupied, we need only a few (even one) $k$ points. However, in the case of metal, on the other hand, since we need to consider the occupation up to the Fermi energy, more $k$ points are needed for obtaining the **Fermi surface** (a closed

[13] If you are a chemist, you can imagine that an energy gap is a kind of HOMO-LUMO gap of a molecule in solid.
[14] For $3 < E_g < 5$ eV, we can say "wide-gap semiconductor".
[15] Carrier is either an electron or a hole that conducts an electronic current in a solid. A hole is an unoccupied state in the almost occupied energy band. Like a going-up beer bubble, the unoccupied states carry a positive charge in the solid in the direction opposite to that of the electron.

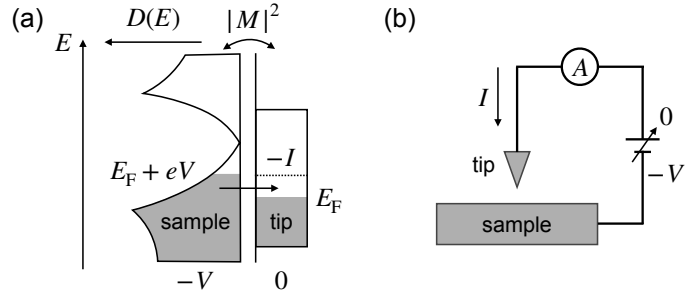


**Figure 5.3** Scanning tunneling spectroscopy. (a) Tunneling current $I$ (Eq. (5.16)) flows from the metallic materials (left) to a scanning metallic tip (right) in the energy region between $E_F$ and $E_F + eV$, in which electrons occupied in the metallic side while not occupied in the tip side. (b) In the experiment, we fix the position of the tip, we change the voltage. Then the value $dI/dV$ is proportional to the density of state $D(E_F + eV)$ (Eq. (5.17)).

surface in the $k$ space on which the energy is the Fermi surface) which costs more CPU times. Total energy depends on the number of the sampling points, which should be checked by increasing the sampling points.

## 5.6 Experiments for $E(k)$ and DOS

The calculated $E(k)$ and DOS $D(E)$ by Quantum ESPRESSO can be directly compared with **ARPES** (angle-resolved photo-electron spectroscopy) and **STS** (scanning tunneling spectroscopy) measurements, respectively. In ARPES, we can measure a kinetic energy $E$ of photo-excited electron which emitted from the materials as a function of the momentum direction of photo-electron $\boldsymbol{k}$ emitted into the vacuum by illuminated by light (photoelectric effect), which can be directly compared with the calculated electronic energy dispersion, $E(k)$. Since the electrons exist in the occupied energy bands, we can compare the $E(k)$ only for the occupied energy bands down to 10–20 eV below the Fermi energy. The range of energy that we can observe by ARPES depends on the light source.

In STS measurement (see Fig. 5.3 (b)), we measure the tunneling electric current $I$ on a sharp metallic tip, which is electrically biased by an applied voltage. If we assumed that the tunneling probability

$|M|^2$ does not depend on the energy of electrons, the tunneling current $I$ is given by

$$I = \int_{E_F}^{E_F+eV} |M|^2 D(E) \mathrm{d}E, \tag{5.16}$$

from which the differential conductance, $\mathrm{d}I/\mathrm{d}V$ is calculated as follows:

$$\frac{\mathrm{d}I}{\mathrm{d}V} = |M|^2 D(E_F + eV) \propto D(E_F + eV). \tag{5.17}$$

We get from Eq. (5.17) that the differential conductance defined by $\mathrm{d}I/\mathrm{d}V$ is proportional to the density of state at $E = E_F + eV$. Thus, we can measure $D(E)$ by changing $V$ near the $E_F$. In the case of STS, the sample should be a conductor to have a finite $I$. Further, in order to avoid thermal broadening of the Fermi distribution function, the STS measurement is performed at a much lower temperature than the room temperature.

## 5.7 Phonon dispersion

Phonon dispersion relation is the phonon frequencies in units of $\mathrm{cm}^{-1}$ (1 eV = 8065 $\mathrm{cm}^{-1}$) as a function of the wavevector of phonon, $q$. In Fig. 5.4, we show (a) phonon dispersion and phonon density of states of graphene. In Quantum ESPRESSO, we specify $q$ by connecting symmetric points in the Brillouin zone, as is the case of the electronic energy band. When we have $N$ atoms in a unit cell, we have $3N$ phonon dispersion in the Brillouin zone in which 3 of the $3N$ phonon dispersion are acoustic phonon modes whose frequency is zero at the zone-center (or the $\Gamma$ point) of the Brillouin zone. The remaining $3N - 3$ phonon modes are optical phonon modes. For the three acoustic modes, one of the three acoustic modes is longitudinal acoustic (LA) phonon mode, in which the oscillational direction is parallel to the propagation direction of the wave of oscillation. The remaining two acoustic phonon modes are transverse acoustic (TA) phonon modes, in which the oscillational direction is perpendicular to the propagation direction. For optical phonon modes, $N - 1$ modes are longitudinal optic (LO) modes, and the remaining $2N - 2$ are

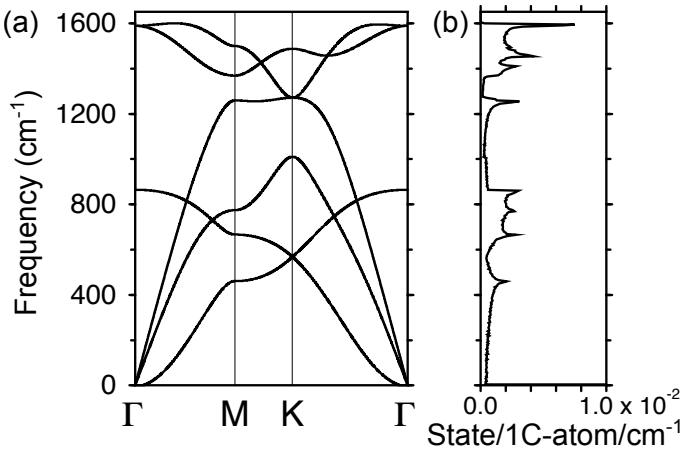


**Figure 5.4** (a) Phonon dispersion of graphene. The unit of frequency is $cm^{-1}$ (1 eV = 8065 $cm^{-1}$). (b) Phonon density of states.

transverse optic (TO) modes. The assignment of LA, TA, LO, and TO is possible by looking at the direction of oscillation of each atom at the Γ point (or near the Γ point for acoustic modes by the Material Cloud (see Sec. 3.3.1.)).

When the material is two-dimensional, such as graphene as shown in Fig. 5.4, TA modes are further classified by in-plane TA (iTA) and out-of-plane TA (oTA), and TO modes are classified by in-plane TO (iTO) and out-of-plane TO (oTO) phonon modes. In LA and LO modes, since the propagation direction is in-plane, we do not usually say iLA or iLO. On the other hand, we sometimes call oTA and oTO modes as ZA and ZO modes which shows that the oscillational direction is in the direction of *z* axis for *xy* plane of two-dimensional materials.

Phonon dispersion of a given material is calculated by solving the so-called dynamical matrix. In the dynamical matrix, we define force constants between two atoms in the crystal. In order to define the force constant, any atom should have a restoring force for all directions of the displacement of the atom. This situation corresponds to the ground state in which the total energy has a minimum at the optimized position as a function of displacement of each atom. The restoring force can be calculated by the gradient of the total energy by displacing an atom in the unit cell with keeping other

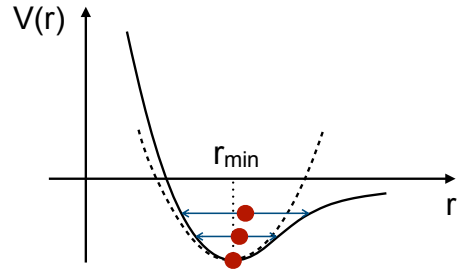


**Figure 5.5** Anharmonicity of oscillation. When we expand the potential $V(r)$ as a displacement $x$ measured from the minimum of $V(r)$, $r_{\min}$ the potential can be approximated by a harmonic potential ($\propto x^2$) as shown in the dashed line. When the amplitude of oscillation becomes relatively large, the centers of oscillation that are shown as dots shift to large values of $r$ because of the deviation of $V(r)$ from the harmonic potential. The shift of dots corresponds to the thermal expansion of the materials. Thus, the anharmonicity of the potential is essential for thermal expansion.

atoms at the optimized position. If the optimization of the lattice structure is not sufficient, some restoring force might be negative, which gives an imaginary phonon frequency for the acoustic phonon modes at the Γ point.

In the phonon calculation by Quantum ESPRESSO, we usually adopt so-called "density-functional perturbation theory (DFPT)" [Baroni *et al.* (2001)] in which we need to optimize structure in relatively high precision by calculating the norm of the restoring forces of each atom, which takes a much more computational time than that of the electronic energy band.

When we get the minimum of the total energy by optimization, we can expand the total energy by a displacement $x$ in which the quadratic function of the displacement, $kx^2/2$, corresponds to the harmonic oscillation with a spring constant $k$. However, when the displacement is relatively large (for example, 10% of the lattice constant, $a$), an anharmonic term which is proportional to $x^3$ can not be neglected anymore as shown in Fig. 5.5. When the amplitude of oscillation becomes relatively large, the center of oscillation that is shown a dot for each amplitude shift to a larger value of $r$ than $r_{\min}$ because of the deviation of $V(r)$ from the harmonic potential (dashed line). The shift of dots corresponds to the thermal expansion of the materials. Thus, the anharmonicity of the potential is essential for thermal expansion.

## 5.8 Electron-phonon interaction

Since both electrons and phonons exist as a function of wavevector in solid, we expect the interaction between an electron and a phonon, that is, electron-phonon interaction, when the energy and momentum conservation satisfies in the interaction. The origin of electron-phonon interaction can be understood by the oscillation of atomic potential by lattice oscillation which modifies the electronic energy. In Quantum ESPRESSO, we obtain the electronic energy band by assuming that the atoms do not move. However, this assumption is an approximation in the case of finite temperature,[16] in which we have a finite amplitude of lattice oscillation, 0.01–0.1 Å, whose energy is the order of $k_{\mathrm{B}}T$ ($k_{\mathrm{B}}$ is the Boltzmann constant). Thus, the oscillation of the lattice accelerates (or decelerates) the velocity of an electron to have a thermal equilibrium state. Because of the law of action and reaction, the motion of an electron can modify the lattice oscillation, too. However, since the mass of an atom is $10^3 - 10^5$ times larger than that of an electron, like a small bird on the shoulder of a person, the energy of the electron depends only on the position but not on the velocity of the atom. This means that the electron can easily follow the motion of the atom without any delay of the motion of the electron. This approximation is called "**adiabatic approximation**". In this approximation, the motion of the lattice is not affected much by the motion of electrons as the motion of the human is not affected by the motion of the bird on the shoulder even though the person feels the bird.

When we denote distortion of an atom, $\delta\boldsymbol{R}$, from the original position of $\boldsymbol{R}$ as shown in Fig. 5.6, the distorted atomic potential $v(\boldsymbol{r} - \delta\boldsymbol{R} - \boldsymbol{R})$ can be expanded by

$$v(\boldsymbol{r} - \boldsymbol{R} - \delta\boldsymbol{R}) = v(\boldsymbol{r} - \boldsymbol{R}) + v'(\boldsymbol{r} - \boldsymbol{R})\delta\boldsymbol{R}, \tag{5.18}$$

in which the second term of the right-hand side of Eq. (5.18) is called deformation potential. When we adopt the adiabatic approximation

[16] Lattice does move even at $T = 0$ K, which is known as zero-point motion of the atom. An origin of the zero-point motion is the uncertainty principles of quantum mechanics. It is known that the zero-point motion gives a not-negligible contribution to thermal properties of materials.

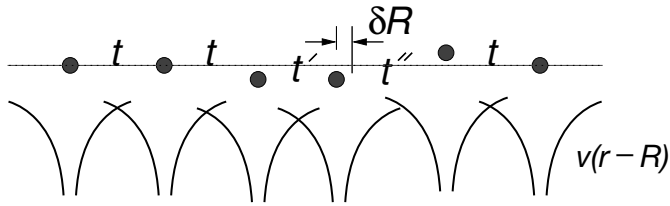


**Figure 5.6** Deformation potential. Solid lines are atomic potentials. When an atom shifts position by $\delta\boldsymbol{R}$, the potential energy for an electron (showing solid circles) of the nearest neighbor atom increases (or decreases) by moving away (or approaching) the atom. Further the absolute value of the transfer integral $|t|$ decreases or increases by moving away (or approaching) the atom.

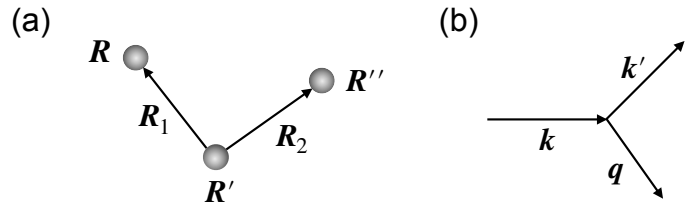


**Figure 5.7** (a) Three-centers integral $M(\boldsymbol{R}', \boldsymbol{R}, \boldsymbol{R}'')$ in Eq. (5.20) is a function of the positions of three atoms, $\boldsymbol{R}', \boldsymbol{R}, \boldsymbol{R}''$. The integration is given as a function of the relative coordinate $\boldsymbol{R}_1 = \boldsymbol{R} - \boldsymbol{R}'$, $\boldsymbol{R}_2 = \boldsymbol{R}'' - \boldsymbol{R}'$. (b) The momentum of an electron $\hbar\boldsymbol{k}$ is scattered to $\hbar\boldsymbol{k}' = \hbar\boldsymbol{k}' - \hbar\boldsymbol{q}$ by emitting a phonon with the crystal momentum $\hbar\boldsymbol{q}$.

that the atomic wavefunction follows the position of the atom, the atomic wavefunction of the distorted atom is given by

$$\varphi(\boldsymbol{r} - \boldsymbol{R} - \delta\boldsymbol{R}) = \varphi(\boldsymbol{r} - \boldsymbol{R}) + \varphi'(\boldsymbol{r} - \boldsymbol{R})\delta\boldsymbol{R}. \tag{5.19}$$

When we consider the integration of the atomic potential by the atomic wavefunction, $\langle\varphi|v|\varphi\rangle$, the correction of $\langle\varphi|v|\varphi\rangle$ by putting Eqs. (5.18) and (5.19), up to the linear term of $\delta\boldsymbol{R}$, we get the expression of electron-phonon interaction. The correction of $\langle\varphi|v|\varphi\rangle$ appears in the diagonal and off-diagonal matrix element of the Hamiltonian matrix, which we call on-site and off-site electron-phonon interaction, respectively.

When we consider electron-phonon interaction in solid, an electron is scattered from $\boldsymbol{k}$ to $\boldsymbol{k}'$ states in the $k$ space. When we

consider the Bloch orbital $\Phi(\boldsymbol{k}, \boldsymbol{r})$ for electronic states and the lattice distortion of a phonon with the wavevector, $\boldsymbol{q}$, $\delta\boldsymbol{R} = A\exp(-i\boldsymbol{q}\boldsymbol{R})$, the matrix element between the Bloch orbitals of $\boldsymbol{k}$ and $\boldsymbol{k}'$ is given by

$$\begin{aligned} V_{\boldsymbol{k}',\boldsymbol{k}} &\equiv A\langle\Phi(\boldsymbol{k}', \boldsymbol{r})|v'(\boldsymbol{r})\exp(-i\boldsymbol{q}\boldsymbol{R})|\Phi(\boldsymbol{k}, \boldsymbol{r})\rangle \\ &= \frac{1}{N}\sum_{\boldsymbol{R},\boldsymbol{R}',\boldsymbol{R}''} \exp(-i\boldsymbol{k}'\boldsymbol{R} + i\boldsymbol{k}\boldsymbol{R}'' - i\boldsymbol{q}\boldsymbol{R}')M(\boldsymbol{R}, \boldsymbol{R}', \boldsymbol{R}''), \end{aligned} \tag{5.20}$$

where $M(\boldsymbol{R}', \boldsymbol{R}, \boldsymbol{R}'')$ is three-centers integral as a function of $\boldsymbol{R}', \boldsymbol{R}, \boldsymbol{R}''$, $M = A\langle\varphi(\boldsymbol{r} - \boldsymbol{R})|v'(\boldsymbol{r} - \boldsymbol{R}')|\varphi(\boldsymbol{r} - \boldsymbol{R}'')\rangle$. When we adopt the relative coordinates $\boldsymbol{R}_1 = \boldsymbol{R} - \boldsymbol{R}'$, $\boldsymbol{R}_2 = \boldsymbol{R}'' - \boldsymbol{R}'$ to the coordinate $\boldsymbol{R}'$, as shown in Fig. 5.7, $M$ can be expressed as a function of $\boldsymbol{R}_1$ and $\boldsymbol{R}_2$, $M(\boldsymbol{R}_1, \boldsymbol{R}_2)$. Then we can take the summation on $\boldsymbol{R}'$ in Eq. (5.20), and we get

$$\begin{aligned} V_{\boldsymbol{k}',\boldsymbol{k}} &= \frac{1}{N}\sum_{\boldsymbol{R}_1,\boldsymbol{R}',\boldsymbol{R}_2} \exp(-i\boldsymbol{k}'\boldsymbol{R}_1 + i\boldsymbol{k}\boldsymbol{R}_2 + i(-\boldsymbol{q} - \boldsymbol{k}' + \boldsymbol{k})\boldsymbol{R}')M(\boldsymbol{R}_1, \boldsymbol{R}_2) \\ &= \delta(-\boldsymbol{q} - \boldsymbol{k}' + \boldsymbol{k})\sum_{\boldsymbol{R}_1,\boldsymbol{R}_2} \exp(-i\boldsymbol{k}'\boldsymbol{R}_1 + i\boldsymbol{k}\boldsymbol{R}_2)M(\boldsymbol{R}_1, \boldsymbol{R}_2) \end{aligned} \tag{5.21}$$

where $\delta(-\boldsymbol{q} - \boldsymbol{k}' + \boldsymbol{k})$ is the delta function that shows the conservation of momentum, $\boldsymbol{k} = \boldsymbol{k}' + \boldsymbol{q}$, before and after the scattering. In Fig. 5.7 (b), we show that the momentum of an electron $\hbar\boldsymbol{k}$ is scattered to $\hbar\boldsymbol{k}' = \hbar\boldsymbol{k} - \hbar\boldsymbol{q}$ by emitting a phonon with the crystal momentum $\hbar\boldsymbol{q}$. It is noted here that the delta function is satisfied even when $\boldsymbol{k} = \boldsymbol{k}' + \boldsymbol{q} + \boldsymbol{G}$ ($\boldsymbol{G}$ is the reciprocal lattice vector) since the exponential function $\exp(i(-\boldsymbol{q} - \boldsymbol{k}' + \boldsymbol{k})\boldsymbol{R}') = \exp(i\boldsymbol{G}\boldsymbol{R}')$ becomes the unity. The scattering with $\boldsymbol{G} \neq 0$ in which additional momentum from the lattice is given (or released) to electron is called the Umklapp process while the scattering with $\boldsymbol{G} = 0$ is called normal process. In both cases the energy and momentum that include the crystal momentum conserved during the scattering processes. The electron-phonon interaction is essential for occurrence of electrical resistance, superconductivity, and Raman spectroscopy.

In Quantum ESPRESSO, the electron-phonon matrix element is calculated as a function of $\boldsymbol{k}$ and $\boldsymbol{q}$ (see Sec. 3.3.3). The calculated

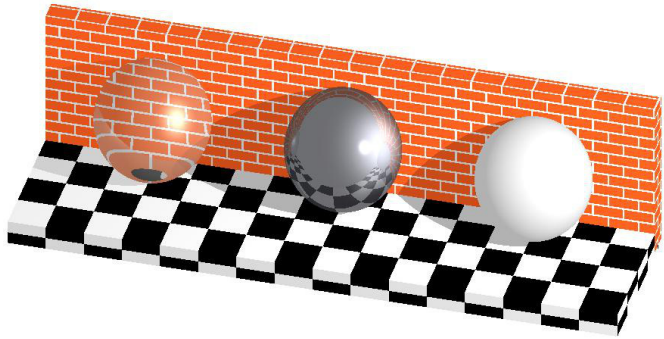

**Figure 5.8** When light comes to a material, the light is transparent (left), reflected (center), or scattered (right). Even for the case of transparent, the direction of light changes after the transmission. Reprinted with permission from Asakura Publishing Co. Ltd.

matrix elements are used for estimating the critical temperature of the superconductivity or resonant Raman intensity.

## 5.9 Optical properties of solid

When light hits a material (see Fig. 5.8), the light is transparent (left), reflected (center), or scattered (right). Even in the case of transparent properties, the direction of light changes after the transmission. It means that all phenomena are related to the interaction of a photon and materials.

Light or a photon interacts with an electron (or electrons) in the materials. The optical properties of the materials consist of (1) absorption, (2) emission, and (3) scattering of light. In the case of semiconductors, optical absorption (or emission) occurs for the photon whose energy is more than the energy gap of the semiconductor. Suppose the momentum and energy of a photon are matched to the difference of momentum and energy between the initial and final electronic states. In that case, the optical absorption occurs by annihilating the photon and by exciting the electron from the initial to the final states. This type of excitation for the electron is called single-particle excitation. On the other hand, for metal or heavily doped semiconductors, an electric field of a photon as

an electro-magnetic wave can excite an electric current of metal. The optical absorption occurs by the Joule heat by the current. In this case, since the current is the collective motion of electrons, this type of excitation is called collective excitation. Usually, the single-particle excitation and collective excitation occur exclusively or simultaneously for a given energy of the photon.

Scattering of light in the semiconductor is defined as a sequential process of optical absorption and emission, in which the emitted light propagates in any direction of solid angle. The scattering amplitude depends on materials as a function of photon frequency, which determines the color of the materials. On the other hand, in metal, the reflection of light occurs by screening the electric field of the photon by the induced electric current, which is the origin of metallic luster.

For the region of the wavelength of the visible light, from 400 to 800 nm, there are two kinds of scattering of light: elastic and inelastic scattering of light, which we call the Rayleigh and Raman scattering, respectively. In the Rayleigh (Raman) scattering, the scattered light does not (does) change the energy from that of the incident light. The scattering amplitude becomes strong if the energy difference of the initial and the final electronic states is the same as the photon energy for either the incident or scattered photon. This effect is called resonant Rayleigh (Raman) scattering. The resonant Rayleigh scattering can be one of the reasons the materials have an intrinsic color.[17]

Optical absorption can be explained by the perturbation theory for electronic structure in which the perturbation Hamiltonian is given by the vector potential of the electromagnetic field as follows:

$$\begin{aligned}\mathcal{H} &= \frac{1}{2m}\left\{-i\hbar\nabla - e\boldsymbol{A}(t)\right\}^2 + V(\boldsymbol{r}) \\ &= \frac{1}{2m}\left\{-\hbar^2\Delta + ie\hbar\boldsymbol{A}(t)\cdot\nabla + ie\hbar\nabla\cdot\boldsymbol{A}(t) + e^2\boldsymbol{A}(t)^2\right\} + V(\boldsymbol{r}).\end{aligned} \tag{5.22}$$

Both electric field ($\boldsymbol{E} = i\omega\boldsymbol{A}$) and magnetic field ($\boldsymbol{B} = \nabla\times\boldsymbol{A} = i\boldsymbol{k}\times\boldsymbol{A}$) of the electro-magnetic wave can be expressed by the vector

[17] Other reasons are (1) absorption spectra by induced current, (2) structural color, and so on.

potential $\boldsymbol{A}(t)$. In Eq. (5.22), we adopt the Coulomb gauge ($\mathrm{div}\boldsymbol{A} = 0$),[18] we get that $\nabla \cdot \boldsymbol{A} = \mathrm{div}\boldsymbol{A} + \boldsymbol{A} \cdot \nabla = \boldsymbol{A} \cdot \nabla$. When we neglect the term of $e^2\boldsymbol{A}(t)^2/2m$ compared with the term $ie\hbar\boldsymbol{A} \cdot \nabla$, which is a good approximation for the conventional power of laser light, we get the perturbation Hamiltonian as follows:

$$\mathcal{H}' = \frac{ie\hbar}{m}\boldsymbol{A}(t) \cdot \nabla. \tag{5.23}$$

When we used the Fermi golden rule,[19] the transition probability per unit time, $dP/dt$ from the initial state $i$ to the final state $f$ is given by

$$\frac{dP}{dt} = \frac{\pi}{\hbar^2} |\langle f|\mathcal{H}'|i\rangle|^2 \delta(E_f - E_i - \hbar\omega), \tag{5.24}$$

where $\delta$ is the Dirac delta function. The delta function tells us that the optical transition occurs when the energy difference between the initial state $E_i$ and the final state $E_f$ is matched to the energy of the phonon $\hbar\omega$, which we call resonant optical transition. In the mathematics, the delta function $\delta(x)$ describes a singular function at $x = 0$. However, in physics, because of the uncertainty principles for the energy, $\Delta E \Delta t \sim \hbar$, the strict condition of $x = 0$ can be relaxed for the fast optical transition with a small $\Delta t$. For example, if $\Delta t = 1$ ps (or 1 THz), $\Delta E$ becomes about 1 meV. $\Delta E = 1$ meV means that the optical absorption spectra have a spectral width of 1 meV. For the case of Raman scattering, a typical value of scattering is $\Delta t = 10$ fs, $\Delta E$ becomes 0.1 eV.[20]

$\langle f|\mathcal{H}'|i\rangle$ in Eq. (5.24), which is called transition dipole moment, is calculated by putting the wavefunction of valence and conduction

[18] The gauge is an additional condition for a vector potential combined with a scalar electro-static potential that does not change the value of electric and magnetic fields. If we adopt the Coulomb gauge, the scalar electro-static potential satisfies the Poisson equation, while if we adopt the Lorentz gauge, the scalar electro-static potential satisfies the wave equation.

[19] The Fermi golden rule is a general formula of the rate of transition from the initial to the final states for a given time-dependent perturbation that has a time dependence of $\exp -i\omega t$. See detail in any textbook on quantum mechanics.

[20] $\Delta E = 0.1$ eV means that the resonance Raman scattering occurs within 0.1 eV energy width as a function of incident laser energy, which we call resonance Raman profile. It is noted that the spectral width of Raman spectra comes from the lifetime of a phonon.

bands for the initial and final states, respectively. Here we can express the vector potential of the light by polarization vector $\boldsymbol{P}$ that is the unit vector in the direction of $\boldsymbol{A}$ (or $\boldsymbol{E}$),

$$\boldsymbol{A} = \frac{i}{\omega}\sqrt{\frac{I_0}{c\varepsilon_0}}\exp\{i(\boldsymbol{k}_{\text{opt}}\cdot\boldsymbol{r}\pm\omega t)\}\boldsymbol{P}, \tag{5.25}$$

where $I_0$ is the intensity of incident laser light (W/m$^2$), $\varepsilon_0$, $\boldsymbol{k}_{\text{opt}}$ and $\omega$ denote, respectively, the permittivity of the vacuum, the wavevector and angular frequency of the light. When we define the dipole vector:

$$\boldsymbol{D}^{fi}(\boldsymbol{k}) = \langle f|\nabla|i\rangle, \tag{5.26}$$

we express the matrix element by an inner product of $\boldsymbol{D}^{fi}$ and $\boldsymbol{P}$, as follows:

$$\langle f|\mathcal{H}'|i\rangle = \frac{e\hbar}{m\omega}\sqrt{\frac{I}{c\varepsilon_0}}\exp\{i(\omega_f-\omega_i\pm\omega)t\}\boldsymbol{D}^{fi}\cdot\boldsymbol{P}. \tag{5.27}$$

In the Quantum ESPRESSO, since the wavefunction is expanded by the plane waves (Eq. (5.9)), by putting Eq. (5.9) to Eq. (5.26), $\boldsymbol{D}^{fi}(\boldsymbol{k})$ is expanded as follows:

$$\begin{aligned}\boldsymbol{D}^{fi}(\boldsymbol{k}) &= i\sum_{\boldsymbol{G}}\sum_{\boldsymbol{G}'}C^{f*}_{\boldsymbol{G}'}(\boldsymbol{k})C^{i}_{\boldsymbol{G}}(\boldsymbol{k})(\boldsymbol{k}+\boldsymbol{G})\int\exp\{i(\boldsymbol{G}-\boldsymbol{G}')\boldsymbol{r}\}d\boldsymbol{r}\\ &= i\sum_{\boldsymbol{G}}\sum_{\boldsymbol{G}'}C^{f*}_{\boldsymbol{G}'}(\boldsymbol{k})C^{i}_{\boldsymbol{G}}(\boldsymbol{k})(\boldsymbol{k}+\boldsymbol{G})\delta_{\boldsymbol{G},\boldsymbol{G}'}\\ &= i\sum_{\boldsymbol{G}}C^{f*}_{\boldsymbol{G}}(\boldsymbol{k})C^{i}_{\boldsymbol{G}}(\boldsymbol{k})(\boldsymbol{k}+\boldsymbol{G}).\end{aligned} \tag{5.28}$$

Thus using the output of the coefficients of the wavefunction, we can calculate the optical absorption spectra.

The optical absorption spectra can be calculated in Quantum ESPRESSO once we calculate the dielectric functions as a function of $\omega$, $\varepsilon(\omega)$ (Sec. 3.4.1). Using the calculated dielectric functions, the real and imaginary part of the refractive index, $n(\omega)$ and $\kappa(\omega)$ are, respectively, given by

$$n(\omega) = \sqrt{\frac{|\varepsilon(\omega)| + \text{Re}(\varepsilon(\omega))}{2}}, \tag{5.29}$$

and

$$\kappa(\omega) = \sqrt{\frac{|\varepsilon(\omega)| - \mathrm{Re}(\varepsilon(\omega))}{2}}. \tag{5.30}$$

The dimensionless reflectance, $R(\omega)$, and absorption coefficient, $\alpha(\omega)$ in units of 1/m are expressed by $n(\omega)$ and $\kappa(\omega)$ as follows:

$$R(\omega) = \frac{(n(\omega)-1)^2 + \kappa(\omega)^2}{(n(\omega)+1)^2 + \kappa(\omega)^2}, \tag{5.31}$$

and

$$\alpha(\omega) = \frac{2\omega\kappa(\omega)}{c}, \tag{5.32}$$

where $c$ denotes the velocity of light. The absorption coefficient, $\alpha(\omega)$, is defined by **the Lambert-Beer law** in which the intensity of the transmitting light, $I(z)$, for a given incident intensity, $I_0$, is expressed by

$$I(z) = I_0 \exp(-i\alpha z). \tag{5.33}$$

The absorption coefficient becomes large when the number of states is large for a pair of the initial and final states for a given energy difference $E$ is large. The number of states for the pair is calculated by Quantum ESPRESSO as **joint density of states** ($JDOS(E)$) which is defined by

$$JDOS(E) = \sum_{\sigma} \frac{V}{(2\pi)^3} \int d\boldsymbol{k}\delta\{E_{c\sigma}(\boldsymbol{k}) - E_{v\sigma}(\boldsymbol{k}) - E\}, \tag{5.34}$$

where the summation is taken for the spin of electrons, $V$ is the volume of the sample, $E_{c\sigma}(\boldsymbol{k})$ ($E_{v\sigma}(\boldsymbol{k})$) represents the energy dispersion of conduction (valence) band with the spin $\sigma$. Here, we assume that the photon wavevector is sufficiently small compared with the reciprocal lattice vector, and thus the photon wavevector is neglected for the momentum conservation. The assumption is valid for $\hbar\omega < 3$eV. In the case of X-ray, on the other hand, the wavevector of the photon can not be neglected in the calculation of X-ray absorption spectra [Chowdhury *et al.* (2012)]. In one-dimensional materials

such as carbon nanotubes, it is known that the JDOS becomes singular ($1/\sqrt{E-E_0}$ at the energy bottom or top ($E = E_0$), which is known as one-dimensional van Hove singularity [Saito *et al.* (1992)]. In the two-dimensional materials, van Hove singularity ($\log|E-E_0|$) appears at the saddle point of energy dispersion. In the case of graphene, the saddle points exist at the M point ($E = E_0$) in the two-dimensional Brillouin zone.

## 5.10 Transport properties of solid

When we apply the voltage to the electrodes at both ends of the materials, electric current flows. If you can control the current electronically, we can make a solid-state device such as a transistor. Further, applying a magnetic field to the devices can create an electric current with the aligned spin of an electron, which we call spin current. In this section, we discuss the electric current as a transport property of solid.

When we consider a cuboid with a width $W$ and a length $L$, electrical resistance $R$ in SI unit Ω (Ohm) is defined by

$$R = \rho\frac{L}{W^2}, \quad (\Omega) \tag{5.35}$$

where $W^2$ is a cross-section of the cuboid and $\rho$ $(\Omega m)$ is called resistivity. The inverse of $R$ is conductance $G$ in SI unit $S$ (Siemens):

$$G = \sigma\frac{W^2}{L}, \quad (S) \tag{5.36}$$

where $\sigma \equiv 1/\rho$ is conductivity (S/m). It is clear from Eqs. (5.35) and (5.36) that $R$ and $G$ depend on the shape of material such as $W$ and $L$ while $\rho$ and $\sigma$ do not depend on the shape but only on the materials.

When an electron (or a hole) feels a constant force of $-e\boldsymbol{E}$ ($e\boldsymbol{E}$) in the presence of the constant electric field $\boldsymbol{E}$, the velocity is proportional to the time $t$, as $e\boldsymbol{E}t/m$, where $m$ is the effective mass of the electron. On the other hand, the electron loses velocity by scattering in the materials. If we assume that the electron loses the velocity after a time $2\tau$, where $\tau$ is called a relaxation time, the averaged velocity, $\bar{v}$ of the electron can be expressed by $e\boldsymbol{E}\tau/m$ since

the velocity changes from 0 to $2e\boldsymbol{E}\tau/m$. The current density $\boldsymbol{J}$ in units of $\mathrm{C/m^2 s}$, is defined by the number of electrons (or holes) passing a unit area of 1 $\mathrm{m}^2$ per unit time, which is given by

$$\boldsymbol{J} = n_c e\bar{v} = \frac{n_c e^2 \tau \boldsymbol{E}}{m}, \tag{5.37}$$

where $n_c$ denotes the carrier[21] density in units of $1/\mathrm{m}^3$. Since the conductivity is defined in electromagnetism by $\boldsymbol{J} = \sigma \boldsymbol{E}$, we get the formula for the conductivity by comparing with Eq. (5.37),

$$\sigma = \frac{n_c e^2 \tau}{m}. \tag{5.38}$$

Further, the conductivity is given by a product of (number of carriers) and mobility. Mobility is a physical quantity of how much velocity increases with respect to a given electric field. When we denote the number of electrons and hole per unit volume by $n$ and $p$, respectively, the **mobility** of electron and hole, $\mu_e$ and $\mu_h$ are defined by

$$\sigma = -ne\mu_e + pe\mu_h. \tag{5.39}$$

The unit of mobility is $\mathrm{m^2/V{\cdot}s}$. By comparing Eq. (5.38) and Eq. (5.39), the mobility can be expressed by

$$\mu_i = e\tau_i/m_i \quad (i = \mathrm{e}, \mathrm{h}). \tag{5.40}$$

Eq. (5.40) means that the mobility is proportional to the recombination time, $\tau_i$, and inversely proportional to the effective mass, $m_i$. In order to get a relatively large current density, $\boldsymbol{J}$, either a large carrier density or a large mobility are needed. In semiconductors, the number of carriers can be controlled by the number of impurities doped to the semiconductor. However, since the impurity can be a center of scattering for carriers, too much doping gives relatively low mobility.

In Quantum ESPRESSO, the relaxation time for the $n$-th band, $\tau_n(\boldsymbol{k})$, is given as a function of $\boldsymbol{k}$ by the inverse of the scattering rate,

[21] Carrier is either an electron or a hole that carries charges.

$\Gamma_{n\boldsymbol{k}}(\boldsymbol{k})$, as

$$\tau_n(\boldsymbol{k}) = \frac{1}{\Gamma_n(\boldsymbol{k})}, \tag{5.41}$$

in which $\Gamma_n(\boldsymbol{k})$ is calculated by EPW package [Poncé *et al.* (2016)] with using the electron-phonon interaction as

$$\begin{aligned}\Gamma_n(\boldsymbol{k}) = \frac{2\pi}{\hbar}\sum_{m\mu j}\int \frac{d\boldsymbol{q}}{\Omega_{\mathrm{BZ}}}|M_{mn}(\boldsymbol{k}+\boldsymbol{q},\boldsymbol{k})|^2 \times \\ \left[\frac{1+j}{2} - jf^0_{m,\boldsymbol{k}+\boldsymbol{q}} + n_{\boldsymbol{q},\mu}\right]\delta\left(\Delta E_{\boldsymbol{k}\boldsymbol{q}} - j\hbar\omega_{\boldsymbol{q}\mu}\right),\end{aligned} \tag{5.42}$$

where $M_{mn}(\boldsymbol{k}+\boldsymbol{q},\boldsymbol{k})$ represents the electron-phonon matrix element for an electron to be scattered from the initial state $(n, \boldsymbol{k})$ to the final state $(m, \boldsymbol{k}+\boldsymbol{q})$ by the $\mu$-th phonon at $\boldsymbol{q}$ with the phonon frequency $\omega_{\boldsymbol{q}\mu}$. The integer $j$ represents either phonon emission $(j = +1)$ or phonon absorption $(j = -1)$. $f^0_{m,\boldsymbol{k}+\boldsymbol{q}}$ and $n_{\boldsymbol{q},\mu}$ denote, respectively, the Fermi and Bose-Einstein distribution functions for the electron and the phonon. $\Omega_{\mathrm{BZ}}$ denotes the volume of the Brillouin zone in the $k$ space. The delta function shows the energy conservation in the Fermi golden rule for the time-dependent perturbation theory. The summation is taken over the possible intermediated states specified by $m$, $\mu$, and $j$ and the integration on $\boldsymbol{q}$ is taken over the Brillouin zone.

It is noted that the $M_{mn}(\boldsymbol{k}+\boldsymbol{q},\boldsymbol{k})$ for a given $\boldsymbol{q}$ is calculated by the so-called Wannier interpolation (see Sec. 5.14.3) in EPW (electron-phonon Wannier) package. The EPW package can usually install directly inside Quantum ESPRESSO by doing `"make epw"` after installing Wannier90 by `"make w90"`. Even though the tutorials for the EPW package are beyond the scope of this book, several tutorials are available at `https://docs.epw-code.org/doc/Tutorial.html`. We also recommend that the readers practice with Quantum ESPRESSO and Wannier90 in Chapter 3 before running the tutorials for EPW.

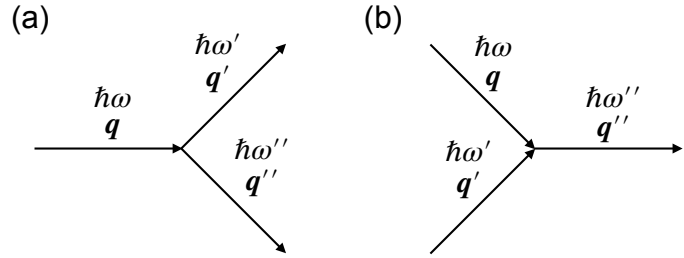


**Figure 5.9** Phonon-phonon scattering by cubic term of the anharmonic potential, (a) phonon-emission and (b) phonon-absorption processes. The energy and momentum before and after the scattering conserve. It is noted that there is the Umklapp scattering in which the reciprocal lattice vector $\boldsymbol{G}$ can be added in the momentum after the scattering.

## 5.11 Phonon-phonon interaction

A phonon with the angular frequency $\omega$ and an energy $E_{\rm ph} = \hbar\omega(n + 1/2)$ $(n = 0, 1, 2, ...)$ is an eigenstate of harmonic Hamiltonian in which the harmonic potential is given by $Kx^2/2$, where $K$ is a spring constant and $x$ is distortion of an atom from $x = 0$. Further, phonon in a crystal is given a propagating wave of oscillation as a function of the wavevector $\boldsymbol{q}$. For a given $\boldsymbol{q}$, we have $3N$ phonon modes in which $N$ is the number of atoms in the unit cell. All the $3N$ modes are orthogonal to one another.

When we consider anharmonic terms of the potential, which is proportional to $x^3$ or $x^4$, as a perturbation Hamiltonian, a phonon state specified by an integer $n$ in $E_{\rm ph} = \hbar\omega(n + 1/2)$ is no more eigenstate but has a finite life-time. When we solve time-dependent perturbation theory for the cubic anharmonic potential that is proportional to $x^3$, a phonon is scattered into two phonons, or two phonons are scattered into a phonon by creating or annihilating a new phonon, respectively. In Fig. 5.9, we show the three phonon scattering processes for a phonon (a) emitting and (b) absorbing processes. This phonon scattering occurs by keeping the energy and momentum of the phonons before and after the scattering. In this scattering, not only the wavevector $\boldsymbol{q}$ but also the phonon modes are changed, which we call phonon-phonon interaction.

When the cubic anharmonic term, $x^3$ is considered, the potential is not symmetric around the minimum of $V(r)$, $r_{\rm min}$, though the

potential minimum still exists at $r_{\min}$ (see Fig. 5.5). As shown in Fig. 5.5, the averaged position of the oscillation is shifted from $x = 0$ whose shifted value increases with increasing the amplitude of the oscillation. This situation corresponds to the phenomena of thermal expansion (Sec. 5.7).

The $x^4$ term, on the other hand, does not contribute to the thermal expansion since the potential is symmetric around $x = 0$ but contributes to the energy transfer from one phonon mode to the other phonon modes. This situation corresponds to the diffusion of the phonon and thus is related to thermal conductivity. It is noted that the $x^3$ term also contributes to the thermal conductivity. Since the terms of $x^3$ and $x^4$ are given by Taylor expansion around $r_{\min}$, the $x^4$ term is generally smaller than the $x^3$ term.

Because of the phonon-phonon scattering, each phonon mode with the wavevector $\boldsymbol{q}$ at a temperature, $T$, has a finite relaxation time $\tau_j(\boldsymbol{q}, T)$ and a mean free path by multiply the $\tau_j(\boldsymbol{q}, T)$ and the group velocity $\partial\omega(\boldsymbol{q})/\partial\boldsymbol{q}$ of the phonon. It is important to note here that the mean free path we discuss here is not the same as the mean free path for calculating the thermal conductivity (see Sec. 5.12). In the thermal equilibrium at $T$, the probability to find the $j$-th phonon with the energy $\hbar\omega_j(\boldsymbol{q})$ is given by the Bose-Einstein distribution function, $n_{\boldsymbol{q}j}$, as a function of $\omega_j(\boldsymbol{q})$ and $T$ as follows:

$$n_{\boldsymbol{q}j} \equiv \frac{1}{e^{\hbar\omega_j(\boldsymbol{q})/k_{\mathrm{B}}T} - 1}, \tag{5.43}$$

since a phonon is a boson. The values of $n_{\boldsymbol{q}j}$ should not be changed even if we consider the phonon-phonon scattering by anharmonicity of the potential because of the detailed valance of the scattering processes.

The scattering rate for the $j$-th phonon at the temperature $T$, $\gamma_j(\boldsymbol{q}, T)$, is inversely proportional of $\tau_j(\boldsymbol{q}, T)$ which is given by the Fermi golden rule as follows:

$$\begin{aligned}\gamma_j(\boldsymbol{q}, T) &\equiv \frac{1}{\tau_j(\boldsymbol{q}, T)} \\ &= \frac{\pi}{\hbar^2 N_{\boldsymbol{q}}} \sum_{\boldsymbol{q}', \boldsymbol{q}'', j', j''} \left| V^{(3)}_{\boldsymbol{q}j, \boldsymbol{q}'j', \boldsymbol{q}''j''} \right|^2 \delta(-\boldsymbol{q} + \boldsymbol{q}' + \boldsymbol{q}'' + \boldsymbol{G}) \\ &\quad \times [(1 + n_{\boldsymbol{q}'j'} + n_{\boldsymbol{q}''j''})\delta(\omega_{\boldsymbol{q}j} - \omega_{\boldsymbol{q}'j'} - \omega_{\boldsymbol{q}''j''}) \\ &\quad + 2(n_{\boldsymbol{q}'j'} - n_{\boldsymbol{q}''j''})\delta(\omega_{\boldsymbol{q}j} + \omega_{\boldsymbol{q}'j'} - \omega_{\boldsymbol{q}''j''})],\end{aligned} \tag{5.44}$$

where $N_{\boldsymbol{q}}$ represents the number of $\boldsymbol{q}$ points in the Brillouin zone in the calculation. Three delta functions corresponds to the momentum and energy conservation in the phonon-phonon scattering processes as shown in Fig. 5.9. Here $\boldsymbol{G}$ denotes the reciprocal lattice vector. When $\boldsymbol{G} = 0$ ($\boldsymbol{G} \neq 0$), we call normal (the Umklapp) scattering process. The Umklapp process is important for thermal conductivity since the normal process does not give a net thermal flow but only contributes to $\tau_j(\boldsymbol{q}, T)$. The factors $(1 + n_{\boldsymbol{q}'j'} + n_{\boldsymbol{q}''j''})$ and $2(n_{\boldsymbol{q}'j'} - n_{\boldsymbol{q}''j''})$ in Eq. (5.44) are factors that the scattering rate for Fig. 5.9 (a) and (b), respectively, which is relevant to the $n_{\boldsymbol{q}j}$ before and after scattering. The derivation of these factors are long, and we do not discuss the origin more. See, for example, Eq. (6.68) in "The Physics of Phonons" [Srivastava (1990)]. It is noted that the two terms are equivalent to more meaningful terms by the identities

$$\begin{aligned} n_{\boldsymbol{q}'j'} - n_{\boldsymbol{q}''j''} &= \frac{(n_{\boldsymbol{q}'j'} + 1)n_{\boldsymbol{q}''j''}}{n_{\boldsymbol{q}j}}, \\ 1 + n_{\boldsymbol{q}'j'} + n_{\boldsymbol{q}''j''} &= \frac{n_{\boldsymbol{q}'j'}n_{\boldsymbol{q}''j''}}{n_{\boldsymbol{q}j}}, \end{aligned} \tag{5.45}$$

where we used Eq. (5.43) and the energy conservation. In the calculation of Eq. (5.44), we used so-called "single-mode relaxation-time approximation (SMTA)". In the SMTA, when we consider the deviation of $n_{\boldsymbol{q}j}$ for the $j$-th phonon mode at $\boldsymbol{q}$ from the thermal equilibrium, we assume that the other phonon-modes are in the thermal equilibrium.

Since the phonon has a finite lifetime, the uncertainty principle ($\Delta E \Delta t \geq \hbar$) tells us that the phonon energy can not be determined precisely. In fact, $\hbar\gamma_j(\boldsymbol{q}, T)$ corresponds an energy width of the energy dispersion of the $j$-th phonon modes. When the width is large, it means that the phonon has a short lifetime, and thus we can see $\hbar\gamma_j(\boldsymbol{q}, T)$ in the spectral width of the $j$-th phonon at $\boldsymbol{q}$ in the neutron scattering measurement of Raman spectra. This is important for us to discuss the resonant conditions of the scattering event. In Quantum ESPRESSO, the linewidth of the phonon energy dispersion is calculated by `d3.x`. However, since version 6.0 of Quantum ESPRESSO, the `d3.x` code has been superseded by the D3Q code (`https://anharmonic.github.io/d3q/`). Please be aware that each release of the D3Q code is developed and tested on top

of a specific version of Quantum ESPRESSO, and it will probably not work on any other version. Therefore, the readers should choose the correct package.

It is noted that there are other origins of phonon scattering besides anharmonicity. For example, isotope or lattice defect breaks the periodicity of the lattice, which makes the phonon scattering. In the case of carbon, 1.1% of carbon is $^{13}$C isotope. When a phonon propagates in two-dimension, a phonon meets a $^{13}$C in $10 \times 10$ unit cells which can not be negligible. Electron-phonon interaction is another origin for phonon scattering indirectly in which a phonon is absorbed to or emitted from an electron, which gives a finite lifetime of the phonon.

## 5.12 Heat conduction in a solid

When there are hot and cold points in material, heat flows from the hot to the cold points. The heat flux $\boldsymbol{J}$ in units of W/m$^2$ at a point is proportional to the gradient of temperature $\nabla T$, (K/m), that is,

$$\boldsymbol{J} = -\kappa \nabla T, \tag{5.46}$$

which is called **the Fourier law**, and the coefficient $\kappa > 0$ is called **thermal conductivity** (W/m/K). In Quantum ESPRESSO, we can calculate the thermal conductivity by Thermal2 code (`https://anharmonic.github.io/thermal2/`), which comes bundled with the D3Q code. Both Thermal2 and D3Q codes can usually install directly inside Quantum ESPRESSO by doing `"make d3q"`. The thermal conductivity $\kappa$ becomes large when the amplitude of the oscillation is large compared with a few % of the bond length. Diamond and carbon nanotubes are known to be materials with a large thermal conductivity since (1) the mass of carbon atoms is relatively small for a given spring constant and (2) the anharmonicity of the potential is large compared with other materials. It is noted here that the thermal conductivity of metal is generally large, too, because phonons are interacted by electron-phonons interactions. Thus, the phonon scattering process is relevant to the thermal conductivity.

When we use the equation of continuity, temporal change of a heat $Q$ at $\boldsymbol{r}$ is given by

$$\frac{dQ}{dt} = -\mathrm{div}\boldsymbol{J}, \tag{5.47}$$

where $Q$ (J/m$^3$) per unit volume is expressed by the density $\rho$ (kg/m$^3$) and the specific heat $C$ (J/kg/K) as follows:

$$Q = \rho CT. \tag{5.48}$$

When we assume that $\rho$ and $C$ are constants for a given material, we put Eqs. (5.48) and (5.46) to Eqs. (5.47) and obtain the following equation:

$$\frac{dQ}{dt} = \rho C\frac{dT}{dt} = -\mathrm{div}\boldsymbol{J} = \kappa\Delta T. \tag{5.49}$$

Eq. (5.49) is a diffusion equation for T, which we call **the heat equation**. The value of $\kappa/(\rho C)$ (m$^2$/s) is called the **thermal diffusivity**.

Temperature of the lattice in thermal equilibrium is defined by the Bose-Einstein distribution function, $n_{\boldsymbol{qj}}$ (Eq. (5.43)). Using the Boltzmann transport theory, the diffusive thermal conductivity $\kappa$ is expressed by [Saito *et al.* (2018)]

$$\kappa = \frac{\hbar^2}{2Vk_BT^2}\sum_{\boldsymbol{qj}}\omega_{\boldsymbol{qj}}^2\tau_j(\mathbf{q},T)n_{\boldsymbol{qj}}(n_{\boldsymbol{qj}}+1)|v_{\boldsymbol{qj}}|^2. \tag{5.50}$$

where $V$ denotes the volume of material, $\tau_j(\mathbf{q},T)$ is defined by Eq. (5.44), and $v_{\boldsymbol{qj}}$ represents the group velocity of the phonon ($\boldsymbol{v}_{\boldsymbol{qj}} = \nabla_{\boldsymbol{q}}\omega_{\boldsymbol{qj}}$). In Eq. (5.50), we can define the specific heat per volume of the lattice for the $j$-th phonon at $\boldsymbol{q}$ and the specific heat $C$ as follows:

$$C_{v\boldsymbol{qj}} = \frac{\hbar^2}{Vk_BT^2}\omega_{\boldsymbol{qj}}^2 n_{\boldsymbol{qj}}(n_{\boldsymbol{qj}}+1), \qquad C = \frac{V}{2N}\sum_{\boldsymbol{qj}}C_{v\boldsymbol{qj}}. \tag{5.51}$$

In Thermal2 code, we can select as an option either (1) single-mode approximation (SMA) or (2) full consideration by "conjugate gradient algorithm with precoding" (CGP) [Atkinson (1988)]. It is

natural that it takes more computational time if we adopt (2). The product of the group velocity and the relaxation time corresponds to the phonon mean free path. When the sample size, $L$, is smaller than the phonon mean free path, thermal conductivity by the phonon becomes "ballistic" in which the phonon with a positive velocity directly contributes to the thermal conductivity as follows:

$$\kappa_{\mathrm{ball}} = L \sum_{\boldsymbol{q}j} C_{\nu \boldsymbol{q}j} v_{\boldsymbol{q}jx} \theta(v_{\boldsymbol{q}jx}), \tag{5.52}$$

where $\theta$ is the Heaviside function. When part of phonon modes becomes ballistic, the diffusive thermal conductivity can not be used. Further, we must consider the thermal resistivity by isotope scattering [Saito *et al.* (2018)] and by electron-phonon interaction if we want to compare the calculated results with the experimental results.

When we decrease the temperature, the thermal conductivity increases monotonically up to the maximum and then becomes zero since the specific heat becomes zero at $T = 0$ K. It is not generally easy to calculate thermal conductivity by first-principles calculation at low temperatures since the mean free path becomes long compared with the size of the computation. Fitting the anharmonicity to the anharmonic results of Quantum ESPRESSO, the tight-binding method for thermal conductivity is a possible way to calculate thermal conductivity at low temperature [Saito *et al.* (2018)].

We note that the D3Q and Thermal2 codes are beyond the scope of this book. The readers can find the tutorials for graphene and silicon at `https://anharmonic.github.io/`. We recommended the readers to practice the phonon tutorials in Sec. 3.3 before running the tutorials of the D3Q and Thermal2 codes.

## 5.13 Non-resonant Raman scattering

Raman scattering is the inelastic scattering of light, in which energy of the incident light is partially consumed for exciting a phonon.[22]

[22] Any other elementary excitations such as a magnon can be an origin of Raman scattering.

The energy difference between the incident light and the scattered light is called the Raman shift, whose unit is $\mathrm{cm}^{-1}$ (1 eV = 8065 $\mathrm{cm}^{-1}$). In the experiment, they observe the intensity of the scattered light as a function of the Raman shift, which is called Raman spectra. The peak positions of Raman spectra correspond to the phonon modes, which are Raman active modes. The Raman active modes are defined by the optical phonon modes in which the photo-excited electron emits a phonon by the electron-phonon interaction. The Raman active modes have the symmetry of quadratic form of $x$, $y$, $z$ such as $x^2+y^2$, $x^2-y^2$, $xz$, etc. The quadratic function for each phonon mode is obtained as functions for the irreducible representation in the character table of point group for the unit cell if we know the information of the irreducible representation of the phonon mode in the point group.[23]

In Quantum ESPRESSO, we can calculate the so-called non-resonant Raman spectra to obtain the phonon mode's frequency and symmetry and the relative intensity in the Raman spectra, which we call density-functional perturbation theory (DFPT). The non-resonant Raman intensities are calculated within the DFPT [Lazzeri and Mauri (2003)] as

$$I(\nu) \propto \left|\vec{e}_s \cdot R(\nu) \cdot \vec{e}_i\right|^2 \frac{n_\nu + 1}{\omega_\nu}, \tag{5.53}$$

in which $\vec{e}_i(\vec{e}_s)$ is the polarization vector of incident (scattered) light. Here the polarization vector is defined by a unit vector of the direction of electric field of the incident (or scattered) light. $n_\nu$ $(=\frac{1}{e^{\hbar\omega_\nu/k_\mathrm{B}T}-1})$ is the occupation number of $\nu^{th}$ phonon at temperature T. $R(\nu)$ is so-called Raman tensor (a $3\times3$ matrix) for the $\nu$-th phonon mode which connects the polarization vectors, $\vec{e}_i$ and $\vec{e}_s$. Depending on the symmetry of the phonon mode, Raman tensor does have non-zero matrix element. For example, the group theory tells us that the degenerate $E_{2g}$ phonon modes with $x^2-y^2$ and $xy$ symmetry have

[23] Number of the Raman active modes and their irreducible representation are obtained by decomposing the reducible character of "atomic site character" × "irreducible representations of $x, y, z$" into irreducible representations [Dresselhaus *et al.* (2008)].

the following shapes

$$R(E_{2g}:x^2-y^2)=\begin{pmatrix} a & 0 & 0\\ 0 & -a & 0\\ 0 & 0 & 0\end{pmatrix},\quad R(E_{2g}:xy)=\begin{pmatrix} 0 & b & 0\\ b & 0 & 0\\ 0 & 0 & 0\end{pmatrix}, \tag{5.54}$$

respectively, where $a$ and $b$ are non-zero constants at $xx$ ($yy$) and $xy$ ($yx$) components, which are calculated by Quantum ESPRESSO. The matrix elements of non-resonant Raman tensor are calculated by DFPT in Quantum ESPRESSO by differentiating the electric energy, $E^{el}$, with electric field components, $\vec{E}_\alpha$ or $\vec{E}_\beta$ ($\alpha,\beta = x,y,z$), and the lattice deformation of a phonon as follows:

$$R_{\alpha\beta}(\nu)=\sum_{\zeta\delta}\frac{\partial^3 E^{el}}{\partial E_\alpha \partial E_\beta \partial r_{\zeta\delta}}\frac{u^{\nu}_{\zeta\delta}}{\sqrt{M_\delta}}, \tag{5.55}$$

where $M_\delta$ the mass of the $\delta^{th}$ atom, $r_{\zeta\delta}$ the position of the $\delta^{th}$ atom along the direction $\zeta$ ($\zeta = x,y,z$), and $u_{\zeta\delta}$ the atomic displacement of the $\delta^{th}$ atom along the $\zeta$ direction for the eigenmode $\nu$.

For the calculated Raman tensor and polarization vectors, we can calculate the relative Raman intensities by $|\vec{e}_s\cdot R(\nu)\cdot\vec{e}_i|^2$ in Eq. (5.53). For example, when the polarization of the incident light lies in the $x$ direction, $\vec{e}_i =^t (1,0,0)$, we get a non-zero intensity for the $x$ or $y$ polarizations of the scattered light $\vec{e}_s = e_x \equiv^t (1,0,0)$, or $\vec{e}_s = e_y \equiv^t (0,1,0)$ for $R(E_{2g}:x^2-y^2)$ or $R(E_{2g}:xy)$, respectively, as follows:

$${}^t e_x R(E_{2g}:x^2-y^2)e_x = (1,0,0)\begin{pmatrix} a & 0 & 0\\ 0 & -a & 0\\ 0 & 0 & 0\end{pmatrix}\begin{pmatrix}1\\0\\0\end{pmatrix} = a, \tag{5.56}$$

or

$${}^t e_y R(E_{2g}:xy)e_x = (0,1,0)\begin{pmatrix} 0 & b & 0\\ b & 0 & 0\\ 0 & 0 & 0\end{pmatrix}\begin{pmatrix}1\\0\\0\end{pmatrix} = b. \tag{5.57}$$

From the calculated phonon dispersion relation as a function of $q$, we obtain the Raman shift frequency of each phonon at the optical phonon frequency at the Γ point in the Brillouin zone, which

is called zone-center phonon mode. The reason why only the Γ point phonon is observed in the first-order Raman spectra is understood by the three Raman sub-processes: (1) optical absorption of an electron with the wavevector $k$ in which the electron can excite almost "vertically" in the k space, (2) the photo-excited electron can emit a phonon with a phonon wavevector $q$, and (3) the scattered electron is recombined with a hole at the original $k$. In order for the scattered electron to recombine with a hole, the phonon wavevector should be $q = 0$.

If we can not find the corresponding phonon frequency in the observed Raman spectra, the Raman spectra might be two-phonon Raman spectra whose frequency is the sum of two-phonons. In the two-phonon Raman scattering, the restriction of $q = 0$ in the case of one-phonon scattering is relaxed, and a pair of $q \neq 0$ and $-q$ can be possible for the wavevectors of the emitted two phonons, which enables the photo-excited electron to recombine with the hole. Thus we expect that the two phonon spectra are generally broad and weak. When two of the three intermediate states are resonant to the electronic states, the Raman intensity of the two-phonon Raman scattering becomes comparable or even larger than the intensity of one-phonon Raman scattering. This situation is called "double-resonance Raman scattering" [Saito *et al.* (2002b), Saito *et al.* (2003), Saito *et al.* (2002a)]. The double resonance Raman occurs, too, when one of the two scattering processes with $q$ and $-q$ is an elastic scattering of a photo-excited electron by impurity. One famous example of defect-oriented, double resonance Raman spectra is the D-band of graphite at 1350 $\mathrm{cm}^{-1}$ [Pimenta *et al.* (2007)] in which iTO phonon mode at the K point is relevant to the Raman spectra. The two-phonon Raman spectra of the iTO phonon mode at the K point appear at 2700 $\mathrm{cm}^{-1}$ which we call G′ band (or 2D band). It is noted that the G′ band is an intrinsic Raman spectra of graphite without any defects.

When the intermediate state of the photo-excited electrons is a real electronic state, the Raman intensity is enhanced significantly compared with non-resonant Raman spectra, which we call **resonant Raman spectra**. In order to calculate the resonant Raman intensity by first-principles calculation, we need to calculate electron-phonon and electron-photon matrix elements. See detail in the references [Tatsumi and Saito (2018), Tatsumi *et al.* (2018)].

## 5.14 Warnier functions

Wannier functions (WFs) [Wannier (1937)] are Fourier-transformed Bloch functions of DFT calculation into a smaller set that is localized in real space. While the Bloch function is oscillating and delocalized in the real spaces, as shown in Fig 5.10 (a), the WFs that are localized in the real space offer more microscopic insights for the chemical and physical properties. In particular, the WFs are useful for analyzing chemical bonding, building accurate tight-binding models, or calculating the material properties that require a dense integration in the Brillouin zone.

Let us start with the Bloch states of energy band $n$, $\psi_{n\boldsymbol{k}}(\boldsymbol{r})$, in terms of a Fourier series of $\boldsymbol{R}$ as

$$\psi_{n\boldsymbol{k}}(\boldsymbol{r}) = \sum_{\boldsymbol{R}} e^{i\boldsymbol{k}\cdot\boldsymbol{R}} w_{n\boldsymbol{R}}(\boldsymbol{r}), \tag{5.58}$$

where $\boldsymbol{R}$ is a lattice vector labeling a unit cell within a supercell that is conjugate to the $\boldsymbol{k}$-points grid. Here, $w_{n\boldsymbol{R}}(\boldsymbol{r})$ is the WF that is localized at each atomic position of $\boldsymbol{R}$, as shown in Fig. 5.10 (b). The Bloch functions of the 1D system can be plotted for $\boldsymbol{k} = 0, \boldsymbol{k}_1$ and $\boldsymbol{k}_2$ in Fig. 5.10 (a). In the case of $\boldsymbol{k} \neq 0$, we can see that the amplitude of $\psi_{n\boldsymbol{k}}(\boldsymbol{r})$ is oscillating with $\boldsymbol{k}_1$ (or $\boldsymbol{k}_2$). The inverse Fourier transformations of $\psi_{n\boldsymbol{k}}(\boldsymbol{r})$ on $\boldsymbol{k}$ for a given $\boldsymbol{R}$ gives a WF [Wannier (1937)]:

$$w_{n\boldsymbol{R}}(\boldsymbol{r}) = \frac{1}{N_{\boldsymbol{k}}} \sum_{\boldsymbol{k}} e^{-i\boldsymbol{k}\cdot\boldsymbol{R}} \psi_{n\boldsymbol{k}}(\boldsymbol{r}), \tag{5.59}$$

where $N_{\boldsymbol{k}}$ is the number of $\boldsymbol{k}$ points. The set of the WFs forms an orthogonal and complete basis set, respectively, as

$$\int w^*_{n\boldsymbol{R}}(\boldsymbol{r}) w_{n'\boldsymbol{R}'}(\boldsymbol{r}) \mathrm{d}\boldsymbol{r} = \delta(\boldsymbol{R} - \boldsymbol{R}')\delta_{nn'}, \tag{5.60}$$

and

$$\sum_{n\boldsymbol{R}} w^*_{n\boldsymbol{R}}(\boldsymbol{r}) w_{n\boldsymbol{R}}(\boldsymbol{r}') = \delta(\boldsymbol{r} - \boldsymbol{r}'). \tag{5.61}$$

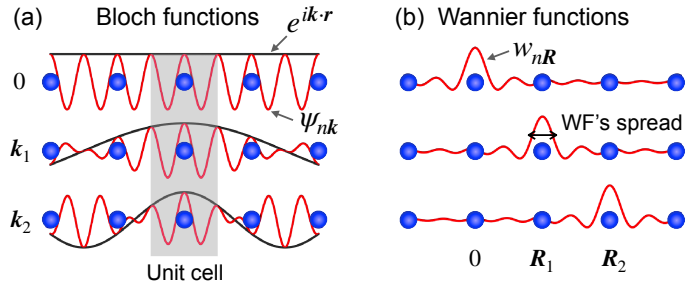


**Figure 5.10** (a) The Bloch functions $\psi_{n\boldsymbol{k}}(\boldsymbol{r})$ of a single band $n$ in 1D system for three different values of the wave vector $\boldsymbol{k}$. (b) The Wannier functions $w_{n\boldsymbol{R}}(\boldsymbol{r})$ for the same band $n$ for the three different values of the lattice vector $\boldsymbol{R}$.

According to the Bloch theorem [Kittel (1976)], $\psi_{n\boldsymbol{k}}(\boldsymbol{r})$ is expressed by

$$\psi_{n\boldsymbol{k}}(\boldsymbol{r}) = e^{i\boldsymbol{k}\cdot\boldsymbol{r}} u_{n\boldsymbol{k}}(\boldsymbol{r}), \tag{5.62}$$

where $u_{n\boldsymbol{k}}(\boldsymbol{r})$ is a periodic function ($u_{n\boldsymbol{k}}(\boldsymbol{r}) = u_{n\boldsymbol{k}}(\boldsymbol{r}-\boldsymbol{R})$). By substituting Eq. (5.62) into Eq. (5.59), we obtain:

$$\begin{aligned} w_{n\boldsymbol{R}}(\boldsymbol{r}) &= \frac{1}{N_{\boldsymbol{k}}} \sum_{\boldsymbol{k}} e^{i\boldsymbol{k}(\boldsymbol{r}-\boldsymbol{R})} u_{n\boldsymbol{k}}(\boldsymbol{r}) \\ &= \frac{1}{N_{\boldsymbol{k}}} \sum_{\boldsymbol{k}} \psi_{n\boldsymbol{k}}(\boldsymbol{r}-\boldsymbol{R}) \\ &= w_{n,0}(\boldsymbol{r}-\boldsymbol{R}). \end{aligned} \tag{5.63}$$

Therefore, $w_{n\boldsymbol{R}}(\boldsymbol{r})$ has the same periodicity as the atomic structure of the crystal, as shown in Fig. 5.10 (b).

It is important to note that the WFs are not unique because the Bloch functions are not unique. For each $\psi_{n\boldsymbol{k}}(\boldsymbol{r})$, we can obtain the same electron density by multiplying a different phase $\alpha$ in front of the Bloch function (i.e., $e^{i\alpha}\psi_{n\boldsymbol{k}}(\boldsymbol{r})$). However, by choosing a different phase of the Bloch functions, we get new Wannier functions that may exhibit very different shapes in real space. When we consider $N_e$ energy bands, $N_e$ Bloch functions at a given $\boldsymbol{k}$ can be rotated by

the unitary operator as

$$\psi_{n\boldsymbol{k}}(\boldsymbol{r}) = \sum_{m=1}^{N_e} U_{mn}^{\boldsymbol{k}} \psi_{m\boldsymbol{k}}(\boldsymbol{r}), \tag{5.64}$$

where $U_{mn}^{\boldsymbol{k}}$ is an $N_e \times N_e$ unitary matrix at each $\boldsymbol{k}$. Then the WFs in Eq. (5.59) can be rewritten as

$$w_{n\boldsymbol{R}}(\boldsymbol{r}) = \frac{1}{N_{\boldsymbol{k}}} \sum_{\boldsymbol{k}} e^{-i\boldsymbol{k}\cdot\boldsymbol{R}} \left[ \sum_{m=1}^{N_e} U_{mn}^{\boldsymbol{k}} \psi_{m\boldsymbol{k}}(\boldsymbol{r}) \right]. \tag{5.65}$$

For Eq. (5.65), the question is how to choose $U_{mn}^{\boldsymbol{k}}$ to obtain a maximally-localized WF in real space.

### 5.14.1 Maximally-localized Warnier functions

Among several methods, **maximally-localized Wannier functions** (MLWFs) [Marzari and Vanderbilt (1997)] are an effective method for minimizing the mean-square spread of the WFs, $\Omega$, to choose $U_{mn}^{(\boldsymbol{k})}$. The MLWFs are employed in Quantum ESPRESSO by Wannier90 package. $\Omega$ is defined as [Marzari and Vanderbilt (1997)]

$$\Omega = \sum_{n=1}^{N_e} \left[ \langle (\boldsymbol{r} - \bar{\boldsymbol{r}}_n)^2 \rangle_n \right] = \sum_{n=1}^{N_e} \left[ \langle \boldsymbol{r}^2 \rangle_n - \bar{\boldsymbol{r}}_n^2 \right], \tag{5.66}$$

where $\bar{\boldsymbol{r}}_n$ and $\langle \boldsymbol{r}^2 \rangle_n$ are the center and the second moment of the average for WF at $\boldsymbol{R} = 0$ that are defined by

$$\bar{\boldsymbol{r}}_n = \langle w_{n,0} | \boldsymbol{r} | w_{n,0} \rangle \text{ and } \langle \boldsymbol{r}^2 \rangle_n = \langle w_{n,0} | \boldsymbol{r}^2 | w_{n,0} \rangle. \tag{5.67}$$

For the 1D system, the spread of the WFs is shown in Fig. 5.10 (b). Since $w_{n,0}$ is a function of $U_{mn}^{\boldsymbol{k}}$ (see Eq. (5.65)), $\Omega$ is a functional of $U_{mn}^{\boldsymbol{k}}$. Thus, it allows us to minimize the spread $\Omega$ by variation of these unitary matrices. To perform this minimization, steepest-descent or conjugate-gradient algorithms can be applied if $\mathrm{d}\Omega/\mathrm{d}U_{mn}^{\boldsymbol{k}}$ is known [Marzari *et al.* (2012b)].

### 5.14.2 Spread of the Wannier functions

As shown by Blount [Blount (1962)], the center of the WFs can be expressed in terms of the Bloch states as

$$\bar{\boldsymbol{r}}_n = \langle w_{n,0}|\boldsymbol{r}|w_{n,0}\rangle = \frac{1}{N_{\boldsymbol{k}}}\sum_{\boldsymbol{k}}\left\langle u_{n\boldsymbol{k}}\left|i\frac{\partial}{\partial \boldsymbol{k}}\right|u_{n\boldsymbol{k}}\right\rangle. \tag{5.68}$$

Thus, the second moment of the WFs can also be expressed as

$$\langle \boldsymbol{r}^2\rangle_n = \langle w_{n,0}|\boldsymbol{r}^2|w_{n,0}\rangle = -\frac{1}{N_{\boldsymbol{k}}}\sum_{\boldsymbol{k}}\left\langle u_{n\boldsymbol{k}}\left|\left(\frac{\partial}{\partial \boldsymbol{k}}\right)^2\right|u_{n\boldsymbol{k}}\right\rangle. \tag{5.69}$$

In a numerical approach, we can use the finite-difference expressions for $\partial/\partial\boldsymbol{k}$ and $(\partial/\partial\boldsymbol{k})^2$ [Marzari and Vanderbilt (1997)] in Eqs. (5.68) and (5.69), respectively, and we get:

$$\bar{\boldsymbol{r}}_n = \frac{i}{N_{\boldsymbol{k}}}\sum_{\boldsymbol{k},\boldsymbol{b}} w_{\boldsymbol{b}}\boldsymbol{b}[\langle u_{n\boldsymbol{k}}|u_{n,\boldsymbol{k}+\boldsymbol{b}}\rangle - 1], \tag{5.70}$$

and

$$\langle \boldsymbol{r}^2\rangle_n = \frac{1}{N_{\boldsymbol{k}}}\sum_{\boldsymbol{k},\boldsymbol{b}} w_{\boldsymbol{b}}[2 - 2\mathrm{Re}\langle u_{n\boldsymbol{k}}|u_{n,\boldsymbol{k}+\boldsymbol{b}}\rangle], \tag{5.71}$$

where $\boldsymbol{b}$ denotes the vectors connecting the points $\boldsymbol{k}$ to neighboring points $\boldsymbol{k}+\boldsymbol{b}$, and $w_{\boldsymbol{b}}$ denotes the associated weights that come from the finite difference representation.

Let us define an overlap matrix element $M_{mn}^{\boldsymbol{k},\boldsymbol{b}}$ as

$$M_{mn}^{\boldsymbol{k},\boldsymbol{b}} = \langle u_{m\boldsymbol{k}}|u_{n,\boldsymbol{k}+\boldsymbol{b}}\rangle. \tag{5.72}$$

It is proved that $M_{mn}^{\boldsymbol{k},\boldsymbol{b}}$ satisfies the following conditions [Marzari and Vanderbilt (1997)]:

$$M_{nn}^{\boldsymbol{k},\boldsymbol{b}} - 1 = i\mathrm{Im}\left(\ln M_{nn}^{\boldsymbol{k},\boldsymbol{b}}\right), \tag{5.73}$$

and

$$2 - 2\mathrm{Re}M_{nn}^{\boldsymbol{k},\boldsymbol{b}} = 1 - \left|M_{nn}^{\boldsymbol{k},\boldsymbol{b}}\right|^2 + \left[\mathrm{Im}\left(\ln M_{nn}^{\boldsymbol{k},\boldsymbol{b}}\right)\right]^2. \tag{5.74}$$

By substituting Eqs. (5.73) and (5.74) into Eqs. (5.70) and (5.71), we obtain:

$$\bar{\boldsymbol{r}}_n = -\frac{1}{N_{\boldsymbol{k}}} \sum_{\boldsymbol{k},\boldsymbol{b}} w_{\boldsymbol{b}} \boldsymbol{b} \mathrm{Im}\left(\ln M_{nn}^{\boldsymbol{k},\boldsymbol{b}}\right), \tag{5.75}$$

and

$$\langle \boldsymbol{r}^2 \rangle_n = \frac{1}{N_{\boldsymbol{k}}} \sum_{\boldsymbol{k},\boldsymbol{b}} w_{\boldsymbol{b}} \left(1 - \left|M_{nn}^{\boldsymbol{k},\boldsymbol{b}}\right|^2 + \left[\mathrm{Im}\left(\ln M_{nn}^{\boldsymbol{k},\boldsymbol{b}}\right)\right]^2\right). \tag{5.76}$$

From Eqs. (5.66), (5.75), and (5.76), we can see that the spread $\Omega$ with respect to the unitary matrix $U_{mn}^{\boldsymbol{k}}$ can be expressed as a function of the overlap matrix element $M_{mn}^{\boldsymbol{k},\boldsymbol{b}}$. Therefore, $M_{mn}^{\boldsymbol{k},\boldsymbol{b}}$ is needed to minimize the spread $\Omega$ to obtain the optimized choice of $U_{mn}^{\boldsymbol{k}}$. On the other hand, the iterative minimization of $\Omega$ will starts with an initial guess orbitals as

$$|\tilde{w}_{n,0}\rangle = \frac{1}{N_{\boldsymbol{k}}} \sum_{m\boldsymbol{k}} A_{mn}^{\boldsymbol{k}} |\psi_{m\boldsymbol{k}}\rangle, \tag{5.77}$$

where $A_{mn}^{\boldsymbol{k}}$ is projected matrix element, which is defined by

$$A_{mn}^{\boldsymbol{k}} = \langle \psi_{m\boldsymbol{k}} | g_n \rangle, \tag{5.78}$$

where $g_n$ are projections such as $s$, $p$, or hybrids. In Quantum ESPRESSO, $M_{mn}^{\boldsymbol{k},\boldsymbol{b}}$ and $A_{mn}^{\boldsymbol{k}}$ are calculated from `pw2wannier90.x` after the Bloch states calculated by `pw.x`.

### 5.14.3 Tight-binding model and Wannier interpolation

The unique set of the MLWFs constitutes an orthogonal and complete basis, which enables us to use these orbitals for setting up the **effective model Hamiltonian** in real space for the tight-binding model as

$$\mathcal{H} = \sum_{\boldsymbol{R}\boldsymbol{R}'} \sum_{nn'} t_{nn'}(\boldsymbol{R}, \boldsymbol{R}') |w_{n\boldsymbol{R}}\rangle \langle w_{n'\boldsymbol{R}'}|, \tag{5.79}$$

where $t_{nn'}(\boldsymbol{R}, \boldsymbol{R}')$ are the hopping parameters that depend on only the distance vector connecting the MLWFs as

$$\begin{aligned} t_{nn'}(\boldsymbol{R}, \boldsymbol{R}') &= \langle w_{n\boldsymbol{R}} | \mathcal{H} | w_{n'\boldsymbol{R}'} \rangle \\ &= \langle w_{n,0} | \mathcal{H} | w_{n',\boldsymbol{R}'-\boldsymbol{R}} \rangle \\ &= t_{nn'}(\boldsymbol{R}' - \boldsymbol{R}). \end{aligned} \tag{5.80}$$

Using a Fourier transformation of $\mathcal{H}$ in the basis of the MLWFs, we can obtain $\mathcal{H}$ in momentum space as

$$\begin{aligned} \mathcal{H}_{nn'}(\boldsymbol{q}) &= \sum_{\boldsymbol{R}} e^{i\boldsymbol{q}\cdot\boldsymbol{R}} t_{nn'}(\boldsymbol{R}) \\ &= \sum_{\boldsymbol{R}} e^{i\boldsymbol{q}\cdot\boldsymbol{R}} \left( \frac{1}{N_{\boldsymbol{k}}} \sum_{\boldsymbol{k}} e^{-i\boldsymbol{k}\cdot\boldsymbol{R}} \left[ (U^{\boldsymbol{k}})^{\dagger} \epsilon(\boldsymbol{k}) U^{\boldsymbol{k}} \right]_{nn'} \right), \end{aligned} \tag{5.81}$$

where $\epsilon(\boldsymbol{k})$ are the Kohn-Sham eigenvalues by given a $\boldsymbol{k}$-grid in the DFT calculation. By diagonalizing the tight-binding Hamiltonian $\mathcal{H}_{nn'}(\boldsymbol{q})$ in Eq. (5.81), we can obtain the energy dispersion, $\epsilon(\boldsymbol{q})$, in which $\boldsymbol{q}$-grid can be much denser than $\boldsymbol{k}$-grid. This calculation is known as the **Wannier interpolation**, which is useful to calculate transport properties (e.g., electrical conductivity) that require a dense $\boldsymbol{k}$-grid in the Brillouin zone.